EARTHQUAKE RISK ASSESSMENT FOR ISTANBUL METROPOLITAN AREA BY DETERMINISTIC APPROACH

by

Bulent Hakan AKMAN

B.S. in C.E., Istanbul Technical University, 1996

Submitted to the Kandilli Observatory and
Earthquake Research Institute in partial fulfillment of
the requirements for the degree of
Master of Science
in
Earthquake Engineering

Boğaziçi University

2001

EARTHQUAKE RISK ASSESSMENT FOR ISTANBUL METROPOLITAN AREA BY DETERMINISTIC APPROACH

APPROVED BY:

Prof. Dr. Mustafa Erdik.....

Prof. Dr. Özal Yüzügüllü.....

Assis. Prof. Eser Durukal.....

DATE OF APPROVAL.....

ACKNOWLEDGEMENTS

I am deeply grateful to my thesis advisor, Prof. Dr. Mustafa Erdik for their invaluable suggestions, criticism and encouraging helps in the preparation of this thesis My gratitude also goes to following institutions: Istanbul Metropolitan Municipality, ISKI (Istanbul Water and Sewer Administration), Turkish Telecommunication Administration, IGDAS (Istanbul Natural Gas Distribution Association), BEDAS (Beyazid Electricity Distribution Association) and General Directorate of Highways due to valuable data they provided.

I am greatly indebted to the members of the Department of Earthquake Engineering especially to Ph.D student, Yeşim Alpay Biro for her support and encouragement throughout the study.

In the end I owe it all to my parents for their great support and devotion.

EARTHQUAKE RISK ASSESSMENT FOR ISTANBUL METROPOLITAN AREA BY DETERMINISTIC APPROACH

Bülent Hakan AKMAN

Department of Earthquake Engineering, Master of Science Thesis, 2001

Thesis Supervisor: Prof. Dr. Mustafa ERDİK

Keywords: Earthquake, Deterministic, Vulnerability, Scenario,

The largest city, İstanbul in Turkey which has a complex tectonic region and is one of the most seismically active regions of the Eastern Mediterranean. Throught the city's history, earthquakes have been the most damaging natural disasters that have affected the area. Therefore, earthquakes constitute one of the most important natural hazards and risks for İstanbul and the mitigation of this risk necessitate immediate preparation of disaster response and management plans.

The primary objective of this study is to develop a hazard map of İstanbul by deterministic approach. This means according to a specified scenario earthquake the damage to buildings and infrastructure with their appropriate physical and socioeconomical consequences were considered. In this study the aim was to investigate the damage to both suffered buildings and the most critical elements at risk

The resulting planning earthquake scenario is intended to contribute to the efforts the local offices with emergency planning responsibilities and private sectors and planners who must understand the scope of the hazard in order to prepare it.

İSTANBUL METROPOLU İÇİN DETERMİNİSTİK OLARAK DEPREM RİSK DEĞERLENDİRİLMESİ

Bülent Hakan AKMAN

Deprem Mühendisliği Ana Bilim Dalı,Yüksek Lisans Tezi,2001

Tez Danışmanı: Prof. Dr. Mustafa ERDİK

Anahtar Sözcükler : Deprem, Deterministik, Hassaslık, Senaryo

Turkiye'nin en büyük şehri olan İstanbul sahip olduğu kompleks yapısı ile dogu akdenizin sismisitesi en aktif bölgelerinden birisi durumundadır. Şehrin tarihi boyunca dpremlerşehreen fazla zarar veren doğal afetler olarak yerini almıştır.Dolayısıyla, İstanbul'a ait afet yönetim planları hazırlanmasında depremler en onemli unsurlardan birisi olmalidir.

Bu çalışmanın amacı İstanbul'a ait risk haritasının deterministik olarak geliştirilmesidir.Belirlenen senaryo depremine göre altyapı ve üstyapıda oluşacak hasarlar ile bu hasarların meydana getirdiği fiziksel ve sosyoekonomik sonuçlarını etraflica tespitidir.

Planlanan bu deprem senaryosu sonucu acil durum plan ve çalışmalarını gerçekleştirmek isteyen yerel ve özel mercilere katkıda bulunabilir

TABLE OF CONTENTS

LIST OF FIGURES

LIST OF TABLES

LIST OF SYMBOLS

M	Moment Magnitude
NAF	North Anatolian Fault
NE	Nort East
SW	South West
Mw	Moment Magnitude
Mpa	Mega Pascal
MMI	Mercalli Intensity
I_0	Maximum Intensity
Ms	Surface Wave Magnitude
D	End to End Contour Interval Distances
σ	Standart Deviation
r^2	Correlation Coefficient
V_s	Shear Velocity
MDR	Expected Damage Ratio
PI	Plasticity Index

1. INTRODUCTION

The location of İstanbul could be placed in a circle lying roughly at the intersection of the 41 st parallel and the 29th meridian. İstanbul is the place where the Continents of Europe and Asia meet too, for it was founded at the point where the Black Sea is linked to the Mediterranean and the islands by the Sea of Marmara. Istanbul is where roads link East and West, where the sea brings North and South together (Figure 1.1). This geographical feature of the city is further stressed by the presence of the Golden Horn, which throughout history has served as a natural harbour for ships of all kinds. The city of Istanbul,stuated astride the Bosphorus

The Bosphorus links the Black Sea, the length of the Bosphorus ranges between 28.5km and 31.7km (depending on where it is measured), which means an average length of 30km. Its width at the northern end is 4700m, and at the southern end, 2500m. The widest place in the Bosphorus is in the Büyükdere vicinity (3300m), and the narrowest place is that which lies between Rumelihisar and Kanlıca (660-700m). It is known that the deepest part of the Bosphorus is 100m in depth (Figure 1.2-1.3).

The largest city in Turkey, which has a complex tectonic region and is one of the most seismically active regions of the Eastern Mediterranean. Throught the city's history, earthquakes have been the most damaging natural disasters that have affected the area. Marmara region faced so many earthquakes concerning with catalogs. In addition to this, it is predicted a credible seismic gap along the extension of the North Anatolian Fault which pases about 15 km south of the city. Plus, in recent decades the earthquake disaster risks have incresead due to owercrowding, faulty land-use planning and construction, inadequate infrastructure and services, and environmental degradation. As such, for Istanbul large earthquakes may have potential to lead to disasters, which is inevitable urgent preparation for disaster response and management plans.

Earthquake scenarios are the best tools describing physical consequences of an earthquake that can occur in earthquake-prone urban areas such as Istanbul. The earthquake planning scenario describes what could happen in Istanbul if the region is shaken by a specific, plausible earthquake. Such scenario has two important inputs. The first is hazard of such region prepared its earthquake scenario. The second is istatistical damages relating to population, buildings, infrastructures and socio-economic structure.

The success of earthquake scenarios and theirs activities depend on not only determining earthquake hazard, fire related earthquake and landslide which are secondary hazard but also exposing theirs vulnerabilities of damage as realistic as possible. Besides all these, it is needed to establish the relation with each other properly.

The objective of this study is to develop hazard maps Istanbul region in deterministic terms including the effects of regional soil condition and evaluate the damage to buildings and lifeline systems according to deterministically specified scenario earthquake consequences defined in deterministic approach.

Earthquake hazard has been measured in terms of intensity. Intensity has been widely accepted parameter used the ground shaking measure in most earthquake scenarios. It is reasonable to predict damage levels on the basis of expected intensity since intensity levels are defined by means of structural damage. Intensity based vulnerability matrices have been used throughout the world estimating the damage ratios of engineering structures at the scope of a deterministic seismic analysis.

In a deterministic seismic analysis, one or more scenario earthquakes are defined on a selected fault without explicit consideration of the probability. Probabilistic seismic hazard analysis is widely applied in earthquake loss estimation involving sources of uncertainty. On the other hand, the physical characteristics of earthquakes such as their magnitude and epicentral location dissapear in the seismic hazard results. From this point view, the physical characteristics of the specific scenario earthquake are

specifically known. The deterministic seismic analysis is particularly useful when the consequences of the scenario earthquake are needed.

While defining the hazard of the region, effect of local site conditions must be taken into consideration by assigning simplified site categories. Actually, such effects should be determined by detailed microzonation studies like microtremor measurements. Five site categories broadly determined from geology maps because of the fact that no such measurements available for the region under the consideration.

Lifeline systems, buildings, populations and socio-economic activities establish Vulnerability and Element at Risk. It is needed the collection of accurate inventory to define the vulnerability of elements at risk in a earthquake scenario. At this scope studied, it is used the street map whose scale is 1/1000 related all Istanbul area, data supplied by local administrations such as Istanbul Metropolitan Municipality, ISKI (Istanbul Water and Sewer Administration),TELEKOM (Turkish Telecommunication Administration),IGDAŞ (Istanbul Natural Gas Distribution),BEDAŞ (Beyazid Electricity Distribution Association) and TKY (Turkish General Directorate of Highways), DİE (Statement Istatistical Institute) and ground surveys can provide the earthquake damage scenario.İn addition to these, demographic information was compiled and prepared population density map for all Istanbul area. By means of above foundations, telephone, natural gas, water, sewage, major roads and public transportaions were compiled. Furthermore, electric power transmission substations and distribution of administrative buildings and switchboards were included in the compilation

At the scope of all information, the hazard map of the specified scenario earthquake in terms of intensity has been delineated utilizing an earthquake simulation method that had been developed based on Turkish earthquake data. The presented hazard maps have been also modified by the local soil condition of the region. The specified scenario earthquake consequences on element at risk are presented on the basis of vulnerability functions that had been produced from available Turkish data as well as adapted U.S.A data. The maps produced in this study can be used in earthquake

resistant design practices, land use management, earthquake insurance activities and emergency planning studies. They can also constitute a basis for more detailed analyses.

FIGURE 1.1 Satellite image of İstanbul

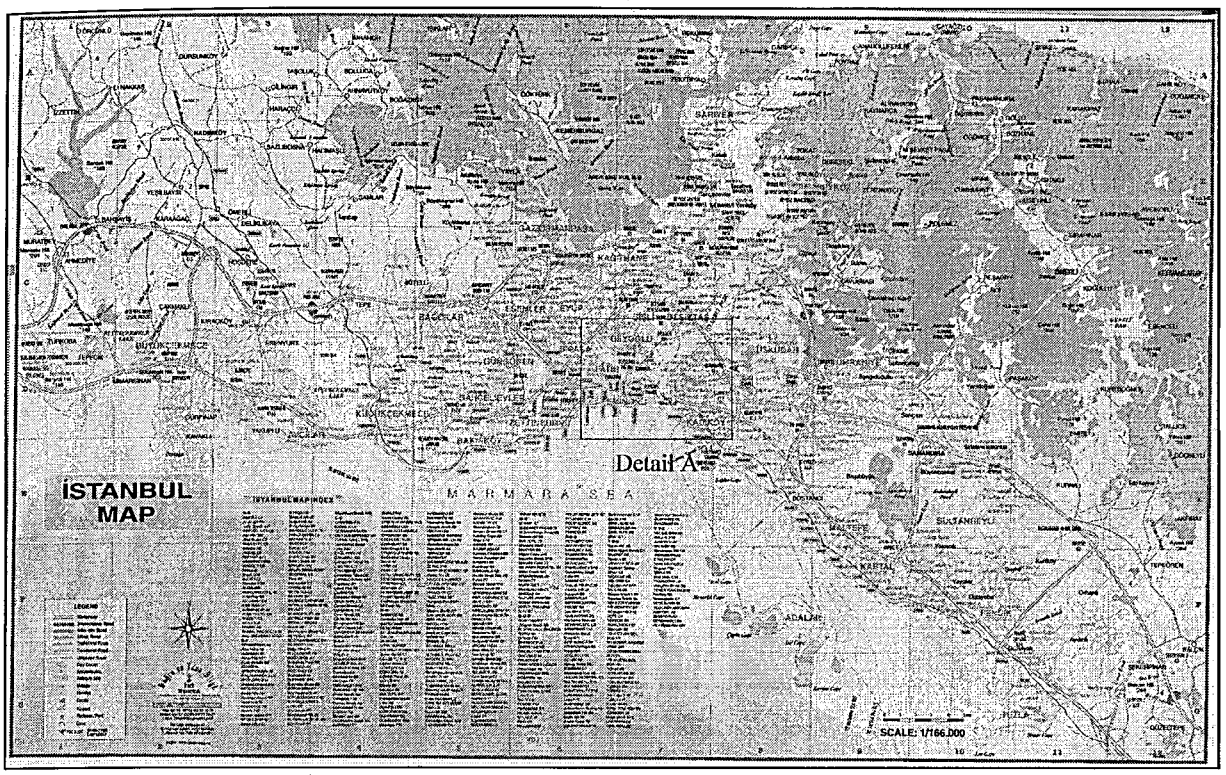

FIGURE 1.2 Istanbul Map

FIGURE 1.3 Satellite Image (Detail "A") of İstanbul

2. NEO-TECTONICS OF MARMARA REGION

General Treatment

The Sea of Marmara is situated at the transition between the North Anatolian fault system and the Aegean one(Figure 2.1). The North Anatolian faulth system is characterized by location of the strain within a single major continuous dextral fault that is the limit between the Anatolian block moving westward at about 24 mm/yr with respect to Eurasia (McCluscky et al.,2000)(Figure 2.2). It is characterized by large (magnitude 7 to 8) earthquakes with rupture lenths significantyly larger than 100 km.The Marmara Sea is located immediately west of the first bifurcation of the North Anatolian fault. It is a topographic depression that is generally assumed to have been created as a pull-apart, following (Ketin, 1948) and (McKenzie, 1972). Thus the Marmara Sea is considered to belong to the Aegean province and the expected fault system there is assumed to be rather complex and consist of short 50 km long segments rupturing in modarate size (6.5 to 7) earthquakes.

It was pointed out by (Le Pichon et al., 1999) that even if the Marmara Sea originated as a pull apart the dense geodetic measurementsin the area (Straub, 1996) indicate that the motion there is purely strike-slip which cannot be reconciled with pull-apart tectonics. Actually geodesy shows that most ot the detxtral strike-slip motion of the North Anatolian fault (about 20 mm/yr) is transmitted through the narrow north Marmara trough(Figure 2.3). Furthermore, (Le Pichon et al., 1999) argued that the Marmara Sea had been affected by historical erathquakes, such as the 1509 and the 1766 ones that appeared to have been significantly larger than typical Aegean earthquakes (Ambraseys and Finkel, 1995). They thus proposed that the North Anatolian fault is continuous across the northern trough of the Marmara Sea. Following (Pınar, 1943), they called it the Marmara fault. They argued that the Marmara fault had recently (about 200,000 years ago) cut through the basins and this process of progressive localization of the fault is to be expected for a fault that has been created in the recent geologic past (Barka, 1992).

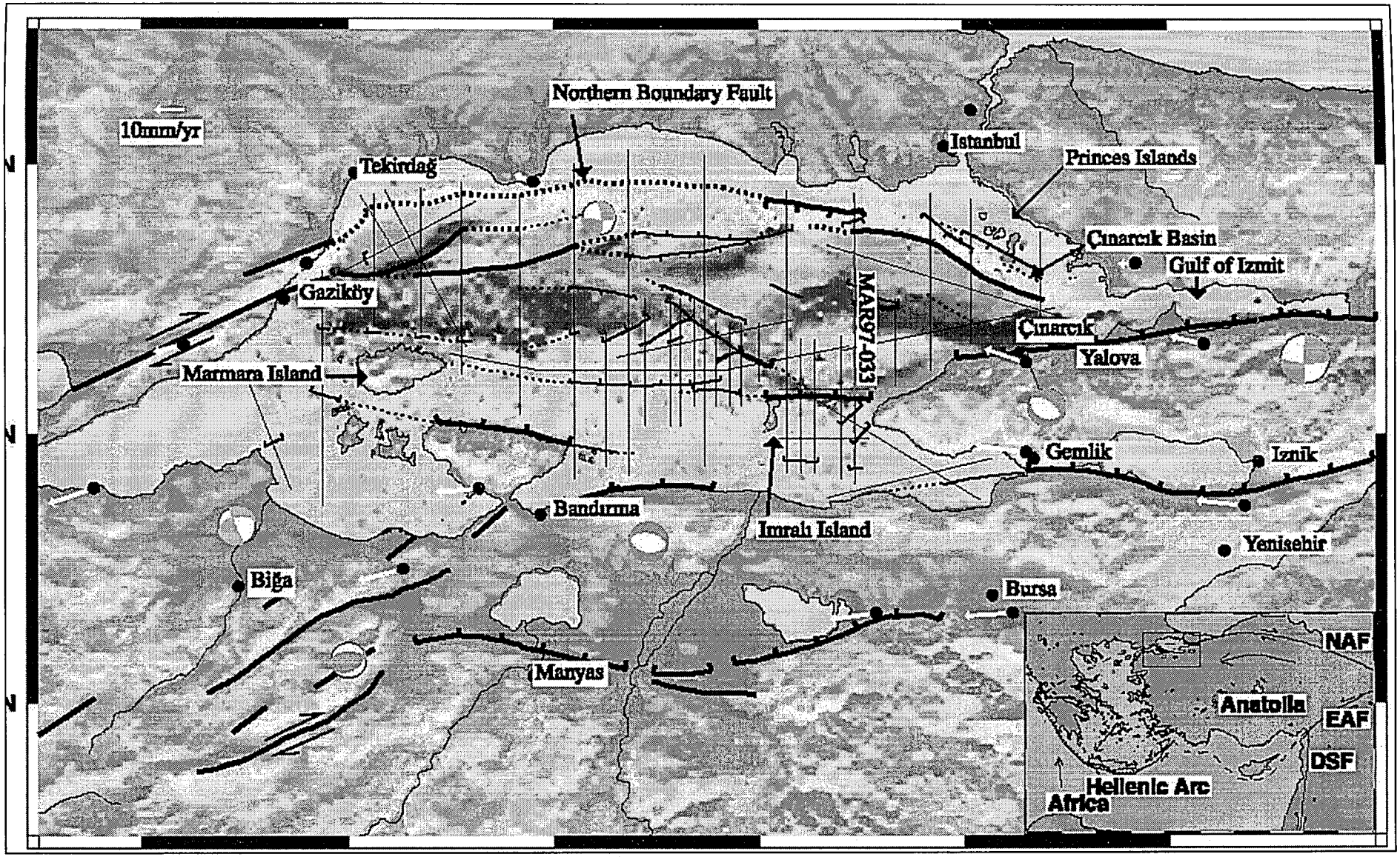

FIGURE 2.1 Tectonic system of Marmara region

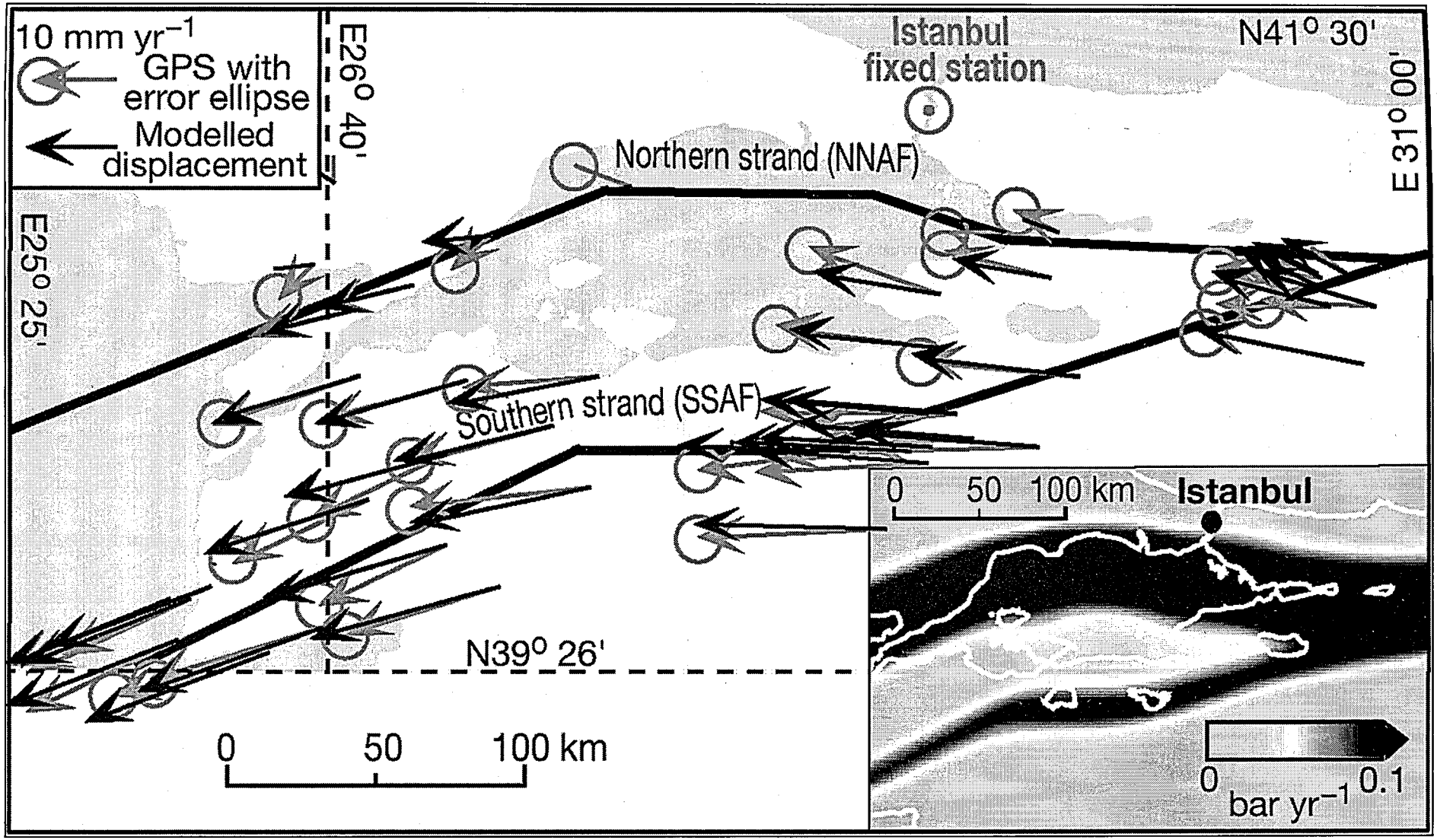

FIGURE 2.2 The displacement model of tectonic structure in Marmara region

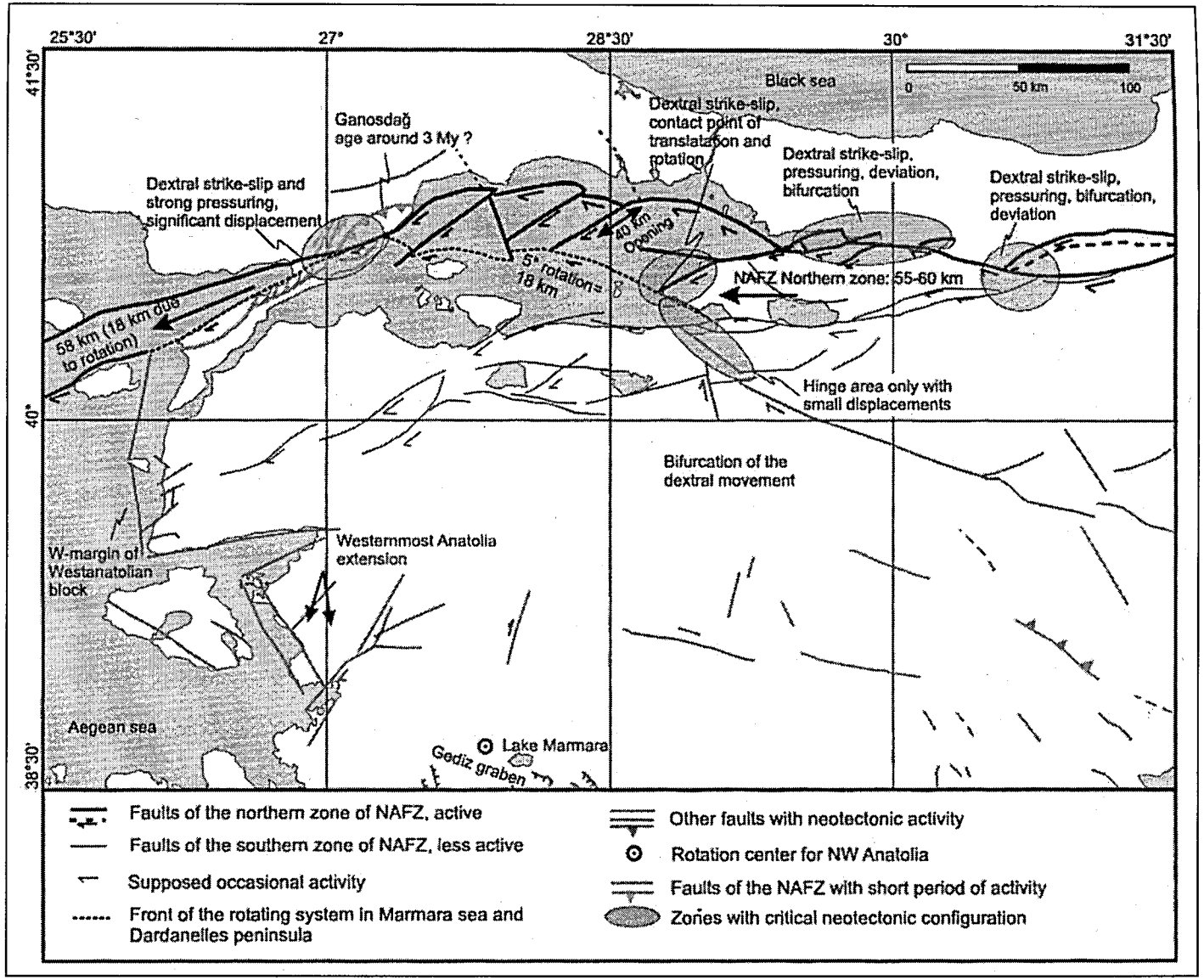

FIGURE 2.3 Neotectonic activities in NW Turkey since The Pliocene critical configurations

The northern Marmara trough is situated between two blocks that show no significant internal deformation at the geodetic level the Thrace one to the north and the South Marmara block to the south. The northern one belongs to Eurasia whereas, in the Eurasian frame, the South Marmara block rotates counterclockwise. As the geodetic data is inverted to determine simultaneously, the rotation of the South Marmara block, the location of the boundary fault between the two blocks assuming that the motion along it is pure dextral strike-slip and the depth of locking on the fault, assuming a fully locked fault in an elastic half-space(Figure 2.4). The inversion is robust for the velocity on the fault. The locking depth is not well determined and is about 10 km. The geodetically determined fault, not surprisingly, coincides with the Ganos fault to the west and the İzmit fault to the east. In between, it follows closely the main active fault mapped by the Suroit cruise in the Sea of Marmara (Le Pichon et al.,2001). There is a 3.5mm/yr component of compression on the Ganos fault in agreement with the field observations (Armijo et al., 1999).

Within the Marmara basin itself, west of 27.43°E, the fault is in the prolongation of the Ganos fault for its first 12 km and thus has the same component of compression. Between 27.47°E and 28.85°E, the main fault is continous over a length of 120 km is nearly pure stike-slip, with a very slight compressional component in its eastern portion. Between 28.85°E and 29.23°E, along the Çınarcık northern slope, the fault has a strong extensional component of 9 mm/yr over a length of 36 km. Finally, between 29.23°E and 29.45°E, near the Hersek delta in the Gulf of İzmit, the 20 km long portion of fault is E-W which should result in a slight compressional component. The most remarkable feature of this system, from the Ganos fault to the İzmit one, is the continuity of main single fault taking about 20 mm/yr of nearly pure dextral motion.In detail, kinematically,one can identify four main units: sea of 140 km long Ganos unit,extending 12 km in the sea of Marmara fault unit that is nearly pure strike-slip and cuts across the northern Marmara basins in a remarkably straight fashion ; the 36 km northern Çınacık slope unit, with a strong extensional component; and finally the İzmit unit that was broken during the Kocaeli earthquake. The Ganos unit was last ruptured in 1912. Thus, the only unruptured units for more than 100 years and probably quite a lot more are the Çınarcık and main Marmara zones(Figure 2.5).Çınarcık Unit should

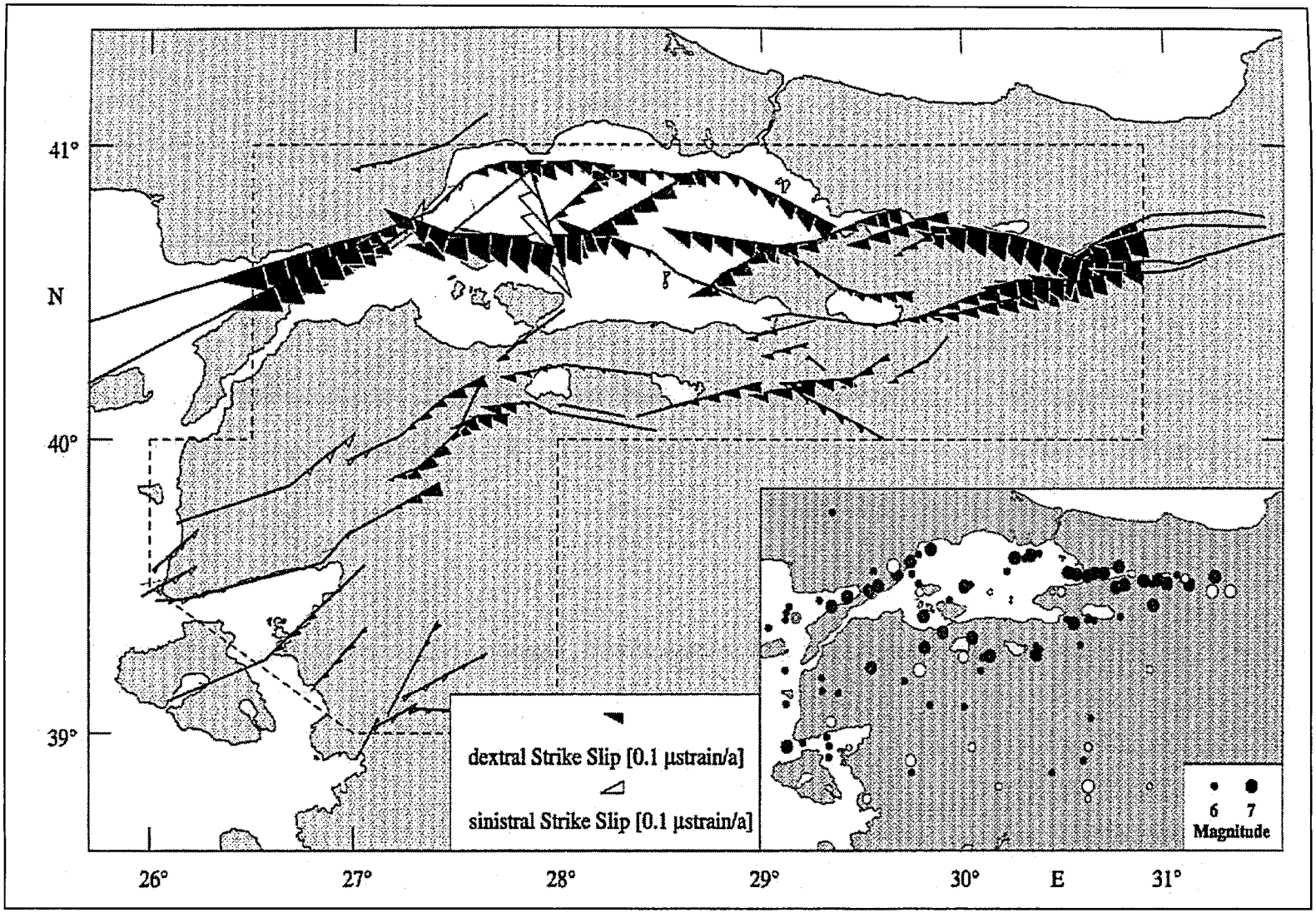

FIGURE 2.4 Scaled and oriented sense of strike along the fault lines

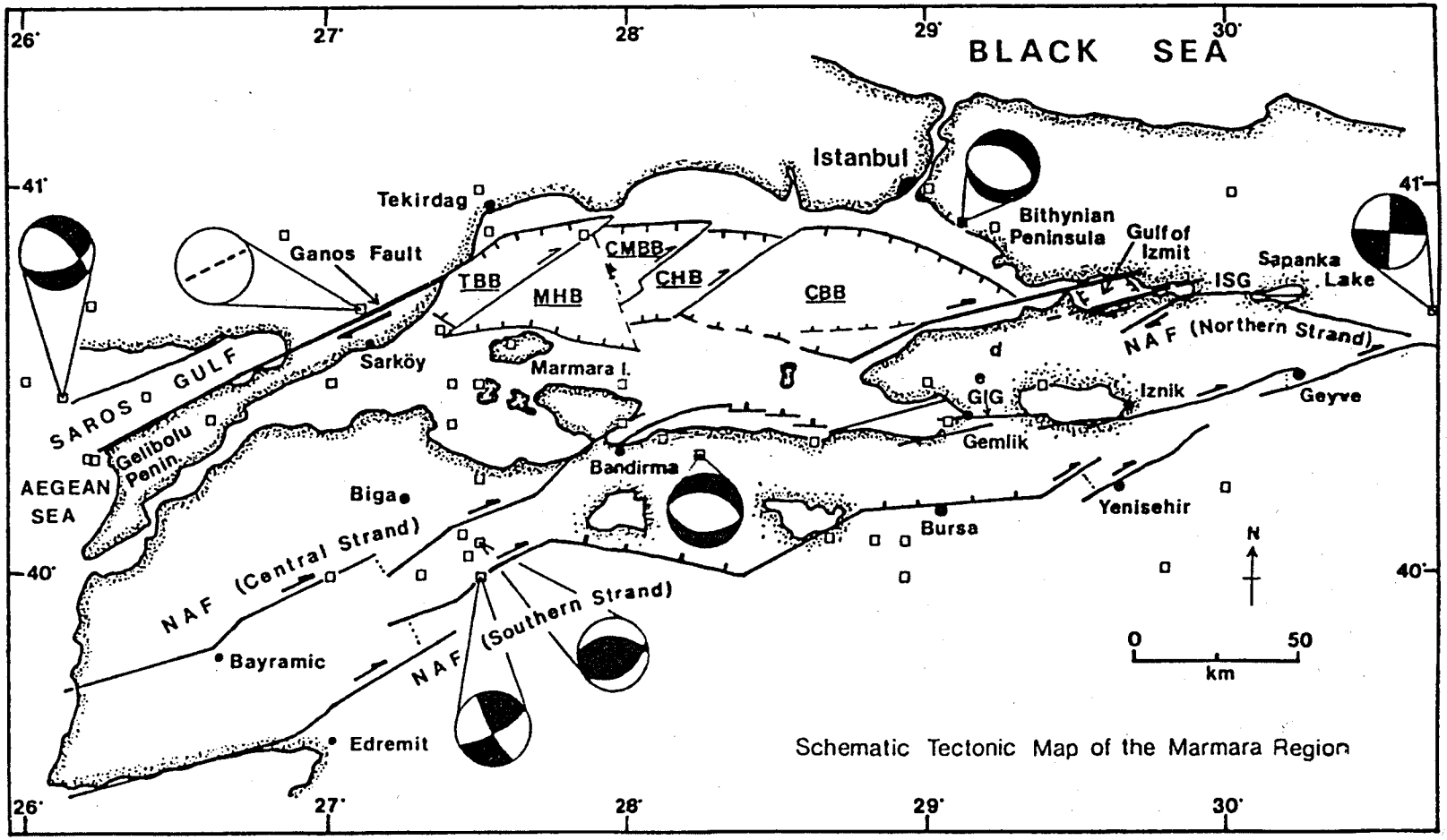

Schematic Tectonic Map of the Marmara Region

Schematic tectonic map of the Marmara region. Earthquake epicenters (open squares) are from Alsan et al. (1975) and Dewey (1976). Earthquake mechanism solutions are from Dewey (1976), Evans et al. (1985), Eyidogan (1988) and Taymaz et al. (1991b). Compressional quadrants are black. TBB: Tekirdag Basin block; MHB: Marmara High block; CMBB: Central Marmara Basin block; CHB: Central High block; CBB: Cinarcik Basin block; NAF: North Anatolian Fault; ISG: Izmit–Sapanca graben; GIG: Gemlik–Iznik graben. The circle without a quadrantal patterns shows only the orientation of the nodal plane. The focal mechanisms are unknown.

FIGURE 2.5 The geometry and distribution of active fault segments belonging to Marmara region

expect there strike-slip with an extensional component (Örgülü and Aktar.2001) have shown that several sizeable Kocaeli aftershocks along this fault unit were pure dextral strike-slip. This suggests that there is partitioning of the motion there and indeed the Suroit cruise has found a system of active normal faults to the southeast of the Çınarcık basin(Le Pichon et al.,2001). The suggest the exintence of a small counterclockwise rotation of the eastern Çınarcık basin with respect to the South Marmara block, that accounts for the pure strike-slip motion along the northern Çınarcık slope(Figure 2.6).

This is the fact that the main Marmara fault unit has a well developed microseismic activity whereas the Çınarcık unit microsesimic activity is model (Gürbüz et al.,2000). According to Ambraseys and Jackson, the Marmara Sea was probably not broken by a large earthquake since more than 500 years. On the other hand, it is difficult to understand in this interpretation on how the two 1766 earthquakes coud have ruptured the same yera independently as in this case their ruptures would be separeted by several tens of kilometres of unruptured and probably creeping fault. However, the elastic effect produced by the locking of the fault within the Sea Marmara is difficult to test in a definitive way with the GPS data available on land.As supporting all these, the present active system in the Sea of Marmara is not compitable with a pull-apart structure. A single continuous fault now cuts through the northern basins(Figure 2.7)

As a result, during the last fifty years, a large number of studies have focused on the NAFZ within and around the Marmara sea. Some of these works are seen as comprasion of the structural models in Figure 2.8

The Izmit bay area

In earlier studies, the bay area was considered as a graben structure (i.e. Crampin and Evans 1986) and some others thought that a single southern strike-slip fault with a vertical component had performed the bay (i.e. Ketin 1969, Saroglu et al. 1987). On the other hand, Barka and Kadinsky-Cade (1988) and Barka and Gulen (1988) introduced a pull-apart model in which they claimed that instead of considering a single segment occurring along the southern shore, en echelon strike-slip segments stepping up

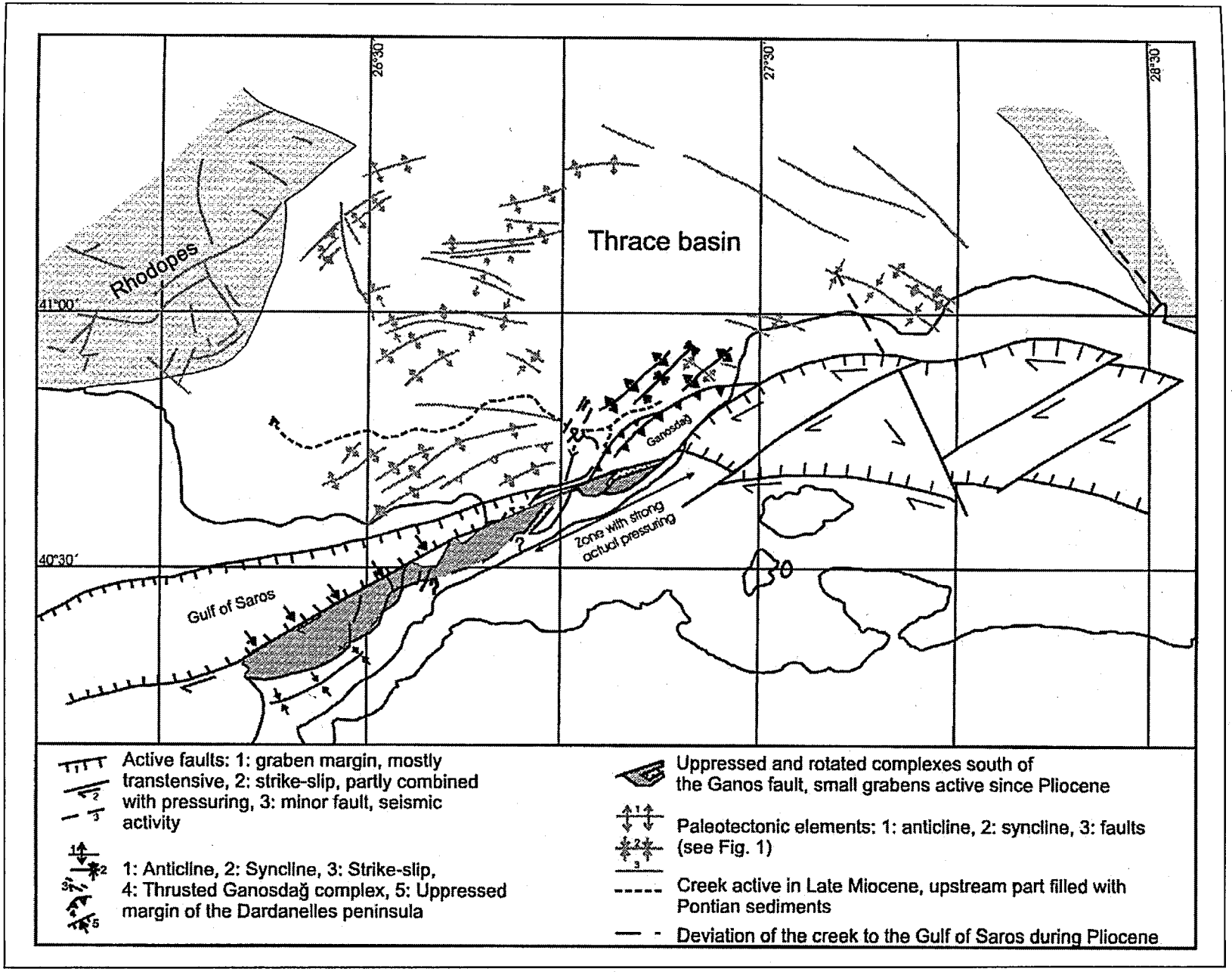

FIGURE 2.6 Neotectonic activity in European Turkey and The Marmara Sea

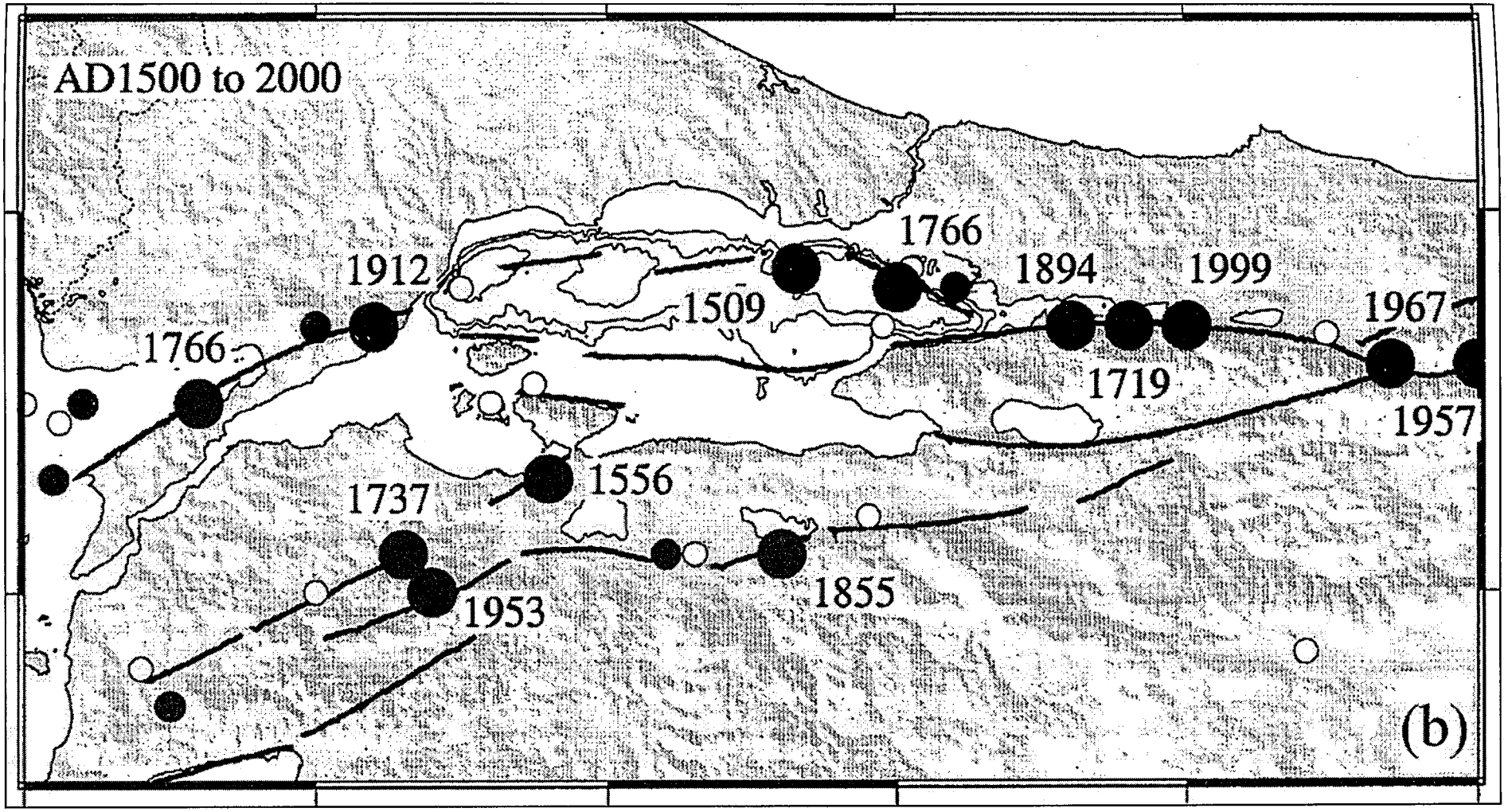

FIGURE 2.7 Large earthquakes since more than 500 years in Marmara region

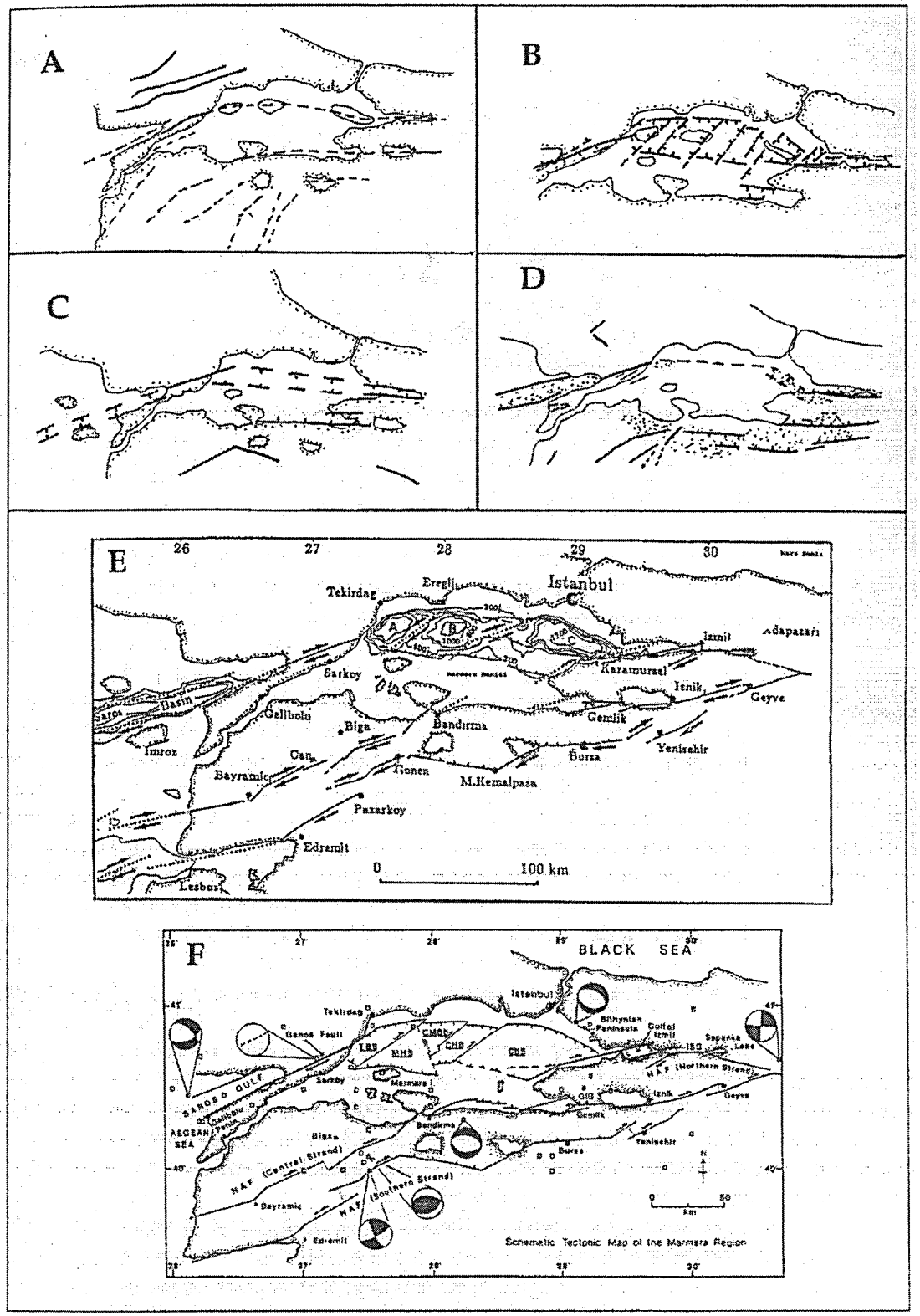

Comparison of the structural models suggested for the Marmara region. (a) Pınar (1943), (b) Pfannenstiel (1944), (c) Crampin and Evans (1986), (d) Şengör (1987), (e) Barka and Kadınsky-Cade (1988), f) Wong et al. (1995), Ergün and Özel (1995).

GURE 2.8 Comparison of the structural models suggested for the Marmara region

westward can give rise to open small basins, such as the Izmit and Karamursel basins, as pull-apart structures . Bargu and Yuksel (1993), Akgun and Ergun (1995), and Koral and Oncel (1995), who studied seismic reflection profiles and onshore geological structures, also concluded that the Izmit bay area consists of a few en echelon strike-slip fault segments and that they form pull-apart basins such as the Izmit and Karamursel basins. Ozhan et al. (1985) and Kavukcu (1990) studied shallow seismic reflection profiles in the bay area and they pointed out that the bay area is not a single graben and that there are two basins separated by basement rocks where the Hersek delta lies over. Thus, it can be suggested that the northern strand of the NAFZ consists of at least three en echelon strike-slip fault segments which form the Izmit bay area (Figure 2.10). These are the Sapanca-Golcuk, Izmit Karamursel and Yarimca-Yalova segments. Between these segments, the Izmit and Karamursel basins open as pull-part basins.

The Izmit basin opens between the Sapanca-Golcuk and Karamursel segments. The E-W trending Sapanca-Golcuk segment extends between Sapanca lake and Izmit bay with en echelon geometry (Figure 2.9) and then it changes direction abruptly to southwestward south of Golcuk. The high elevations in the southern block are related to the compressional component of this segment. These mountains are also the main source of the Hersek delta. The shore-line between the Hersek delta and Golcuk is very straight, indicating a near shore strike-slip fault . This segment is named the Karamusel segment and it initiates near the city of Izmit and extends to the southeastern corner of the Hersek delta (Figure 2.10).

Geyve, Iznik lake and Gemlik areas

(Figure 2.11) shows the extent of the middle strand between Geyve and Gemlik. This strand has been studied in detail by Sipahioglu and Matsuda (1986), Tsukuda et al. (1988), Ikeda et al. (1989, 1991) and Barka (1993). There is abundant evidence of morpho-tectonic features along this section of middle strand. Fault expressions are well developed in Mekece and south of Iznik lake. The Geyve-Pamukova basin has been interpreted as a pull-apart basin (Tsukuda et al. 1988, Kocyigit 1988, Barka 1993). In this basin, the Sakarya river has about 14-21km right-lateral offset (Sipahioglu and Matsuda 1986, Kocyigit 1988). Iznik lake is a pull-apart depression formed between

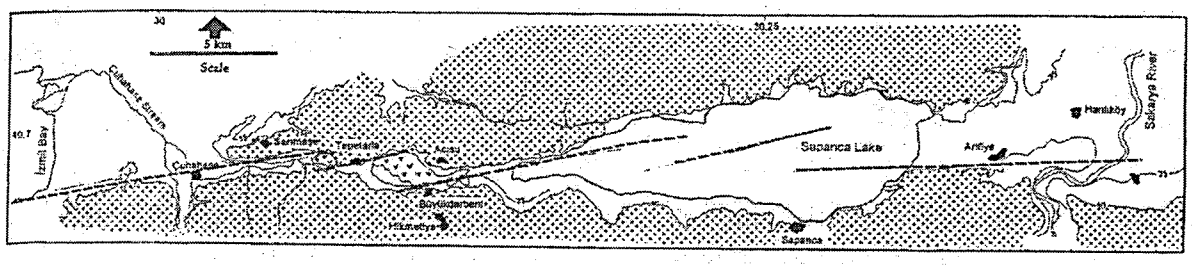

FIGURE 2.9 Geometry and segmentation of the northern strand of the NAFZ between Sapanca lake and İzmit bay

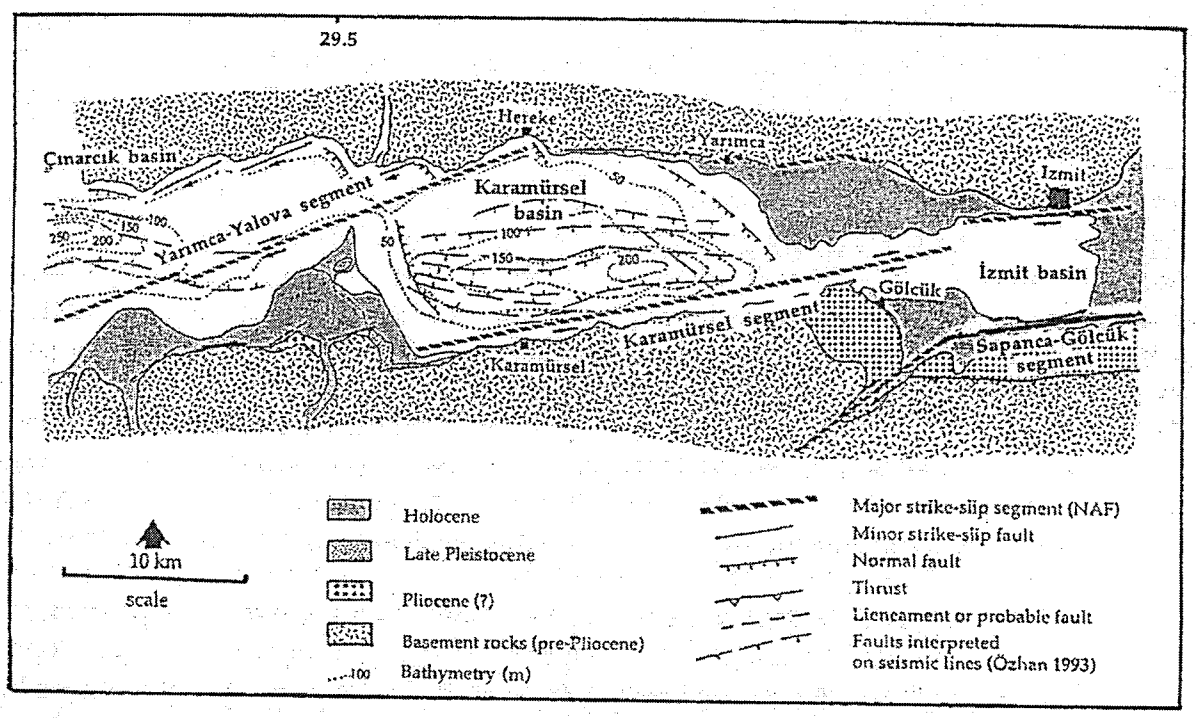

FIGURE 2.10 Neotectonic map of the İzmit bay area

Iznik and Soloz. Between Iznik lake and Gemlik bay this strand splays into two faults; the NE-SW trending one is called Gencali fault (Tsukuda et al. 1988), (Figure 2.12). The Gencali fault extends to Mudanya and forms the southern boundary of the Gemlik basin (Figure 2.13). The Gemlik bay area was studied by Kurtulus (1985), who interpreted the structures from high resolution shallow (effective to 300m) seismic reflection profiles which were obtained by MTA Sismik-1 in 1984. According to the bathymetric map, the maximum depth was about 110m and was located NE of Mudanya. The long axis of the low area trends NW-SE (Figure 2.13). The pattern of active fault segments, both those interpreted from seismic profiles in Gemlik bay and onshore areas and offsets along them, suggests that the Gemlik bay area is a pull-part structure. (Figure 2.13) shows fault geometry between the Gemlik and Bandirma bays which is identical with the northern (Cinarcik basin) and southern strand (Karacabey basin) at the same longitudes.

The Ganos-Saros region

In the northwestern Marmara sea, the northern strand extends from Gazikoy to Saros bay and is approximately 100km long, connecting the Marmara pull-apart basins to the Saros basin (Figure 2.14). The geological studies in the area revealed that the Late Miocene units on the southern block are folded and some thrusting has been identified subparallel to the main trace of the northern strand, both in the Sarkoy area and also on the Gelibolu peninsula (Saner 1985, Onal 1986, Sumengen et al. 1987, Yaltirak 1995). Uplifted shorelines exist all along the Gazikoy to the Gelibolu peninsula (English 1904, Erol 1992, Sakinc and Yaltirak 1995a, b). (Figure 2.15) is a spot image showing the active fault morphology of the central part of the main trace between Saros and Gazikoy, illustrating the linear fault line scrap and right-laterally dragged stream valleys and some linear ridges. The 1912 earthquake occurred along this part and it created right-lateral surface breaks which can be documented from Macovei (1912), Mihalinovic (1927), Ates and Tabban (1976), Ates (1982), Ambraseys and Finkel (1987), Oztin (1987) and Eyidogan et al. (1991), (Figure 2.16). Ambraseys and Finkel (1987) also reported that some parts of the shoreline in the Sarkoy area were uplifted. Although some of the Mihalinovic (1927) photographs show extensional features

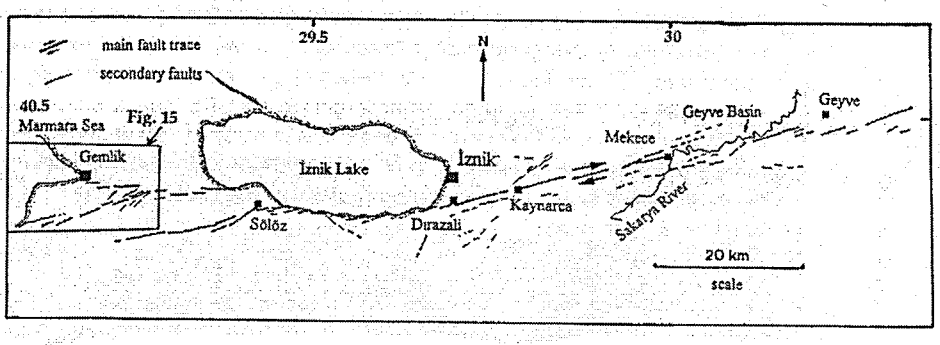

FIGURE 2.11 The extent of the fault traces between Geyve and Gemlik

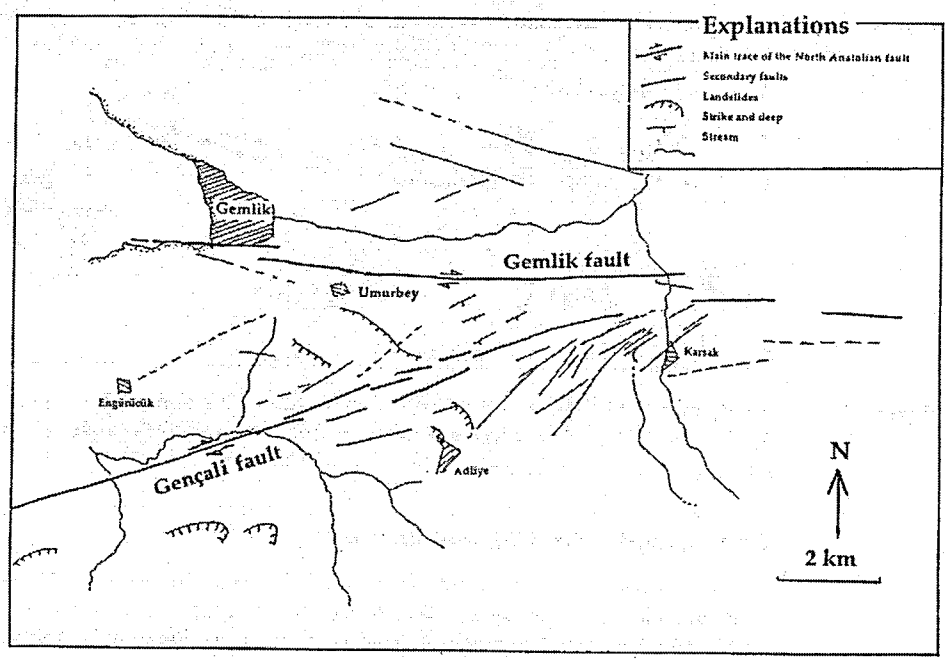

FIGURE 2.12 Fault segments between İznik lake and Gemlik

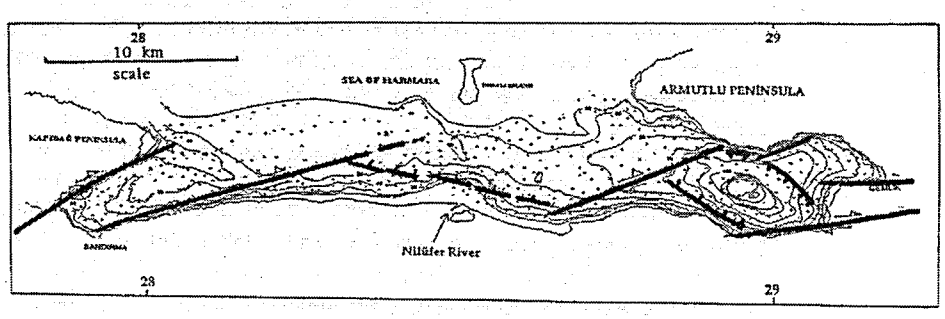

FIGURE 2.13 Distribution of the active fault segments between Gemlik and Bandırma

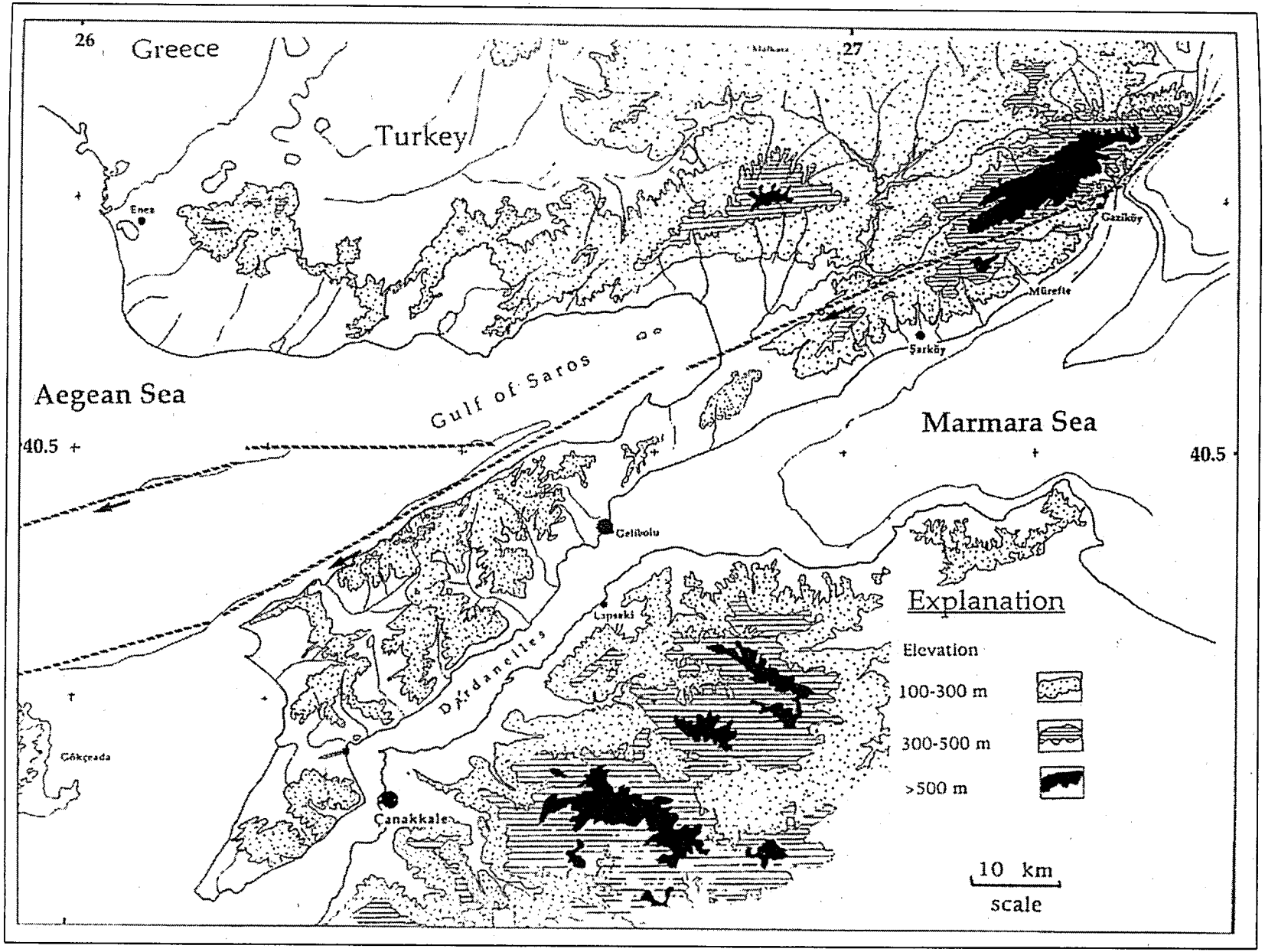

FIGURE 2.14 Morphotectonic map of the Gaziköy-Saros area along the northern strand

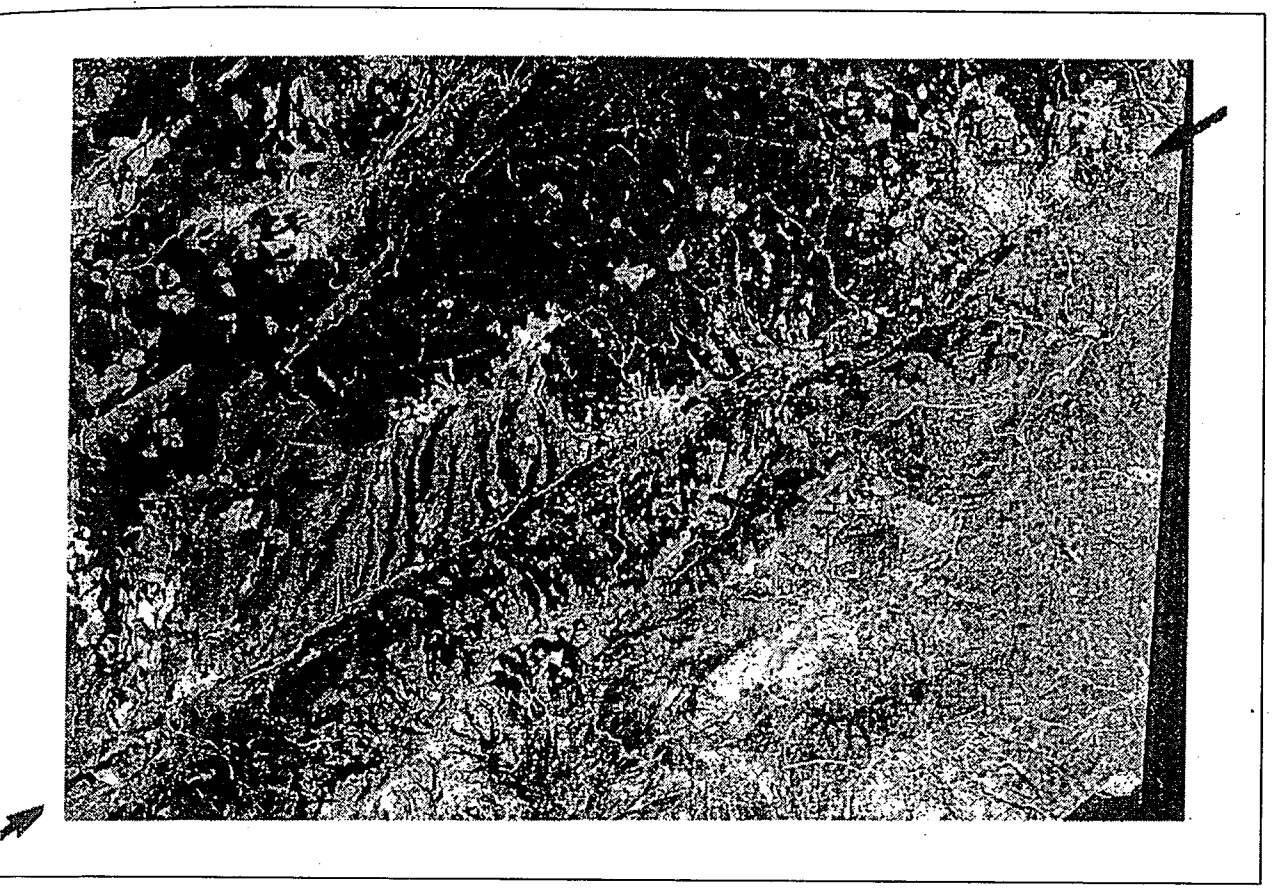

FIGURE 2.15 A spot image of the central part of the Gazikoy-Saros segment

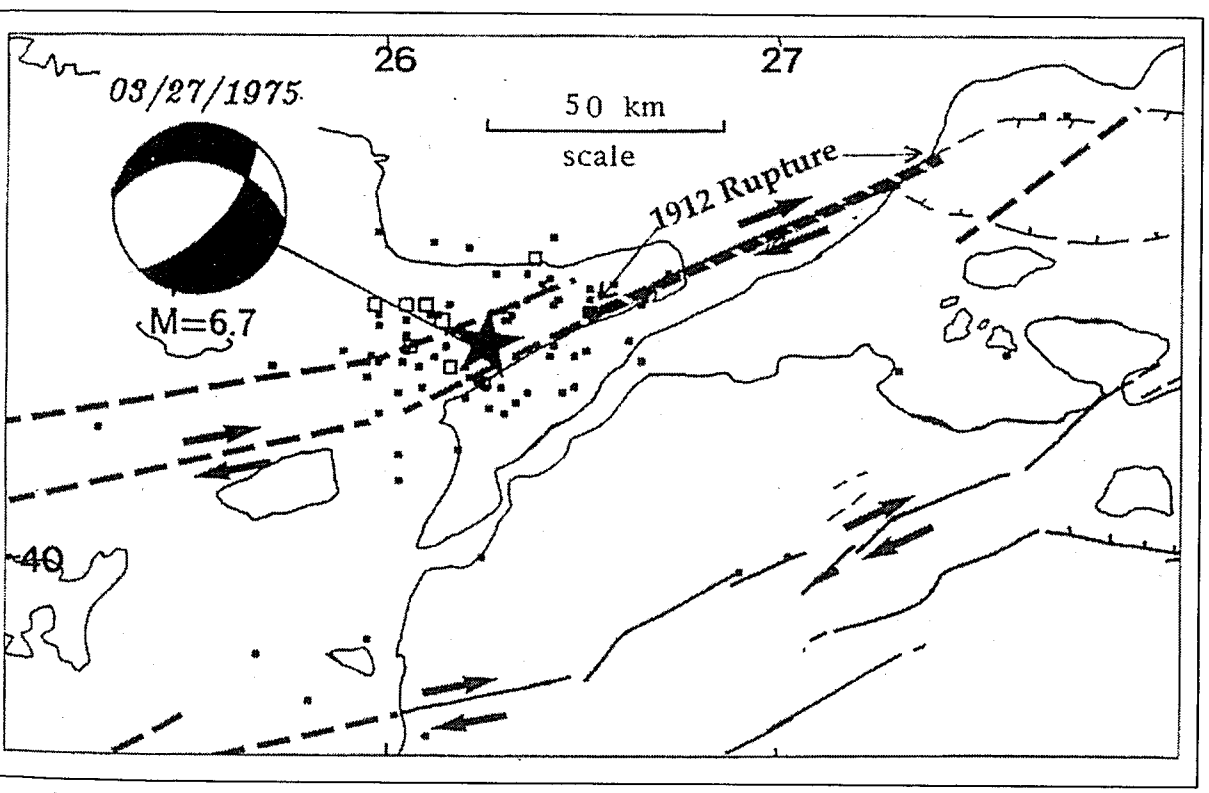

FIGURE 2.16 The Saros earthquake of 27/3/1975

resulting from the 1912 earthquake, these could be related to landslides. Otherwise, active fault morphology and geological structures indicate that this earthquake should have had dominantly right-lateral strike-slip with a thrust component.

GPS data show that most of the motion along the fault, about 10-15mm/y, is taken up by the northern strand (Straub 1996). This is consistent with both paleoseismological data and historical earthquake records. Stein et al. (1997), who modeled failure stress distributions of the migrating earthquakes along the NAFZ between 1939-1967, reported that high failure stress accumulation on both strands of the fault, Sapanca-Izmit and Geyve-Iznik. However, from the above results it appears that the northern strand has more potential than the middle strand.

A study of the Ganos mountain area is particularly important, because this section of the fault could be used as an analogue for Marmara sea ridges occurring along the northern strand in order to understand the structure, active fault morphology and earthquake activity of the strike-slip origins of the NE-SW trending ridges. (Figure 2.14) shows the morpho-tectonic map of the Gazikoy-Saros area indicating the Enez-Ganos and Ganos-Gelibolu highs and the Saros and Marmara sea basins. Simple boundary element modeling (Bilham and King 1989) was carried out to test the kinematics of the faults. The results of the modeling illustrated that the segments extending from Ucmakdere to Gelibolu should have a thrust component of at least 50% This modeling agrees with a kinematic model produced from GPS measurements (Straub 1996). This model also is consistent with the seismicity pattern of the region, for example, the extensional areas (pull-parts) show continuous seismic activity, while the strike-slip segments with thrust components have infrequent large earthquakes as reported by Ambraseys and Finkel (1991). This thrust component is also supported by a few moderate thrust earthquake

The Biga peninsula

Barka and Kadinsky-Cade (1988), Siyako et al. (1989), Herece (1990), Barka(1992) and Saroglu et al. (1987) described active faults in the Biga peninsula

(Figure 2.17). In this area, there are several NE-SW trending strike-slip faults parallel to each other, also showing en echelon geometry giving rise to a few pull-apart basins, such as the Asagiinova, Bayramic, Ezine and Yenice basins. Between basins, the area is morphological elevated. In the Biga peninsula, the southern strand continues to Aegean via Gonen, Yenice and Edremit bay, while the middle strand goes through Sarikoy, Can, Bayramic and Ezine. The area between Ezine and Aegean sea has not been studied for active faults and recent studies did not show the continuity of the fault. Whether the fault does not continue further southwest, or whether these studies failed to recognize the fault is not clear. However, the 1968, M=7.2, earthquake in the Aegean may indicate that this strand continues toward the Aegean sea. As far as historical earthquakes are concerned, the 155, 543 and 1737 earthquakes and a few other moderate to large events can be associated with this strand (Figure 2.18). Nevertheless, during the present century, this strand has been seismically quiet. The 1953 Yenice-Gonen earthquake, M=7.4, along the southern strand formed the NE-SW trending strike-slip rupture zone with 3.5m maximum right-lateral motion (Ketin and Roesli 1953). The 1969 Gonen earthquake, M=5.7, had a dominant thrust component, indicating that the Biga peninsula has been uplifted by a thrust component (Figure 2.17), (e.g. Taymaz et al. 1991). The 1983 Biga earthquake, M=6.1, has a controversial solution, between thrust and normal faulting: the ISC solution reveals dominant normal faulting while solution obtained by Alsan et al. (1984) and Kiyak (1986) suggest dominantly thrust, very similar to the solution of the 1996 earthquake which occurred in Ganos region. The direction of thrust being similar the strike-slip faults suggest also that there is a slip partitioning (e.g. Molnar 1992) along these segments including the Gazikoy-Saros segment where oblique faulting is taken up by two different faults: strike-slip and thrusts which are parallel to each other.

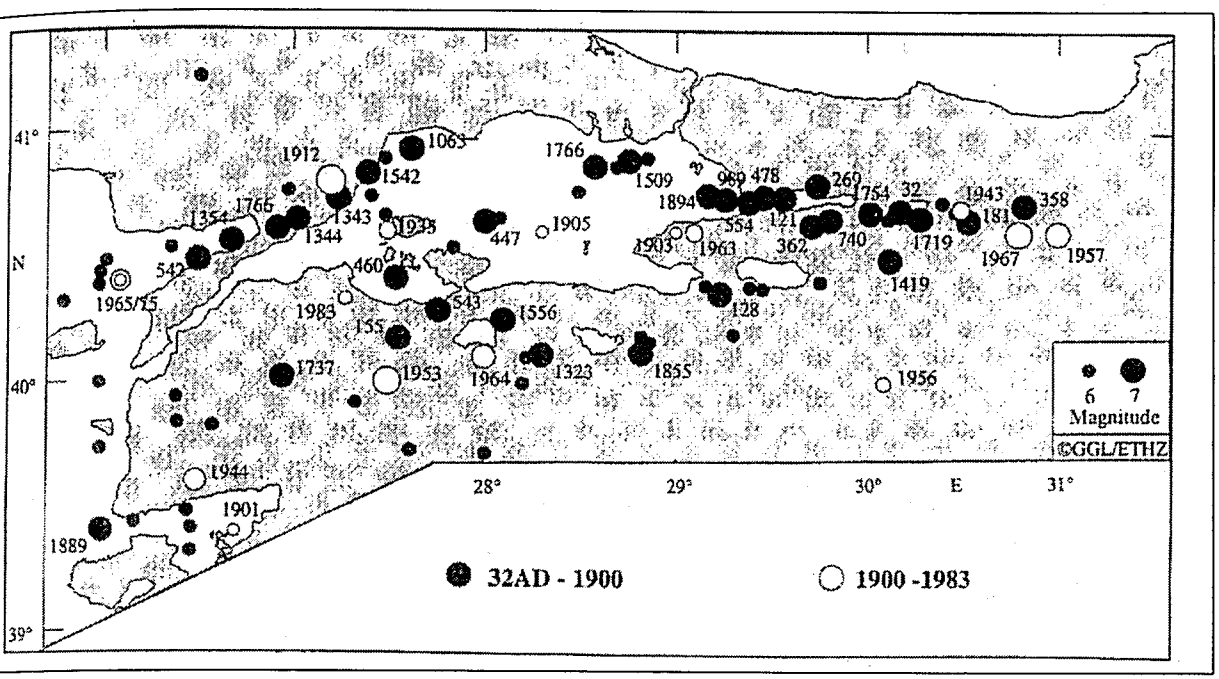

FIGURE 2.18 Historical earthquakes in the Marmara sea region

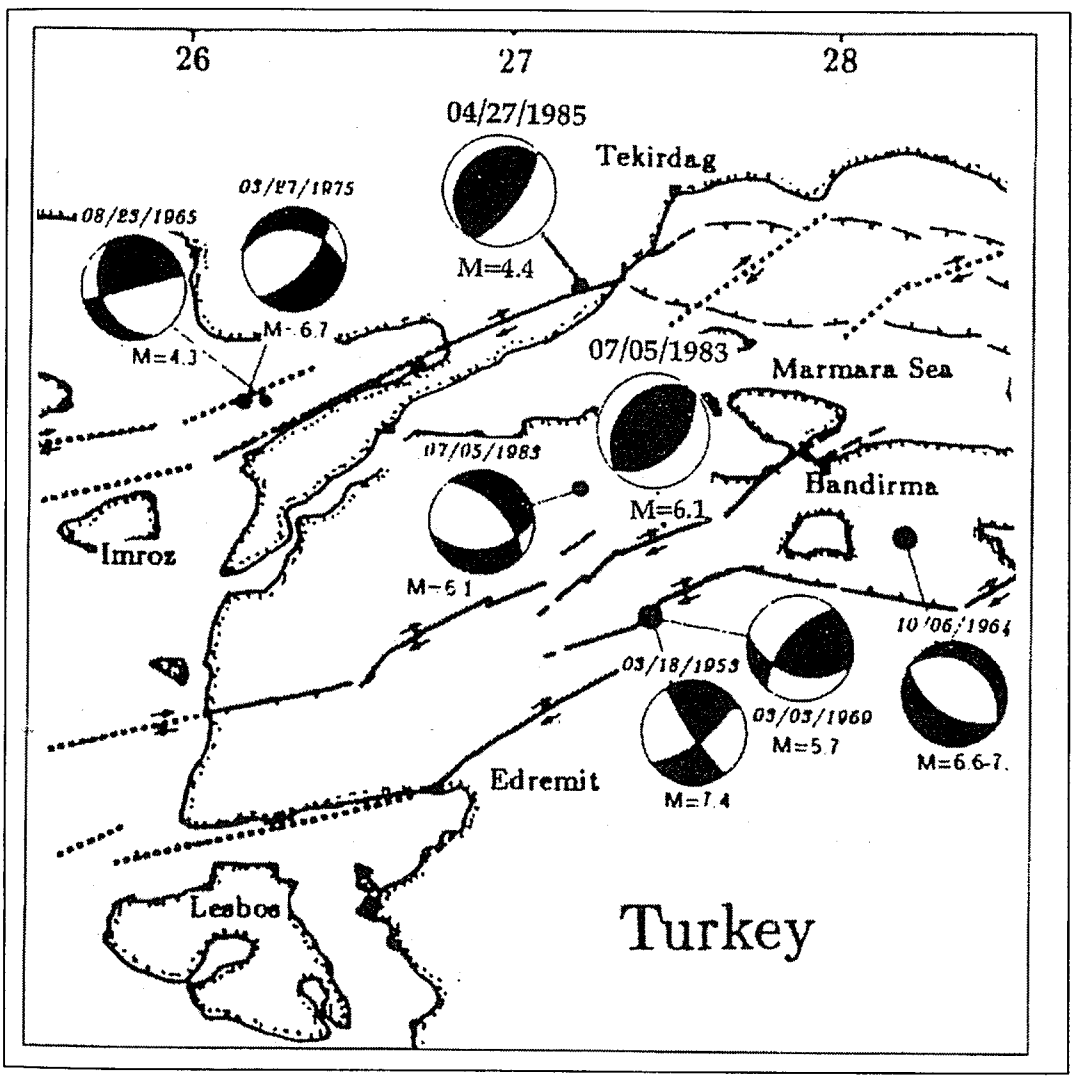

IGURE 2.17 Fault plane solutions of the significant earthquakes in the western Marmara region

3. SEISMICITY OF MARMARA REGION

General Treatment

Ambraseys and Finkel (1991) have shown that in the Marmara Region during the period of 1AD to 1899 there have been 38 earthquakes with magnitude 7 or greater and a further 23 events of Ms>=5.9 since 1900 (5 of which were large magnitude Ms>=7 events in 1912, 1953, 1957, 1967 and 1970). This is equivalent to one large earthquake every 45 years, but it has been noted that the occurrence of large earthquakes in the area tends to be clustered and then followed by long periods of relatively quieter periods. In the early years two such active periods have been identified namely, the 2nd century and the period between 355 and 557 AD for which 4 and 9 large earthquakes are documented respectively. Especially in the three years between 555 and 557 AD there have been 3 large earthquakes. In the following 800 years until 1357 AD there have been only 4 such events, in 740, 989, 1063, and 1344. Starting from 1344 another period of clustered activity has been documented that lasted until 1509 AD, during which 6 large earthquakes are known to have occurred culminating with the great earthquake of 1509 that destroyed much of Istanbul. In Istanbul, earthquake records spanning two millennia indicate that, on average, at least one medium intensity (Io=VII-VIII) earthquake has affected the city every 50 years. The average return period for high intensity (Io=VIII-IX) events has been 300 years. However, the temporal distribution of the earthquakes has not been uniform. (Figure 3.1)

In the Marmara region, there are some potential seismic gaps. For example, along the middle strand from the Mudurnu Valley region to the Aegean Sea there has not been any significant earthquake for the last 400 years, except the 1737 earthquake, in the Biga peninsula (Ambraseys & Finkel, 1991). The most western portion of the southern strand has not ruptured since 1855, except two small segments, the Pazarköy-Edremit and Yenişehir segments. It is difficult to delineate a particular earthquake to a particular fault segment. Nevertheless, recent seismicity maps indicate a potential seismic gap in the central part of the Marmara Sea. There are two potential historical earthquakes that

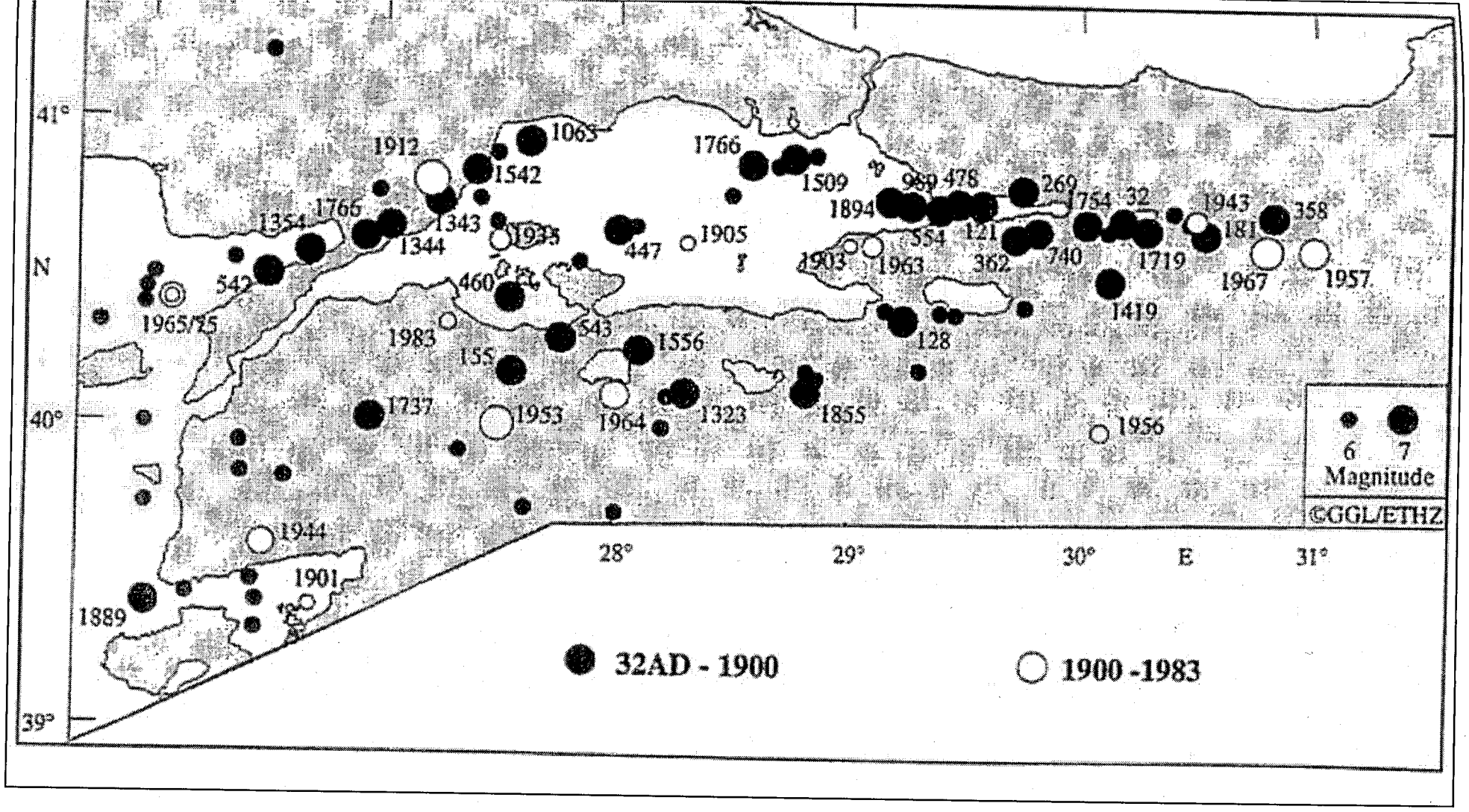

FIGURE 3.1 Historical Earthquakes in the Marmara Sea region, originally from Ambraseys and Finkel (1991)

might have occurred in this gap, one in 1766 and another in 1509. If one considers the slip rate as being approximately 0.5 cm/yr, this area might be safe except for the 1766 earthquake (400 years recurrence interval, 2 m. slip). But if we take the 1509 earthquake with the same slip rate, we see that 2.4 of slip have been accumulated along this segment. In short, in the Marmara region by looking at recent seismicity pattern, one can suspect that there might be some seismic gaps in this area(Figure 3.2)
(Figure 3.3) shows the epicentral distribution of the significant earthquakes occurred in Marmara Region after 1500. It can be seen from the figure there is significant earthquake activity after the 19^h century around Izmit Bay. There are three major historical earthquakes occurred in this region in 1719, 1754 and 1894. 1963 Çınarcık – Yalova (M=6.3) earthquake is the last major event before 1999 Kocaeli Earthquake.

The epicentral location of the earthquakes that has taken place in the Marmara Region after 1900 is provided in (Figure 3.4). It is observed from the earthquake occurrence data that there was almost no activity until 1999 earthquake at Yarimca-Yalova and Karamürsel Basins. Microseismic earthquakes recorded from 1976-1999 shows higher activity in the Izmit and Armutlu peninsula. On the other hand, aftershocks of recent 1999 earthquakes are mostly concentrated around the Armutlu Peninsula.

Parsons et al. (2000) have carried out an assessment of tectonic stresses in the Marmara Sea Region using the concept of earthquake interaction, where the fault rupture and the associated stress release results in the increase in stress and triggering of rupture on adjacent faults. They state that the Kocaeli earthquake have increased the stress at the termini of the ruptured area. It is further hypothesized that this stress increase triggered the 12.11.1999 Duzce earthquake and also increased the aftershock activity on the Yalova Segment. On the basis of damage distribution of past earthquakes they infer three earthquakes on the Yalova Segment (1509, 1719 and 1894) yielding an inter-event period assessment of about 190 years. Using fault rupture recurrence statistics and the earthquake interaction assessments Parsons et al., (2000) estimate the median probabilities of rupture for the Yalova Segment as: 1.7%, 14% and 33% respectively for the next 1, 10 and 30 years. Thus the current enhanced average return

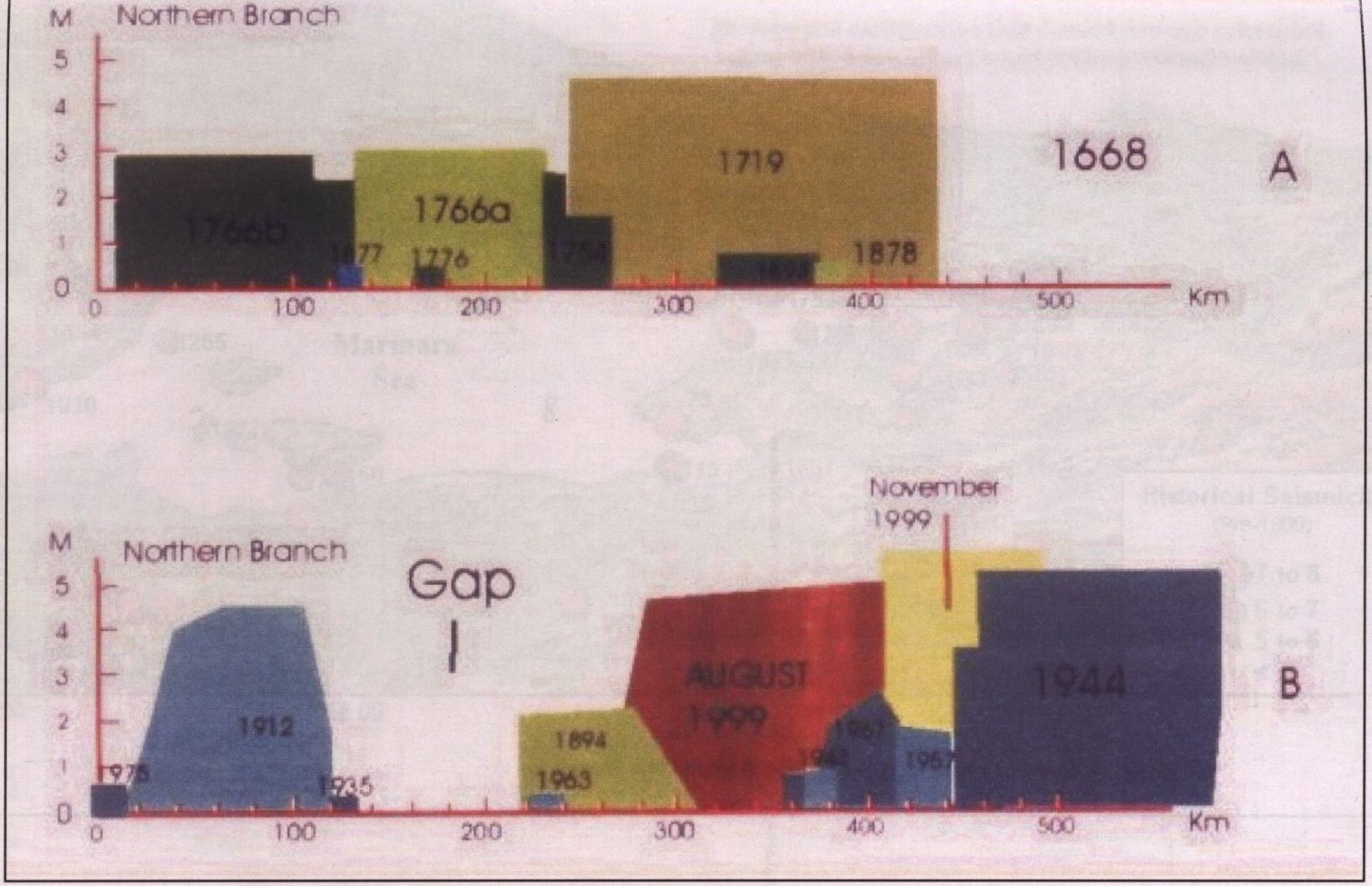

FIGURE 3.2 Earthquake activity along the northern starnd of the North Anatolian fault since 1700 AD.

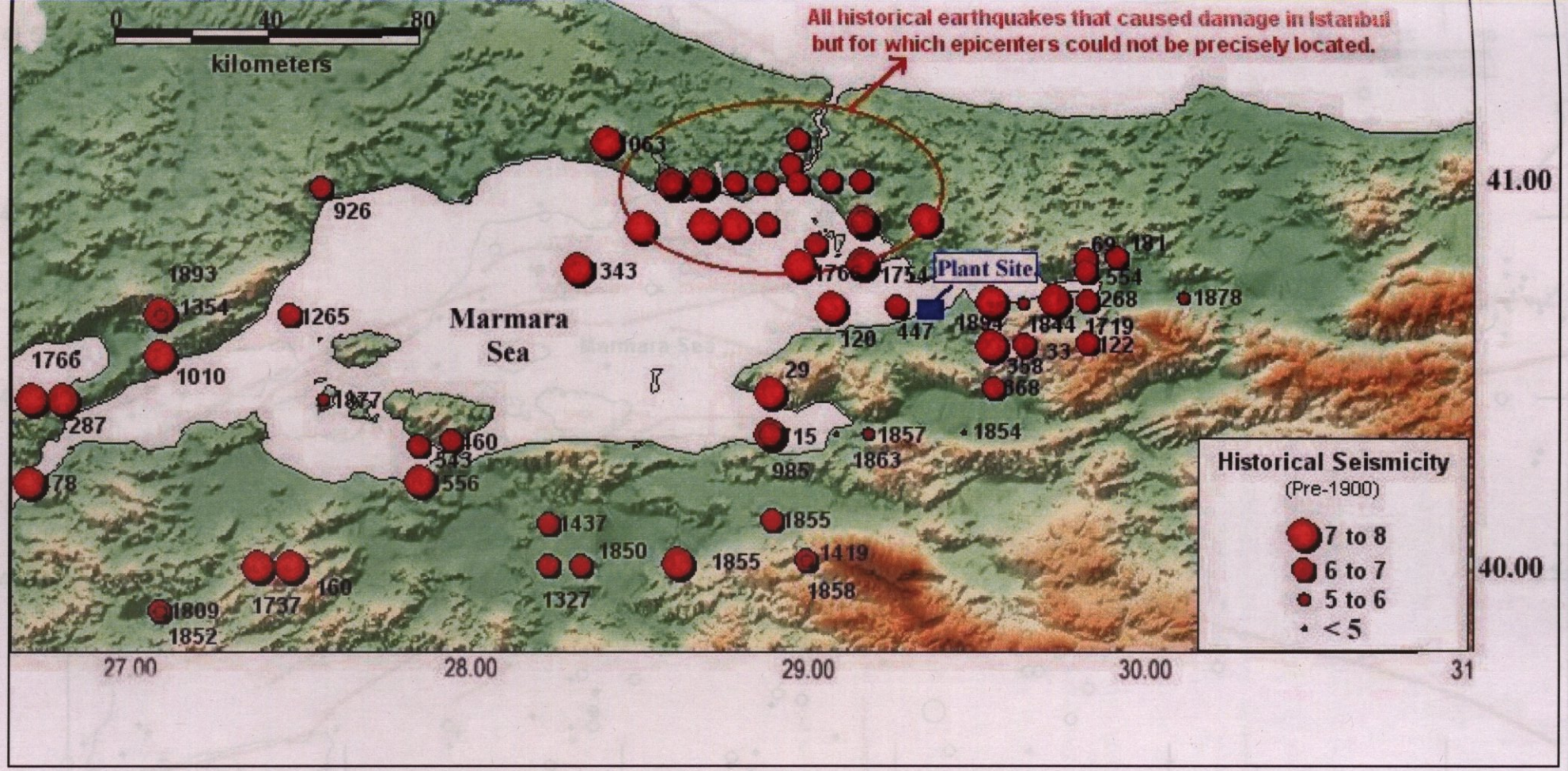

FIGURE 3.3 Historical seismicity of Marmara region.

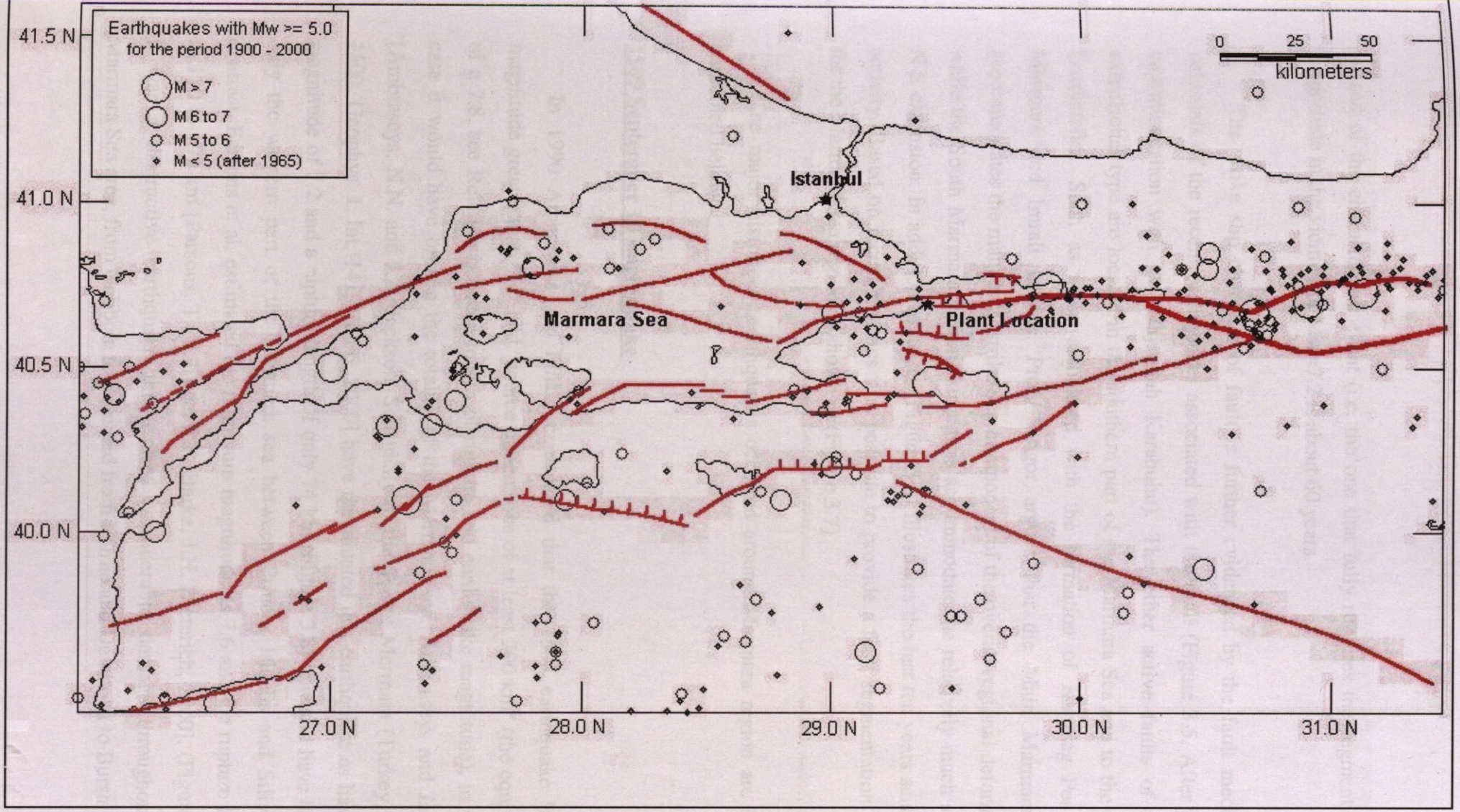

FIGURE 3.4 Seismictiy of the Marmara region between 1900-2000.

period of the characteristic event (i.e. the one that fully ruptures the segment with a magnitude in the vicinity of Mw=7.2 is about 60 years.

The strike slip character of fault is further evidenced by the fault mechanism solutions of the recent earthquakes associated with the fault (Figure 3.5, After private communication with Dr. Hayrullah Karabulut). The other active faults of mostly extensional type are located in the southern part of the Marmara Sea and to the east of Dardanelles. Such as those associated with the formation of Kapidag Peninsula, Marmara and Imrali Islands. Prof. Sengor argues that the Main Marmara fault accommodates the main E-W strike-slip component of the overall regional deformation, while the South Marmara tectonic structures accommodate the relatively much smaller N-S extension. In addition to these, (Figure 3.6) illustrates the last ten years seismicity activity. Based on recent findings it is possible to provide a fault segmentation model for the Marmara Sea region as shown as (Figure 3.7)

The major historical earthquakes occurred around Marmara region are briefly explained below:

1509 September 10 Earthquake

In 1990 Ambraseys and Finkel considered that the 1509 earthquake "had a magnitude greater than 7.4" and "source dimensions of at least 200 km" (the equivalent of a 7.8, see Relation between length of rupture and earthquake magnitude), in which case it would have broken the totality of the Marmara sea. Ambraseys and Jackson [Ambraseys, N.N. and J.A. Jackson, Seismicity of the Sea of Marmara (Turkey) since 1500, Geophys. J. Int. 141, F1-F6, 2000] have reevaluated this earthquake as having a magnitude of 7.2 and a rupture length of only 74 km (Figure 3.8) It would have broken only the western part of the Marmara sea between Princes Islands and Silivri. In contrast, Parsons et al. estimated the minimum magnitude as 7.6 and the rupture length as 110 to 190 km [Parsons, T., S. Toda, R.S. Barka, J.H. Dieterich, 2000]. (Figure 3.9) It was a destructive earthquake that caused considerable damage throughout the Marmara Sea area, from Gelibolu to Bolu and from Edirne and Demitoka to Bursa.

period of the characteristic event (i.e. the one that fully ruptures the segment with a magnitude in the vicinity of Mw=7.2 is about 60 years.

The strike slip character of fault is further evidenced by the fault mechanism solutions of the recent earthquakes associated with the fault (Figure 3.5, After private communication with Dr. Hayrullah Karabulut). The other active faults of mostly extensional type are located in the southern part of the Marmara Sea and to the east of Dardanelles. Such as those associated with the formation of Kapidag Peninsula, Marmara and Imrali Islands. Prof. Sengor argues that the Main Marmara fault accommodates the main E-W strike-slip component of the overall regional deformation, while the South Marmara tectonic structures accommodate the relatively much smaller N-S extension. In addition to these, (Figure 3.6) illustrates the last ten years seismicity activity. Based on recent findings it is possible to provide a fault segmentation model for the Marmara Sea region as shown as (Figure 3.7)

The major historical earthquakes occurred around Marmara region are briefly explained below:

1509 September 10 Earthquake

In 1990 Ambraseys and Finkel considered that the 1509 earthquake "had a magnitude greater than 7.4" and "source dimensions of at least 200 km" (the equivalent of a 7.8, see Relation between length of rupture and earthquake magnitude), in which case it would have broken the totality of the Marmara sea. Ambraseys and Jackson [Ambraseys, N.N. and J.A. Jackson, Seismicity of the Sea of Marmara (Turkey) since 1500, Geophys. J. Int. 141, F1-F6, 2000] have reevaluated this earthquake as having a magnitude of 7.2 and a rupture length of only 74 km (Figure 3.8) It would have broken only the western part of the Marmara sea between Princes Islands and Silivri. In contrast, Parsons et al. estimated the minimum magnitude as 7.6 and the rupture length as 110 to 190 km [Parsons, T., S. Toda, R.S. Barka, J.H. Dieterich, 2000]. (Figure 3.9) It was a destructive earthquake that caused considerable damage throughout the Marmara Sea area, from Gelibolu to Bolu and from Edirne and Demitoka to Bursa.

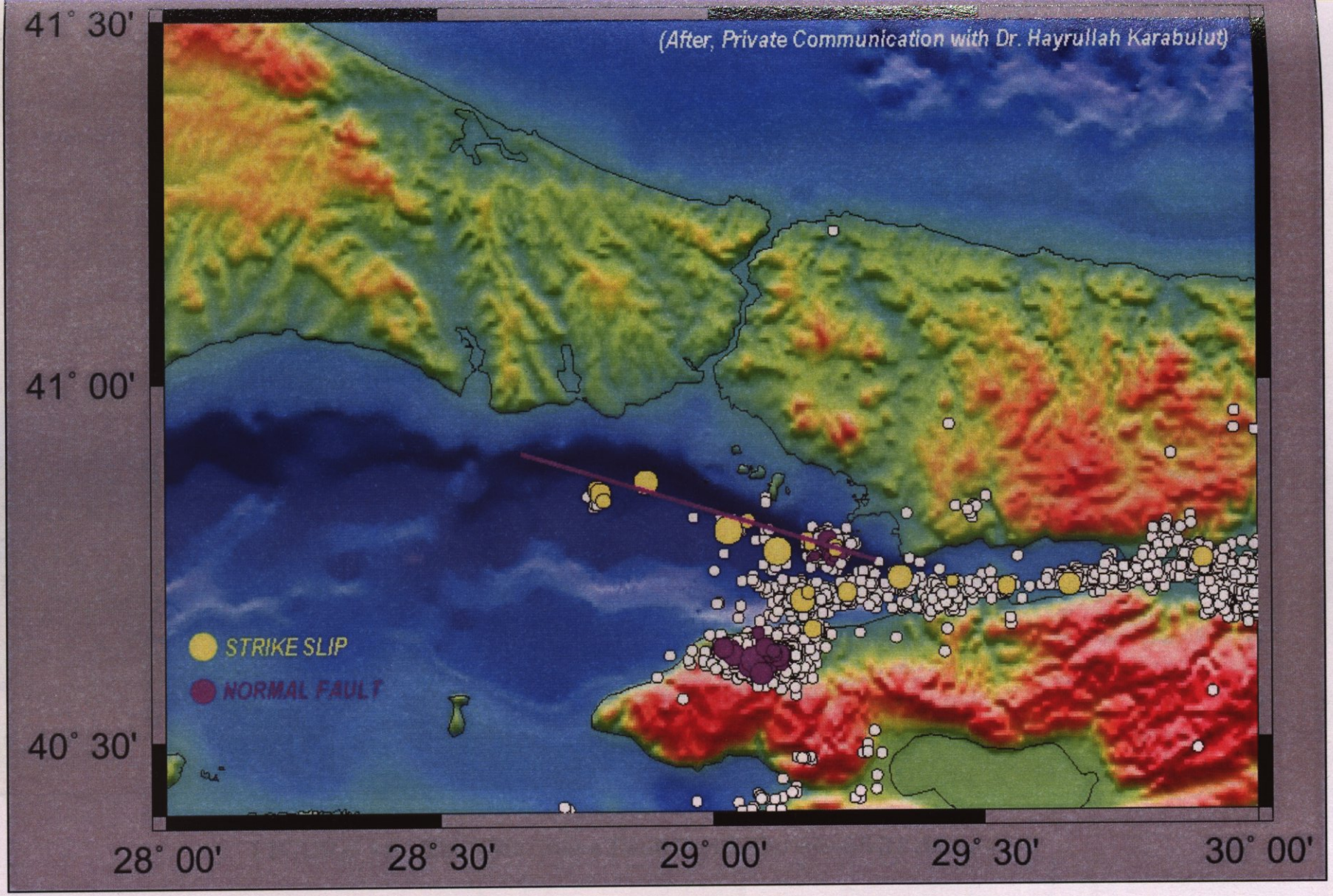

FIGURE 3.5 The Marmara Fault with the seismicity data

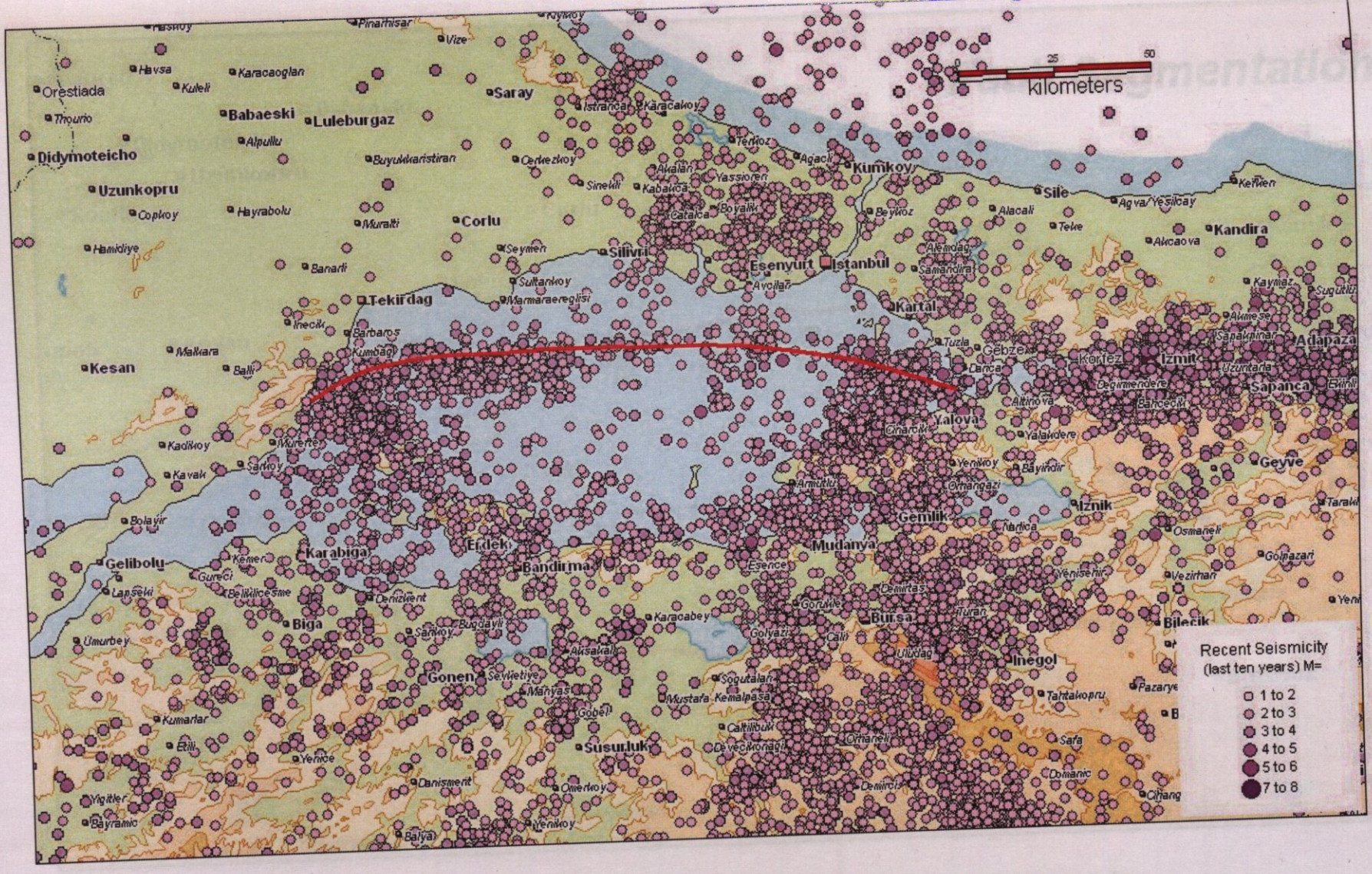

FIGURE 3.6 The "Marmara Fault" with the seismicity data.

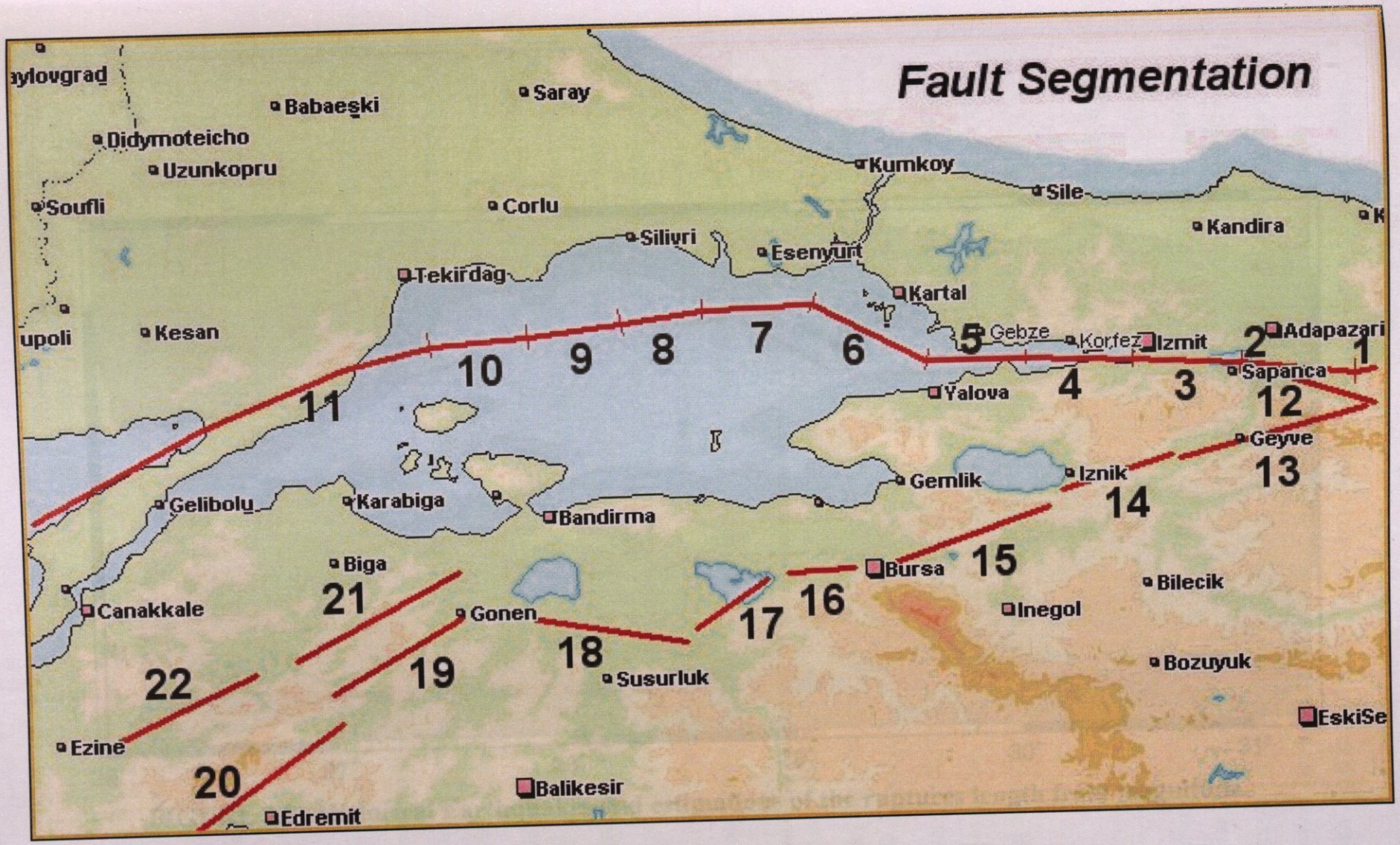

FIGURE 3.7 Fault segmentation model for the Marmara region

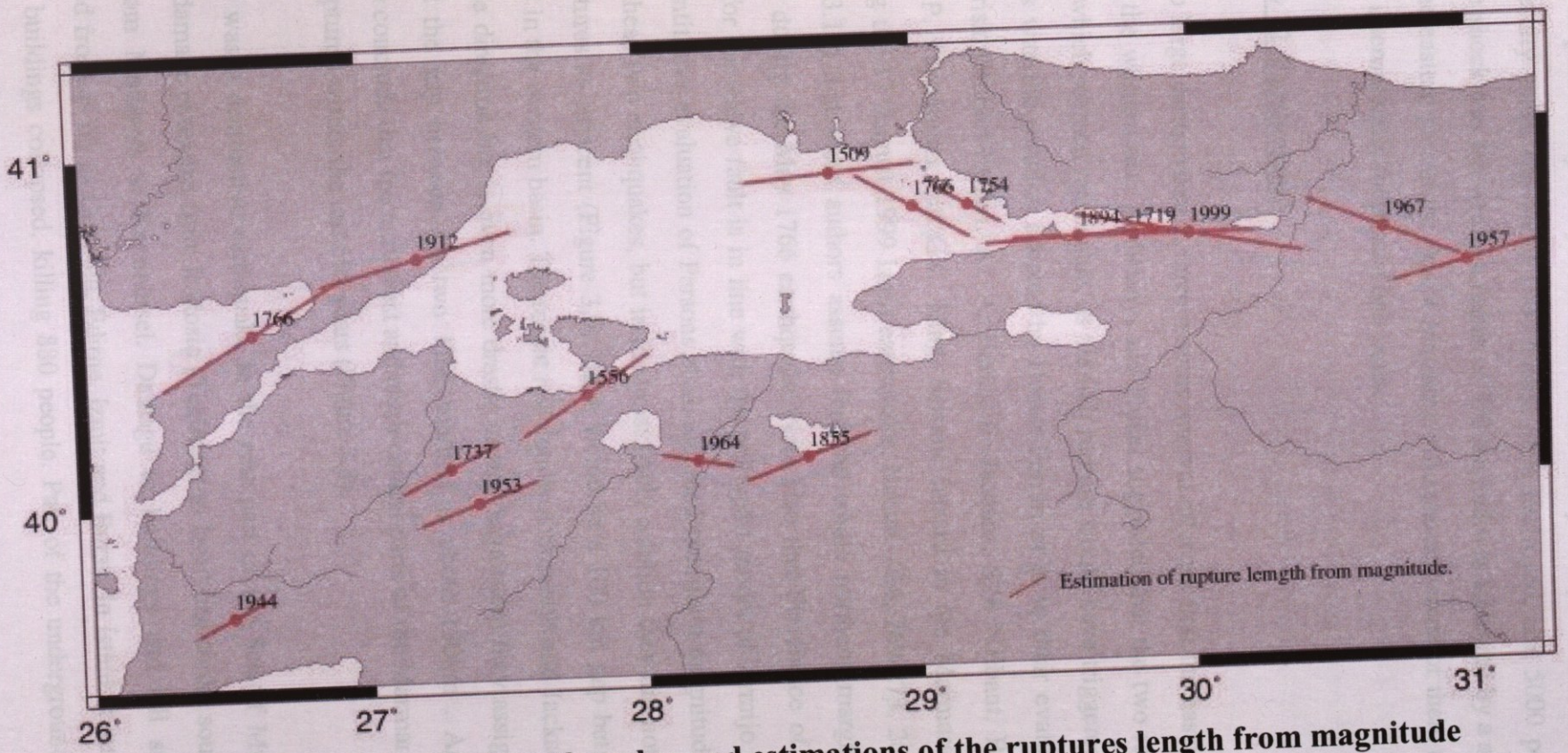

FIGURE 3.8 Historical Earthquakes and estimations of the ruptures length from magnitude

Damage was particularly heavy in Istanbul where many mosques and other buildings, part of the city walls, and about 1000 houses were destroyed, and 5000 people were killed. The shock was felt within a radius of 750 km and was followed by a seismic sea-wave in the eastern part of the Sea of Marmara. Aftershocks, some of them destructive, continued intermittently for almost two years.

1766 May 12 Earthquake

Two large earthquakes at three months interval affected first the eastern Marmara sea, then the western one. Ambraseys and Finkel suggested that the two ruptures were adjacent which seemed reasonable, as the first rupture would have triggered the second one. This was the solution adopted by Hubert-Ferrari et al in their evaluation of the seismic risk [Hubert-Ferrari, A., A. Barka, E. Jacques, S.S. Nalbant, B. Meyer, R. Armijo, P. Tapponnier and G.C. King, Seismic hazard in the Marmara Sea region following the 17 August 1999 Izmit earthquake, Nature, 404, 269-273, 2000]. Note in (Figure 3.10) that these authors assume that the whole northern margin of the sea ruptured during the May 1766 earthquake. Note also that the choice of the northern margin for the active fault is in line with the pull apart model of Armijo et al. (1999). The quantitative evaluation of Parsons et al. assumed minimum magnitudes of 7.2 and 7.6 for these two earthquakes, but in the most likely solution they did not consider the two ruptures as adjacent (Figure 3.9) There would be a 100 km gap between the two ruptures in the western basin. The recent revision by Ambraseys and Jackson goes along the same direction but is even more drastic as the magnitudes they assign are 7.1 and 7.4 and the gap between the two 1766 ruptures is about 130km . Ambraseys and Jackson conclude that the northwest and north-central parts of the Marmara sea have not been ruptured within the last 500 years (Figure 3.8).

It was a destructive earthquake in the east part of the Sea of Marmara caused heavy damage extended from Rodosto (Tekirdağ) to Izmit and to the south coast of the Sea from Mudanya to Karamürsel. Damage to buildings and tall structures were reported from as far as Gelibolu, Edirne, Izmit and Bursa. In Istanbul many houses and public buildings collapsed, killing 880 people. Part of the underground water supply

system was destroyed. The Ayvad dam on the upper Kağithane, north of Istanbul, was damaged, and in the vicinity of Sultanahmet, the roof of an underground cistern caved in. The earthquake was associated with a seismic sea-wave which was particularly strong along the Bosphorus. Damage extended inland, mainly to the north and west, as far as Edirne and to Gelibolu. In Çatalca and surrounding villages all masonry houses were totally destroyed. It is said that about 4000 people lost their lives. The shock was felt strongly along the west coast of Black Sea. Damaging aftershocks continued for weeks, the sequence lasting for over a year.

1894 July 10 Earthquake

A destructive earthquake in the Gulf of Izmit and further to the east caused extensive damage in the area between Silivri, Istanbul, Adapazarı and Katırlı. Maximum effects were reported from the region between Heybeliada, Yalova and Sapanca where most villages were totally destroyed with great loss of life. The shock caused the Sakarya river to flood its banks and the development of mud volcanoes. In Adapazarı 83 people were killed and another 990 in the Sapanca area. In Istanbul damage was widespread and in places very serious. Many public buildings, mosques, and houses were shattered and left on the verge of collapse, while most of the older constructions fell down, killing 276 and injuring 321 people. Three of the dams for the water supply of Istanbul were badly damaged. The shock was associated with a sesimic sea-wave, which at St. Stephanos (Yeşilköy) had a height of 1.5 m., and caused the failure of submarine cables. Liquefaction of the ground and landslides were reported from the epicenter region, particularly from the area between Sapanca and Adapazarı. The shock was felt as far as Bucharest, Sofia, Yannina, Crete and Konya, and it was not followed by a significant aftershock sequence.

To conclude, the estimations on the magnitudes and lengths of the different ruptures have varied widely. Until the recent revision of Ambraseys and Jackson, the magnitude estimates for the 1509 earthquake were about 7.6 or more. It was assumed further that the 18th century earthquake sequence broke the whole Marmara sea (Figure

3.10). This implied long ruptures along a continuous fault joining the Izmit gulf to the east to the Ganos fault to the west.

Earthquakes in the Marmara region have been relatively few in the 20th century. Detailed descriptions of the major events are given below. Fault segment numbers, that are based on the new segmentation presented in Figure 3.7, and are associated with earthquakes that took place in the region in the 20th century are provided in parenthesis following the description of each earthquake.

1909 October 9 Karamürsel Earthquake, Ms = 5.8, Io = VII

The earthquake caused considerable damage in Koğlacık region located between İzmit Bay and İznik Lake. Two more shocks with approximately the same magnitude followed the first event. Several houses and churches have been damaged by the events. The shocks were also felt in Çatalca, Terkos, İstanbul, Göynük, Bolu and Bursa (Ambraseys and Finkel, 1987b).

1912 August 9 Murefte-Sarkoy Earthquake, 40.50N - 27.00E, Ms = 7.4, Io=X

This earthquake destroyed more than 300 villages and towns mainly to the north of the Dardanelles, killing over 2000 people. The shock was associated with a 50 km long fault-break and with the liquefaction of the ground up to epicentral distances of 180 km. Damage extended over a relatively large area and long-period ground motions were responsible for serious damage to public buildings as far as Edirne and Istanbul. The shock was accompanied by a small seismic sea-wave and it was felt within a radius of about 450 km. The intensity distribution of the earthquake as given by Ambraseys and Finkel (1987a) is given in (Figure 3.11). This earthquake can be associated with fault segment 11 (Figure 3.12) (Ambraseys (2000), Hubert-Ferrari et al. (2000)).

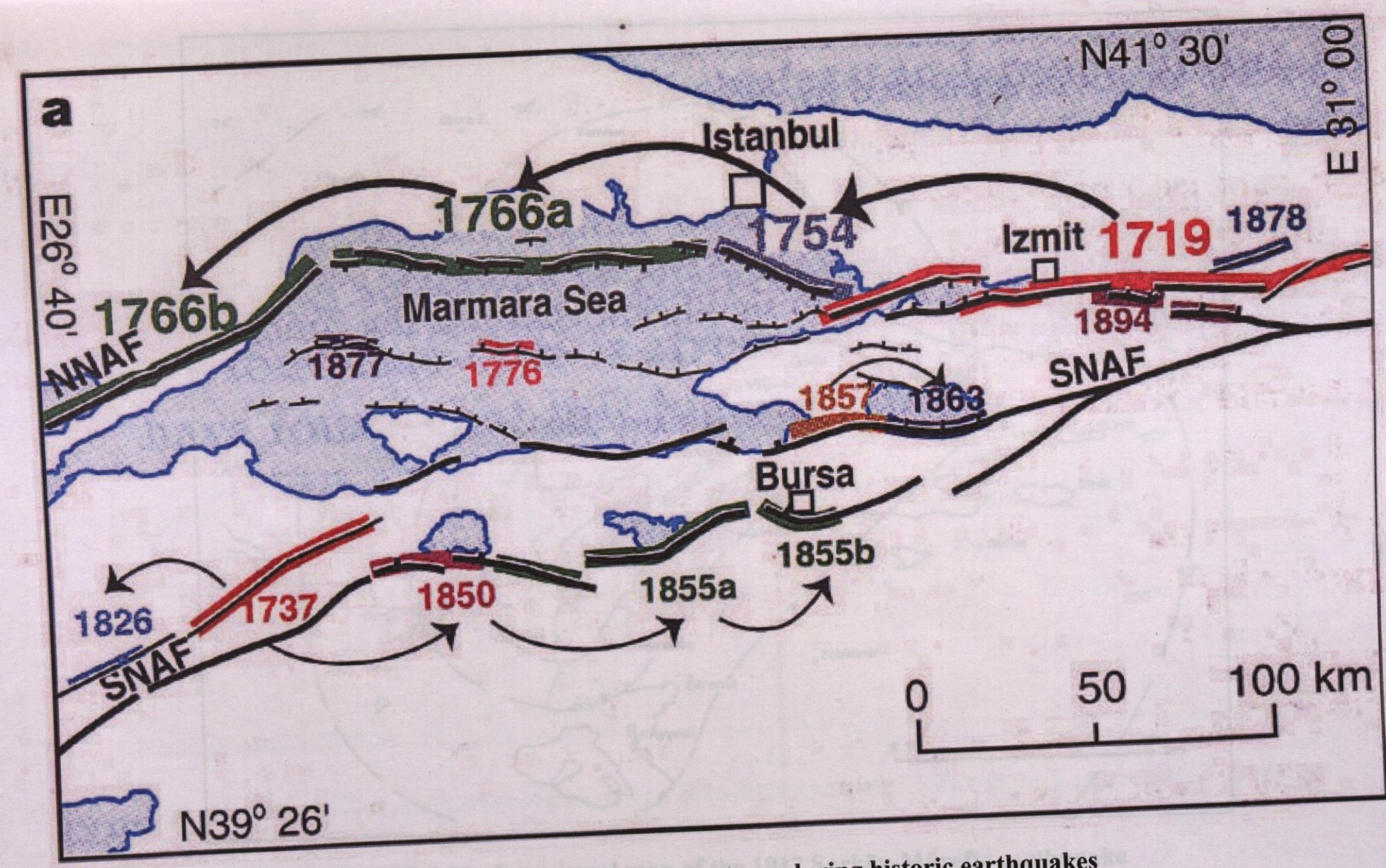

FIGURE 3.10 Locations of fault ruptures during historic earthquakes

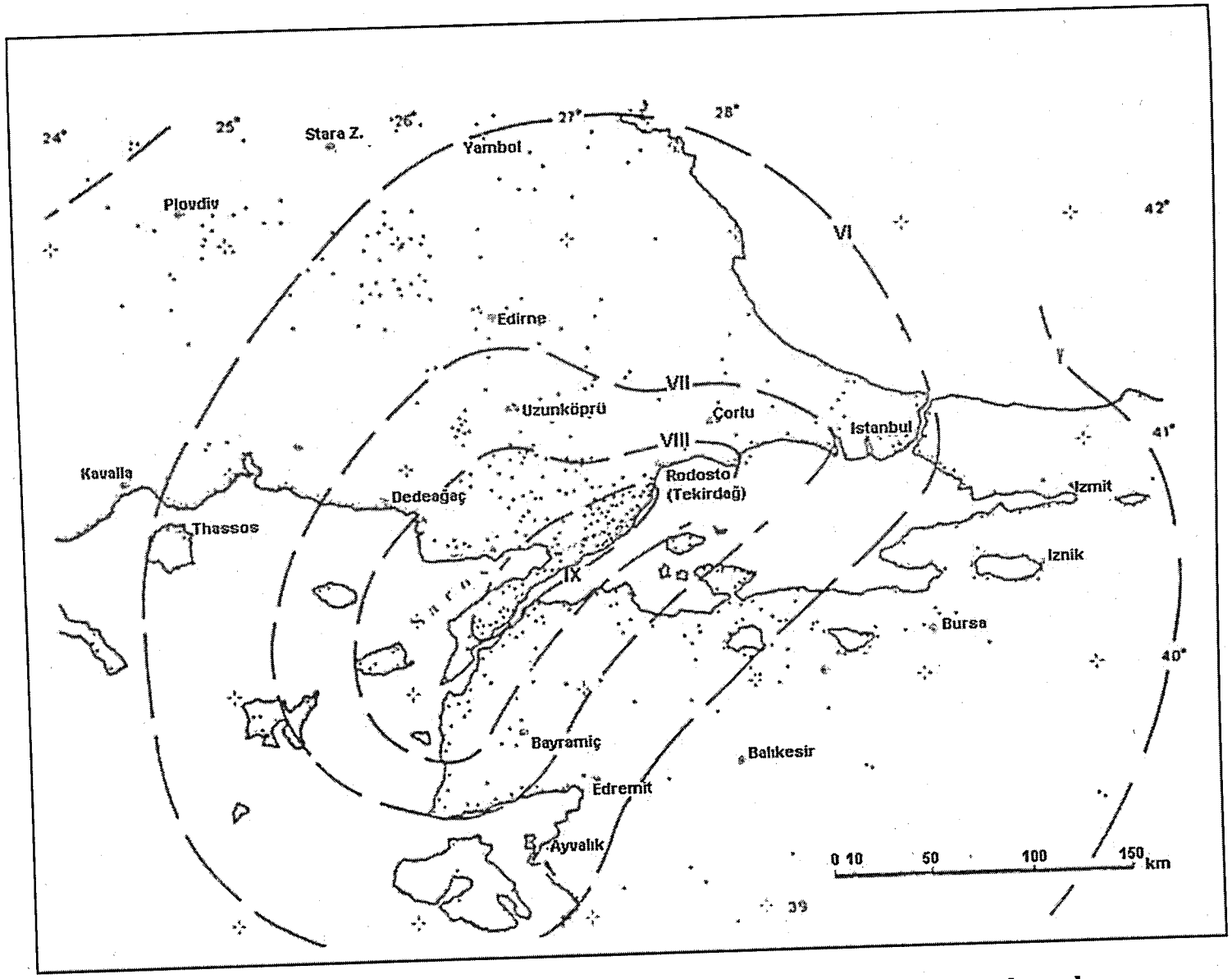

FIGURE 3.11 Iso-seismal map of the 1912 Şarköy-Mürefte earthquake

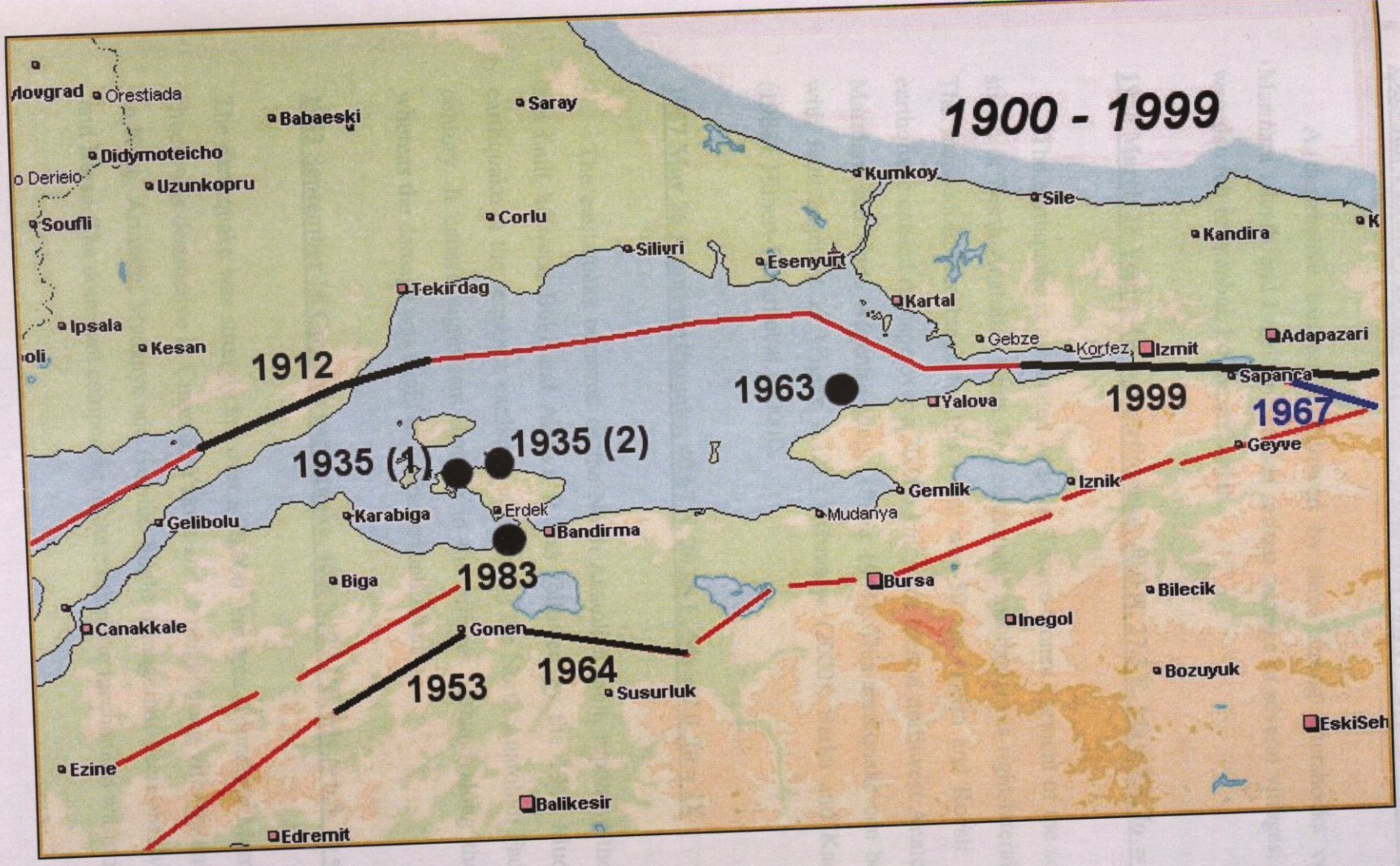

FIGURE 3.12 Historical Earthquakes between 1900-1999 associated with the fault segmentation model

1935 Jan 4 Erdek-Marmara Islands earthquake, 40.0 N – 27.5 E, Ms = 6.4, Io = IX

A destructive earthquake followed by three strong aftershocks occurred in Marmara Islands and Erdek and caused serious damage in several villages. The shock was also felt in Istanbul, Edirne and İzmir.

1953 March 18 Yenice-Gonen earthquake, 40.0 N, 27.3 E, Ms = 7.2, Io = IX

The earthquake is associated with the Yenice-Gonen segment of the southwestern strand of North Anatolian Fault. The earthquake mechanism is right-lateral strike-slip. The mapped surface break for this event was 50 km (Ketin and Roesli, 1953). The earthquake caused damage over a 30,000 km^2 wide area in northwest Anatolia between Marmara and North Aegean regions. (Pınar 1943). This earthquake can be associated with fault segment 19 (Figure 3.12) (Ambraseys (2000), Barka and Kadinsky-Cade (1988), Hubert-Ferrari et al. (2000)).

1957 May 26 Abant earthquake, 40.67 N, 30.86 E, Ms = 7.0, Io = IX

The earthquake occurred on the North Anatolian fault, rupturing the segment of the fault between Bolu and Akyazı. It was followed by the 1967 Mudurnu Valley earthquake in the sequence earthquakes rupturing the North Anatolian Fault in the 20^{th} century. It caused significant damage in the villages situated along the fault zone, whereas the damage was slight in Adapazarı and Abant.

1963 September 18 Çınarcık earthquake, 40.8 N, 29.1 E, Ms = 6.3, Io = VIII

The earthquake was strongly felt over a $70,000^2$ km area around the Marmara Sea. The shock was destructive in Çınarcık, Yalova and in neighboring villages and strongly felt in Kılıç, Armutlu, Mudanya and Gemlik. Slight damage has been observed in Istanbul and Bursa. The dominant component of the earthquake mechanism was normal.

1964 October 6 Manyas earthquake, 40.30 N, 28.23 E, Ms = 6.9, Io = IX

The earthquake occurred in the southern shores of Manyas Lake, south of Marmara Sea, having landslide and liquefaction effects and causing damage in Manyas, M. Kemalpaşa, Gonen, Susurluk, Karacabey and Bandırma and it was strongly felt Istanbul. The earthquake mechanism was determined as normal. This earthquake can be associated with fault segment 18 (Figure 3.12) (Ambraseys (2000), Barka and Kadinsky-Cade (1988), Hubert-Ferrari et al. (2000)).

1967 July 22 Mudurnu Valley earthquake, 40.67 N, 30.69 E, Ms = 6.8, Io = X

This earthquake was the preceding one of the 1999 Kocaeli event in the westward moving series of earthquakes that ruptured the whole length of the North Anatolian Fault between Erzincan and İzmit in the 20th century. The fault rupture was 80 km long between Sapanca and Abant Lakes. The right lateral displacements on the eastern 20 km, that had already ruptured in the 1957 Abant earthquake were in the range of a few cm, whereas the displacements reached 190 cm along the western segments of the rupture zone. Vertical displacements up to 120 cm were also observed. This earthquake can be associated with fault segment 12 (Figure 3.12) (Ambraseys (2000), Barka and Kadinsky-Cade (1988), Hubert-Ferrari et al. (2000)).

1999 August 17 Kocaeli earthquake, 40.702 N, 29.987 E, Mw=7.4

An earthquake of magnitude Mw 7.4 occurred on the North Anatolian Fault Zone with a macroseismic epicenter near the town of Gölcük in the western part of Turkey. (Figure 3.13.) illustrates the ruptured fault segments and the fault slip distribution model associated with this earthquake. The total observable length of the rupture was about 100 km. The lateral offsets varied between 1.5 and 5 m. Most of the aftershock activity is confined to the region bounded by 40.5-40.8N and 29.8-30.0E, which covers the area between Izmit and Adapazari to the east of the epicenter (Figure 3.14). The damage caused by the earthquake covered a very large region extending from Tekirdağ to Eskişehir, cities mostly affected being, Sakarya, Yalova, Kocaeli, Bolu and Istanbul.

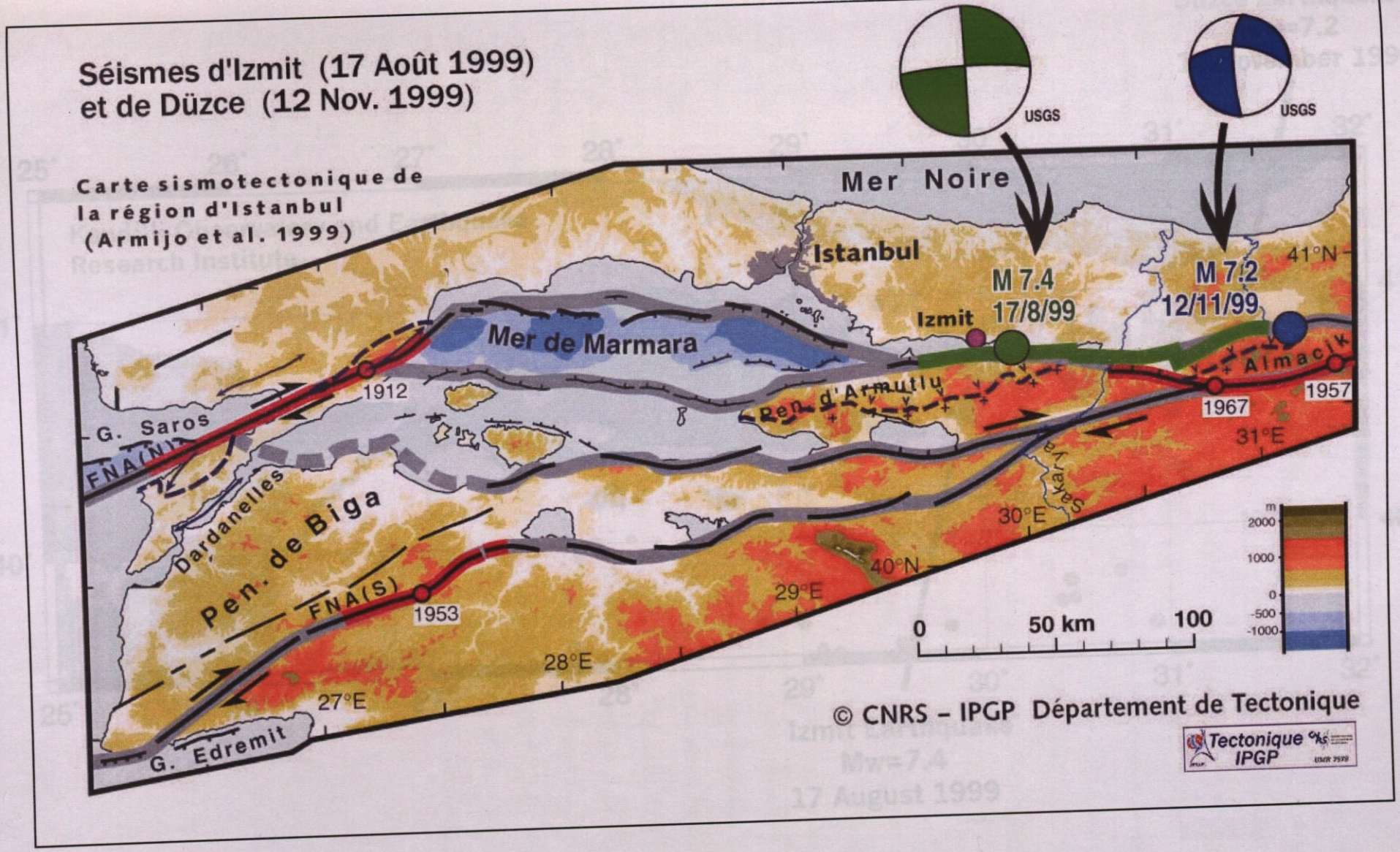

FIGURE 3.13 Surface fault ruptures and slip model of the 17 / 8 /99 and 12 / 11/ 99 Earthquakes

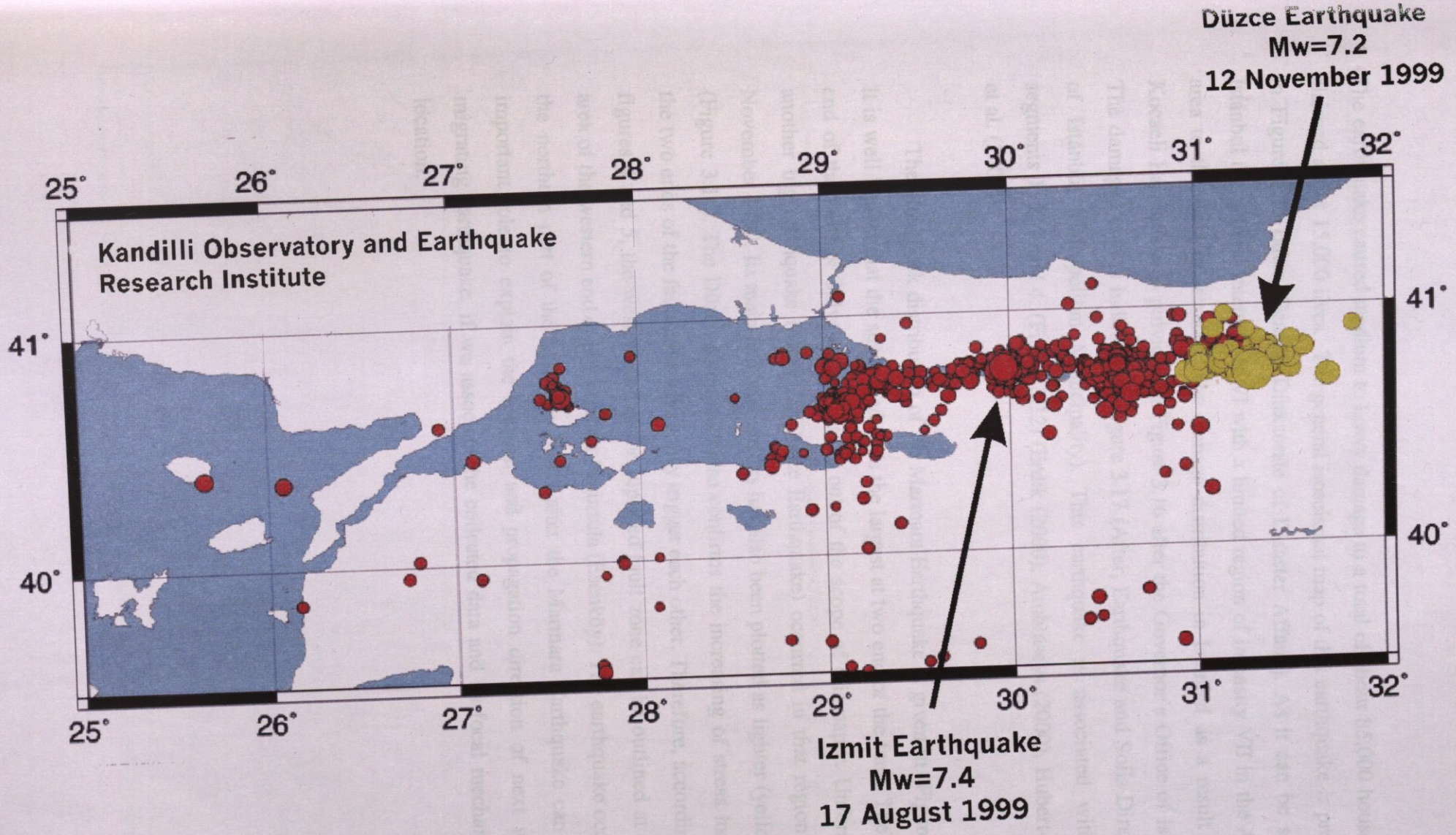

FIGURE 3.14 Locations of İzmit and Duzce Earthquakes, the location of aftershocks

The earthquake caused medium to heavy damage to a total of about 85,000 houses and claimed about 15,000 lives. The general isoseismal map of this earthquake is provided in Figure 3.15 (after, General Directorate of Disaster Affairs). As it can be seen in Istanbul the general intensity is VI with a limited region of intensity VII in the Avcilar area to the west of Istanbul. The damage distribution in Istanbul as a result of the Kocaeli Earthquake is provided in Figure 3.16 after the Governor's Office of Istanbul. The damaged area is indicated in Figure 3.17 (After, Earthquake and Soils Directorate of Istanbul Metropolitan Municipality). This earthquake is associated with fault segments 1, 2, 3 and 4. (Figure 3.12) (Erdik (2000), Ambraseys (2000), Hubert-Ferrari et al. (2000)).

The aftershock distribution of the Marmara Earthquake is given in (Figure 3.14). It is well known that the stress loading is the largest at two end of the fault. The eastern end of the fault is Gölyaka, and that is out of the scope of this paper. Unfortunately another big earthquake (Mw=7.2, Düzce Earthquake) occurred in that region in 12th November 1999. Its main and after shocks has also been plotted as lighter (yellow) dots (Figure 3.14). The Düzce earthquake also confirms the increasing of stress loading at the two ends of the fault zone where may trigger each other. Therefore, according to the figures 4 and 5, the western end of the ruptured fault zone can be outlined at offshore area of the western end of the Armutlu Peninsula (Esenköy). The earthquake occurred at the northern part of the Marmara Island after the Marmara Earthquake can play an important role to explain the location and propagation direction of next westward migrating earthquake, if we associate the collected data and its focal mechanism and location.

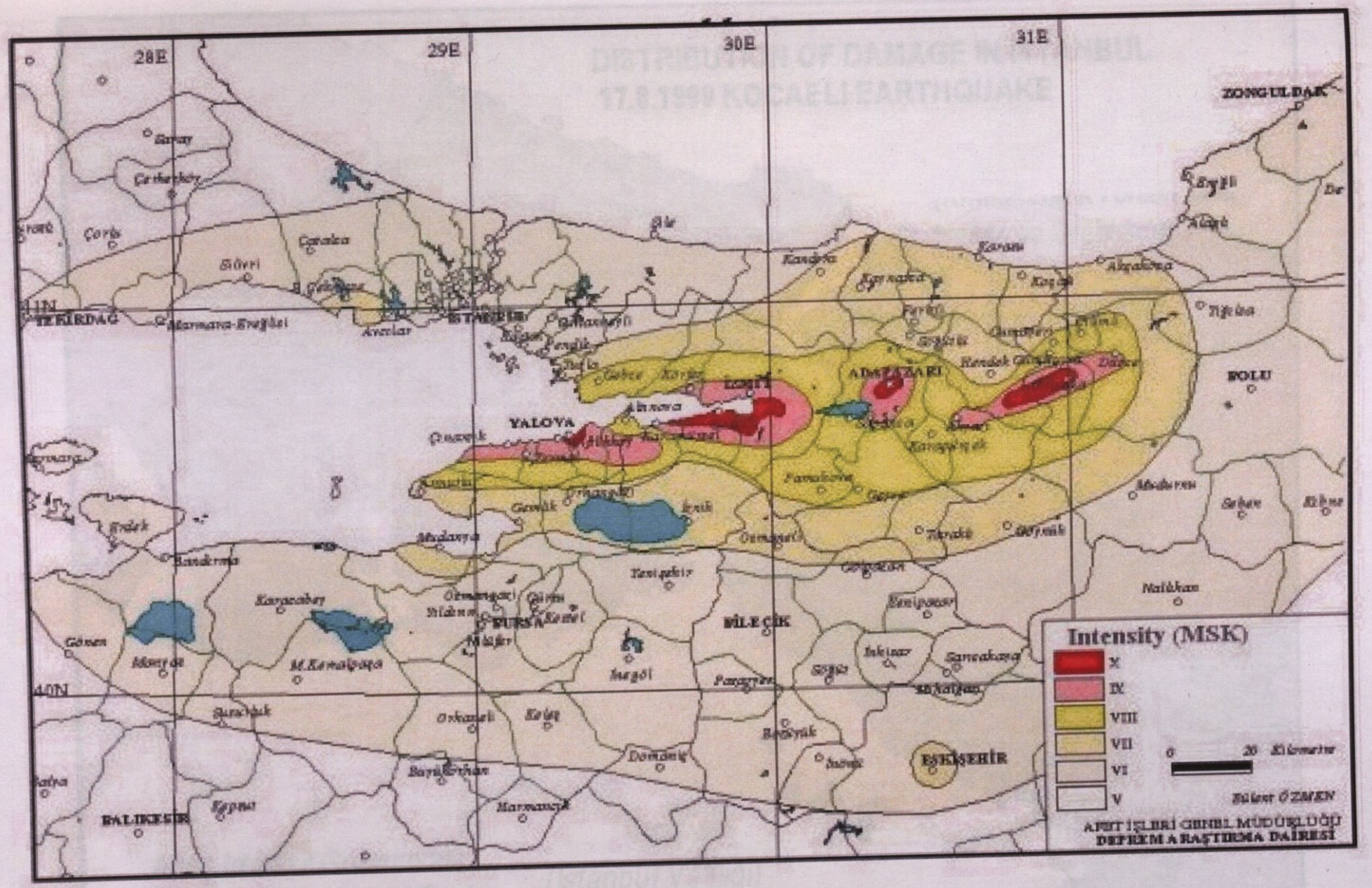

FIGURE 3.15 Isoseismal map of the 17 August 1999 Kocaeli Earthquake

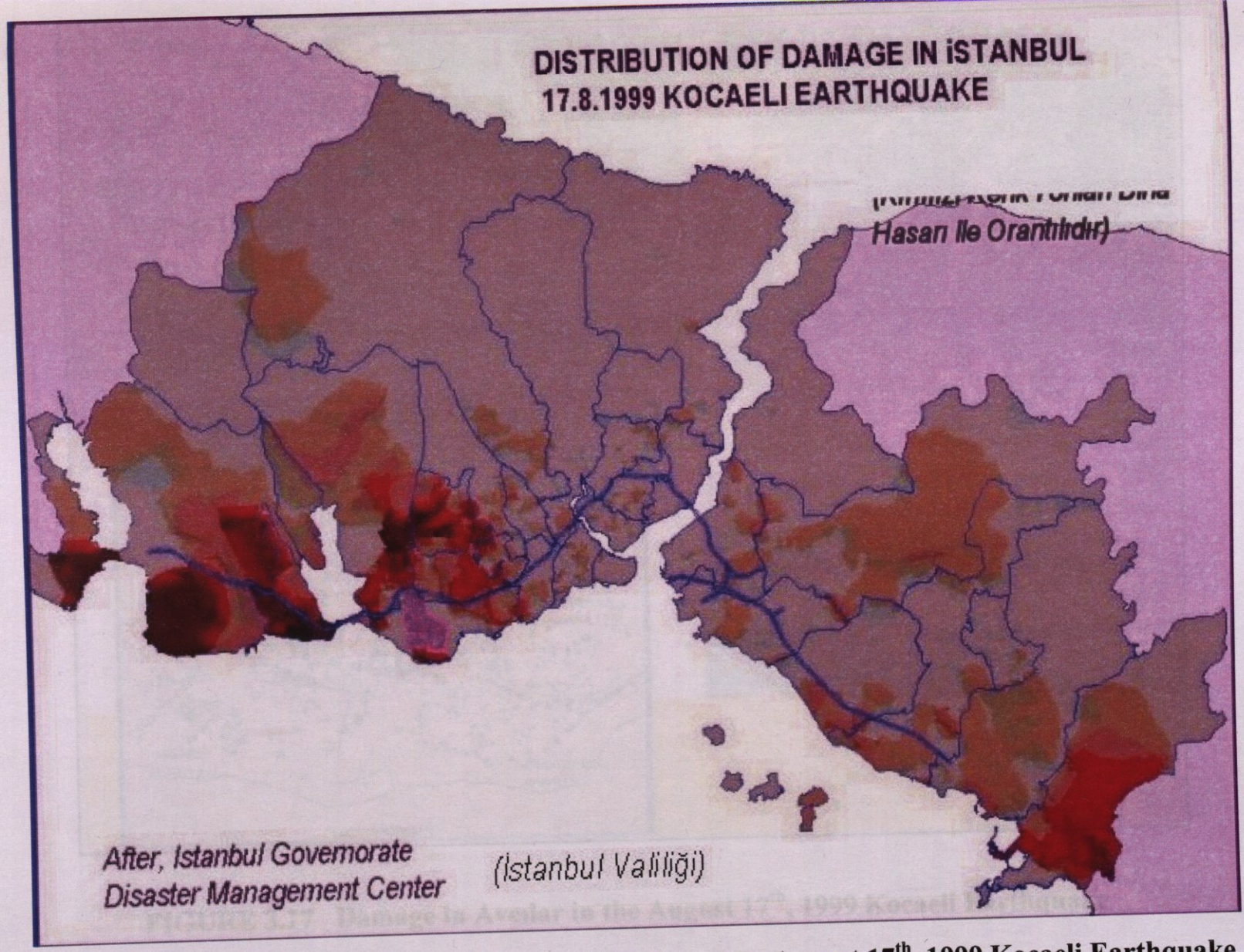

FIGURE 3.16 Distribution of damage in Istanbul due to the August 17th, 1999 Kocaeli Earthquake

FIGURE 3.17 Damage in Avcılar in the August 17th, 1999 Kocaeli Earthquake

4. PROBABILITY OF STRONG SHAKING

Stress Triggering

Earthquakes release part of the stress that slowly accumulates as the earth's plates move toward or past each other. An earthquake drops the stress on the fault which slipped, so that earthquake will not recur until the stress rebuilds, typically hundreds to thousands of years hence. But an earthquake also raises the stress elsewhere, at sites off the slipped fault hence. All other things being equal, the regions where the stress rises will be the sites of the next earthquakes to occur, both large and small. That's our approach in a nutshell. It can be calculated these 'Coulomb' stress changes, and find that aftershocks and subsequent mainshocks tend to occur where the stress rises, and are largely absent where the stress drops. This tendency is strongest immediately after the triggering shock, and fades over the ensuing decades. Thus, such work explores the 'conversation' between earthquakes on nearby faults, so that learn how one event can promote or inhibit earthquakes on other faults. Earthquake probability There are so many features of earthquake behavior that we do not understand that the best use of our limited insight is to 'play the odds,' in other words to calculate the probability of future earthquakes and their uncertainties. This permits the hazard of one fault or city to be compared with another, and the threat of earthquakes to be compared to other hazards, such as pollution, storms, or industrial accidents. Probabilistic seismic hazard assessments typically assume that earthquakes are uncorrelated in space and time. Occasionally, one assumes that the probability of an earthquake drops after large event, but does not rise elsewhere.

However, clustering of earthquakes in space and time is the outstanding feature of seismic catalogs and prehistoric earthquake occurrence, and such clustering is incompatible with such an approach, because it implies that the prospect of an earthquake rises after an event. Stress triggering overcomes this deficiency, and offers a new approach to improve seismic hazard assessments.

The Probability of Shaking In Istanbul

The probability of strong shaking in Istanbul–an urban center of 12 million people–from the description of earthquakes on the North Anatolian fault system in the Marmara Sea during the past 500 years was calculated by (R. Stein and A. Barka) and tested the resulting catalog against the frequency of damage in Istanbul during the preceding millennium. Departing from current practice, it is included the time-dependent effect of stress transferred by the 1999 moment magnitude M=7.4 İzmit earthquake to faults nearer to Istanbul. It is found a 62±15% probability (one standard deviation) of strong shaking during the next 30 years and 32±12% during the next decade. The 17 August 1999 M=7.4 İzmit and 12 November 1999 M=7.1 Düzce earthquakes killed 18,000 people, destroyed 15,400 buildings, and caused $10-25 billion in damage. But the İzmit event is only the most recent in a largely westward progression of seven large earthquakes along the North Anatolian fault since 1939 (Figure 4.1). Just northwest of the region strongly shaken in 1999 lies Istanbul, a rapidly growing city that has een heavily damaged by earthquakes twelve times during the past 15 centuries. Here, ıt will be explained (R.Stein and A. Barka) calculated the probability of future earthquake shaking in Istanbul using new concepts of earthquake interaction, in which the long-term renewal of stress on faults is perturbed by transfer of stress from nearby events.

Stress triggering has been invoked to explain the 60-year sequence of earthquakes rupturing toward Istanbul [Toksoz et al ref](1-3), in which all but one event promoted the next. Although an earthquake drops the average stress on the fault that slipped, it also changes the stress elsewhere. The seismicity rate has been observed to rise in regions of stress increase and fall where the off-fault stress decreases (R.Harris, J.Geophys). The M=7.4 Izmit earthquake, as well as most background seismicity, occurred where the failure stress is calculated to have increased 1-2 bars (0.1-0.2 MPa) by M³6.5 earthquakes since 1939 (Figure 4.2A) (R.Stein and A. Barka). The Izmit event, in turn, increased the stress beyond the east end of the rupture by 1-2 bars, where the M=7.2 Düzce earthquake struck, and by 0.5-5.0 bars beyond the west end of the 17 August rupture, where a cluster of aftershocks occurred (Figure 4.2B). The

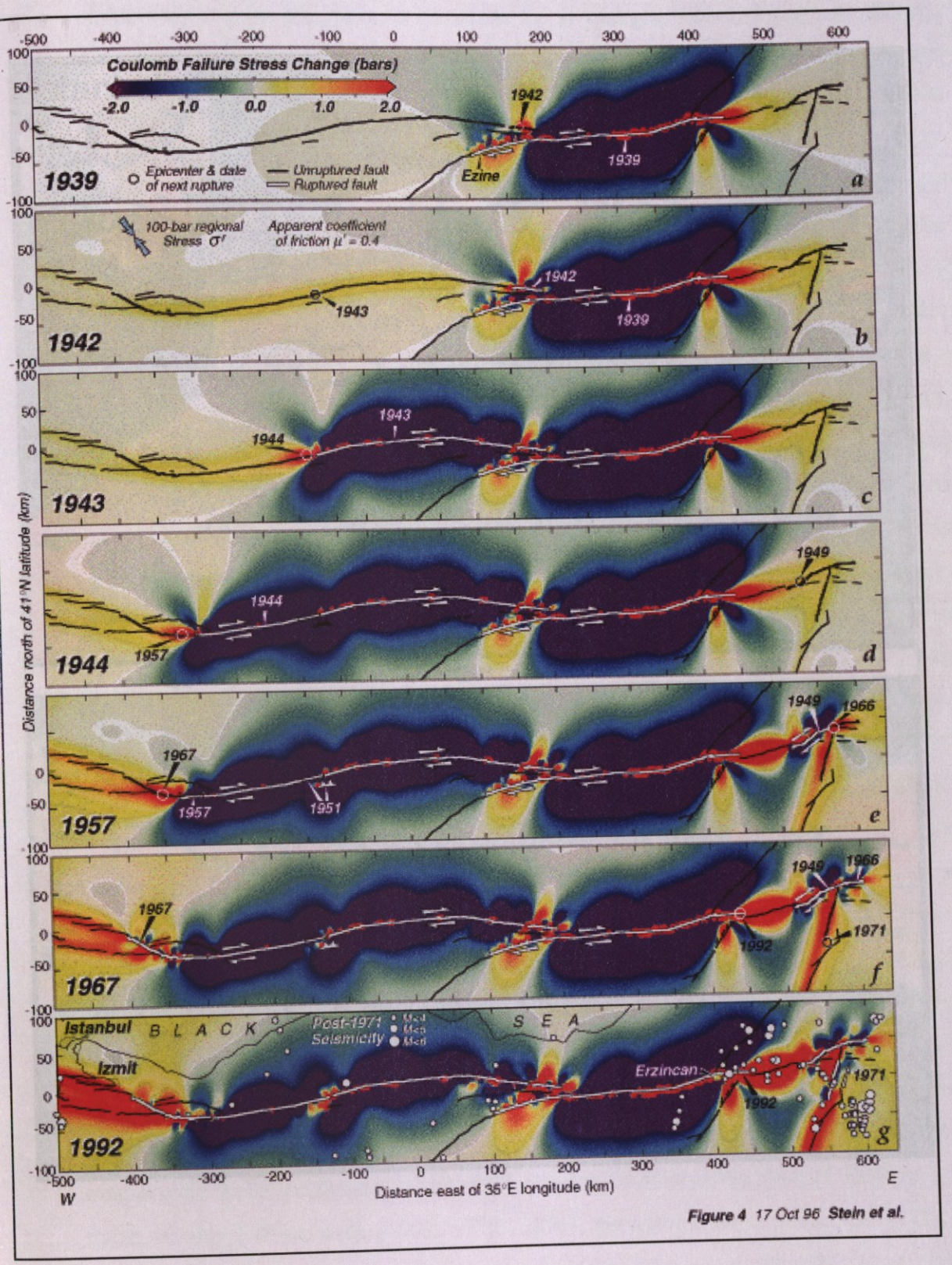

FIGURE 4.1 Stress change of the earthquakes along North Anatolian Fault

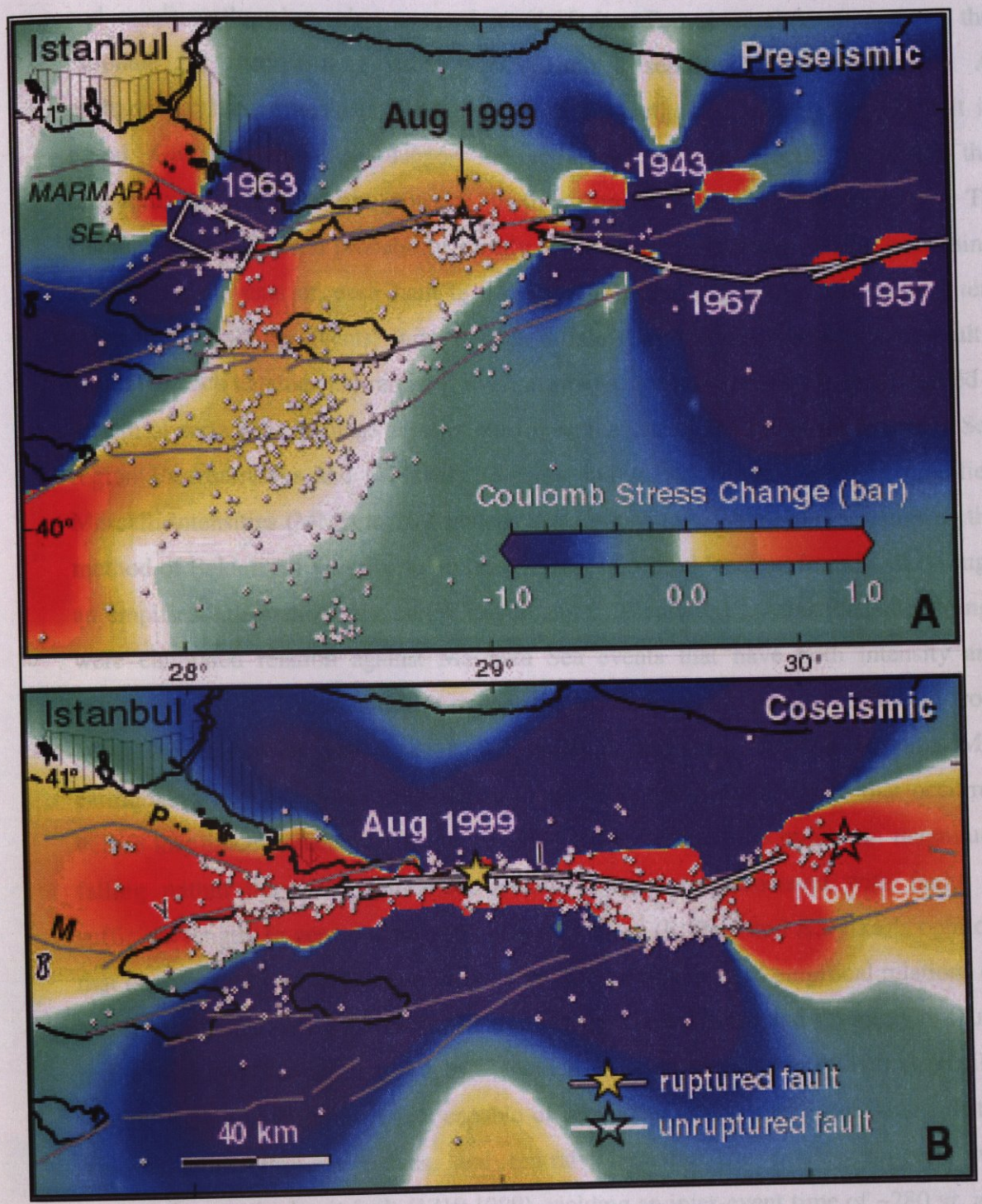

FIGURE 4.1A Stress change caused by earthquakes since 1900

FIGURE 4.1B İzmit aftershocks are associated with seismicity rates

correspondence seen here between calculated stress changes and the occurrence of large and small earthquakes, also reported in (A.Hurbert-Ferrari et al.,), strengthens the rationale for incorporating stress transfer into a seismic hazard assessment. A probabilistic hazard analysis is no better than the earthquake catalog on which it is based. Global observations support an earthquake renewal process in which the probability of a future event grows as the time from the previous event increases . To calculate such a renewal probability, ideally one wants an earthquake catalog containing several large events on each fault to deduce earthquake magnitudes, the mean inter-event time of similar events, and the elapsed time since the last shock on each fault . Although such catalogs are rarely, if ever, available, Ambraseys and Finkel compiled a wealth of earthquake damage descriptions for events since AD 1500 in the Marmara Sea region (N.Ambraseys and C.Finkel). (R.Stein and A.Barka) had assigned modified Mercalli intensities (MMI) to 200 damage descriptions (available online), and used the method of Bakun and Wentworth to infer M and epicentral location from MMI through an empirical attenuation relation (W.Bakun and C. Wentworth). After that, such things were calibrated relation against Marmara Sea events that have both intensity and instrumental data. Uncertainties in earthquake location were explicitly calculated from MMI inconsistencies and inadequacies. Such catalog thus consists of nine $M^{3}7$ earthquakes in the Marmara Sea region since 1500. For the six events that occurred before instrumental recording began in 1900, ıt was selected the minimum magnitude falling within the 95% confidence bounds at locations associated with faults of sufficient length to generate the event (Figure 4.3). In (R.Stein and A.Barka)'s opinion, that is estimated which is rupture lengths and the mean slip from empirical relations on M for continental strike-slip faults (J.Parke et al.,). The locations and geometry of faults in the Marmara Sea are under debate which is based on seismic reflection profiles (Figure 4.3), and find four faults capable of producing strong shaking in Istanbul: the Yalova, Izmit, Prince's Islands, and central Marmara. The catalog suggests two earthquakes on the Izmit fault (1719,1999), yielding an inter-event time of ~280 yr, and three on the Yalova fault (1509, 1719, 1894), permitting an estimate of ~190 yr (D.Wells and K.Coppersmith). (R.Stein and A.Barka) infer one earthquake (May 1766) on the Prince's Islands fault and one (1509) on the central Marmara fault (Figure 4.3). For these, these were gauged by (R.Stein and A.Barka) inter-event times by dividing the

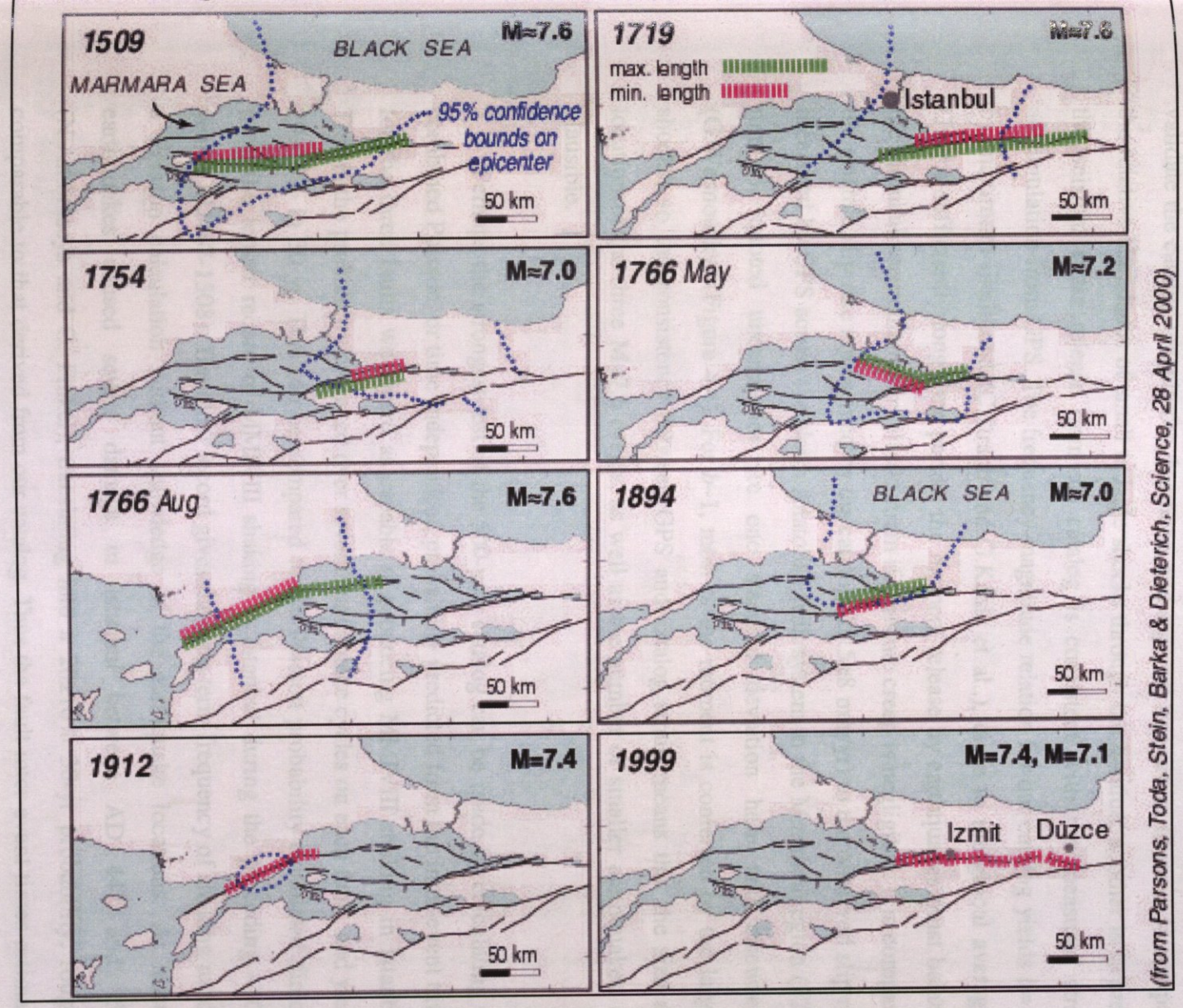

FIGURE 4.3 Large historical earthquakes since 1500

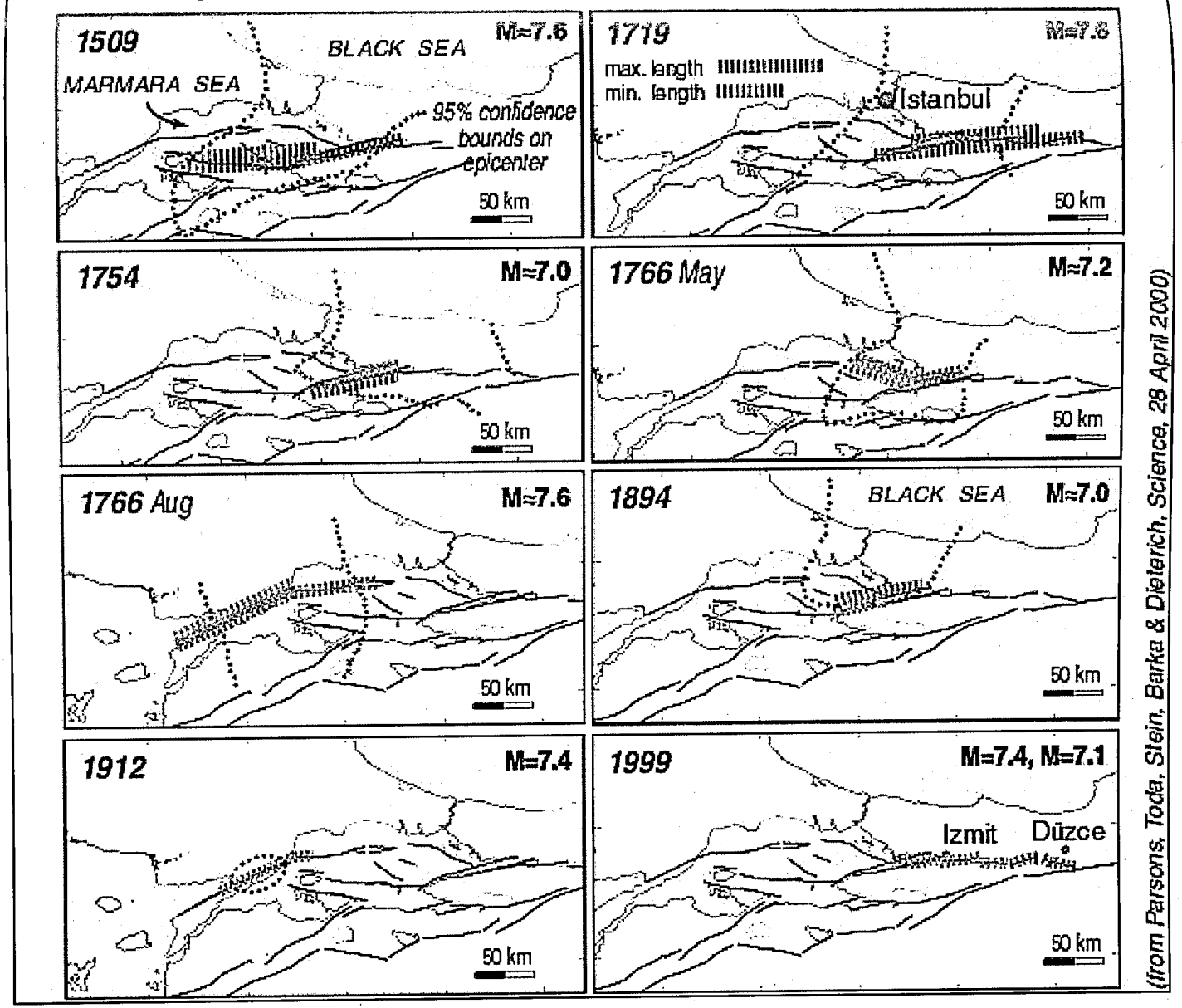

FIGURE 4.3 Large historical earthquakes since 1500

seismic slip estimated from the catalog by the GPS-derived slip rate, yielding a ~210 yr inter-event time for the Prince's Islands fault and ~540 yr for the central Marmara fault. Thus at least two of the four faults are likely late in their earthquake cycles. One way to validate the catalog magnitudes, locations, and segment inter-event times is to compare the relative abundance of small to large shocks through the *b*-value; another is to see if the seismic strain release from the catalog is consistent with the measured strain accumulation from GPS. The frequency-magnitude relation for our catalog yields b=1.1 by maximum likelihood (C.Straub and G.Kahle et al.,), close to the global average . Over a sufficiently long time period, the moment release by earthquakes must balance the moment accumulation by elastic strain if aseismic creep is negligible. It is compared the seismic slip rate represented by the catalog (23.5±8 mm/yr) to the observed slip rate measured by GPS across the North Anatolian fault system in the Marmara region (22±3 mm/yr) (quoted uncertainties are one standard deviation here and elsewhere) (G.Wesnousky) (Figure 4.4). For b~1, most of the moment is conferred by the largest shocks, so the consistency between GPS and catalog strain means that the size and location of the three M~7.6 events, as well as the number of smaller earthquakes, are plausible.

Perhaps the strongest test of the 500-year catalog can be made by calculating the combined Poisson, or time-independent, probability predicted from the inter-event times for the three faults we regard as capable of producing MMIVIII shaking in Istanbul. This is the probability averaged over several earthquake cycles on each fault, and yields 29±15% in 30 yr. This can be compared to the Poisson probability calculated directly from the longer record of MMIVIII shaking in Istanbul during the preceding ~1000 years (AD447-1508). The older record gives the long-term frequency of shaking used in a Poisson calculation without knowledge of the earthquake locations. At least 8 earthquakes caused severe damage in Istanbul between AD 447 and 1508 (N.Ambraseys and C. Finkel), translating into a 20±10% 30-yr probability, roughly comparable to that derived from our catalog. Thus the fault inter-event times estimated from the 500-yr catalog are consistent with the independent record of shaking in Istanbul during the preceding millennium.

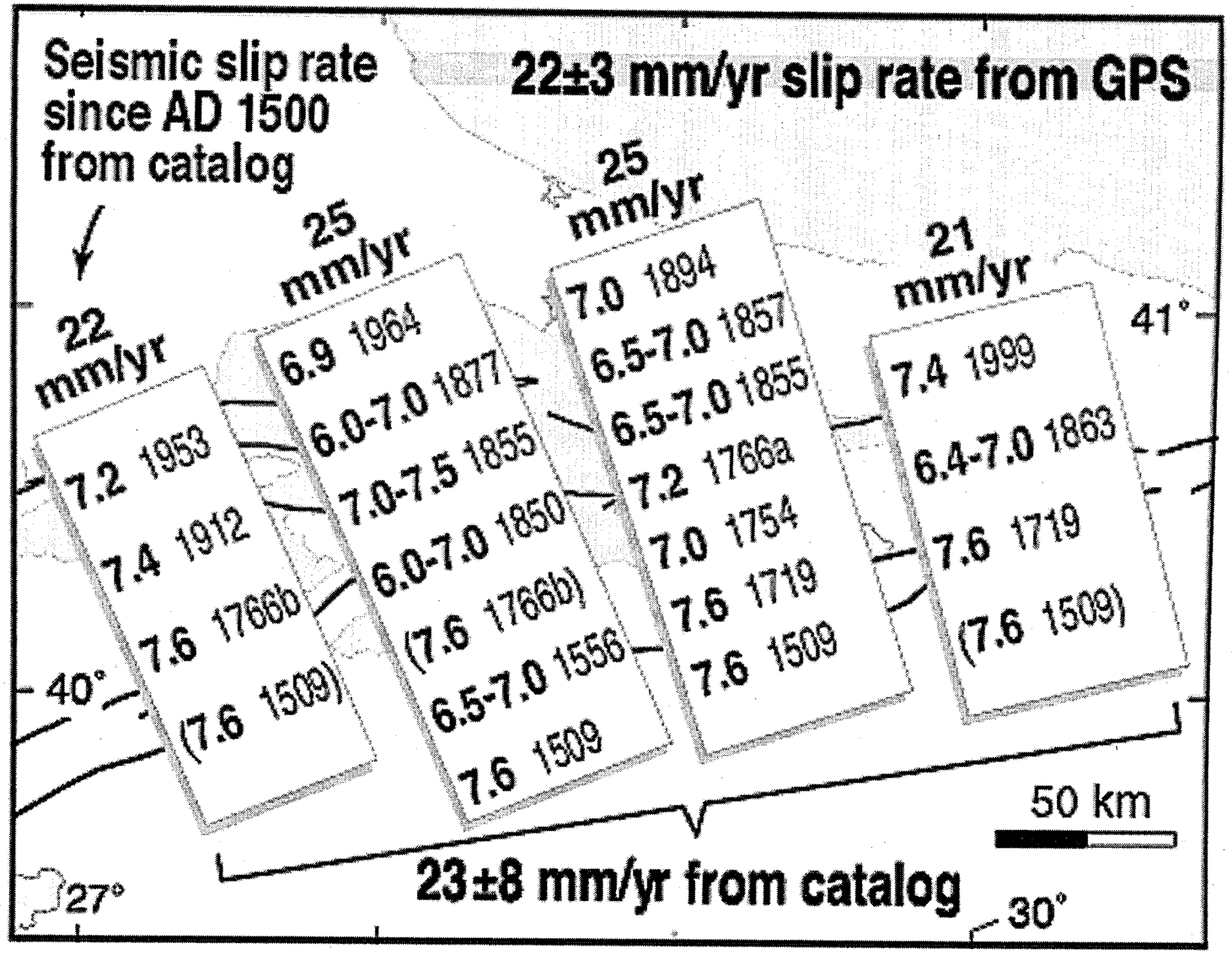

FIGURE 4.4 Seismic slip rate since AD 1500 from catalog

(R.Stein and A. Barka) explained they combined earthquake renewal and stress transfer into the probability calculation on the basis that faults with increased stress will fail sooner than unperturbed faults. Because two out of the three faults within 50 km of Istanbul are interpreted to be late in their earthquake cycles, the renewal probability is higher than the Poisson probability. Additionally, the permanent probability gain caused by stress increase is amplified by a transient gain that decays with time. The transient gain is an effect of rate- and state-dependent friction (J.Dieterich and B.Kilgore), which describes behavior seen in laboratory experiments and in natural seismic phenomena, such as earthquake sequences, clustering, and the occurrence of aftershocks. (R.Stein and A.Barka) defined they estimated the duration of the transient decay directly from the times between triggering and rupturing earthquakes on the North Anatolian fault (Figure 4.5A). Because parameter assignments used in the calculation are approximate, (R.Stein and A.Barka) perform a Monte Carlo simulation to explore the uncertainties. The resulting probability functions (Figure 4.5B) exhibit a gradual rise as the mean time since the last shock on each fault grows, and a sharp jump in August 1999 followed by a decay.

(R.Stein and A.Barka) drew a conclusion which is that a 62±15% probability of strong shaking (MMIVIII; equivalent to a peak ground acceleration of 0.34-0.65g (32)) in greater Istanbul over the next 30 yr (May 2000-2030), 50±13% over the next 22 yr, and 32±12% over the next 10 yr (Table 4.1). Inclusion of renewal doubles the time-averaged probability; interaction further increases the probability by a factor

The twelve earthquakes that damaged Istanbul during the past 1500 yr attest to a significant hazard, and form the basis for a 30-yr Poisson, or time-averaged, probability of 15-25%. Because the major faults near Istanbul are likely late in their earthquake cycles (with no major shocks since 1894), the renewal probability climbs to 49±15%. According to (R.Stein and A.Barka)'calculations, the stress changes altered the rate of seismicity after the 1999 Izmit earthquake, promoting the M=7.2 Düzce shock and the Yalova cluster. Because the 1999 Izmit shock is calculated to have similarly increased stress on faults beneath the Marmara Sea, the interaction-based probability and (R.Stein and A.Barka) advocate climbs still higher, to 62±15%.

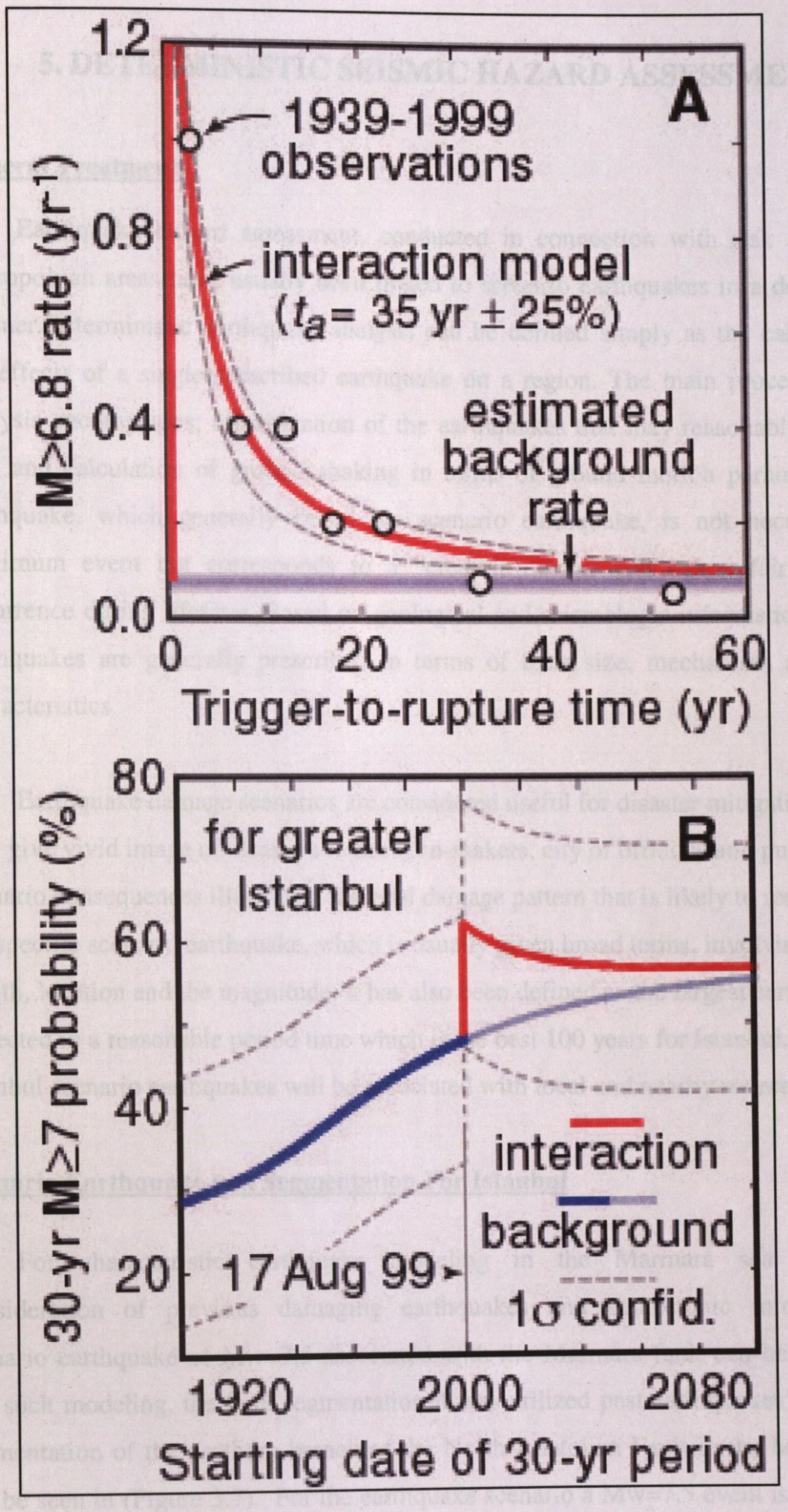

FIGURE 4.5A Observed and modeled transient response to stress transfer

FIGURE 4.5B Calculated probability of a M>=7 earthquake as a function of time

5. DETERMINISTIC SEISMIC HAZARD ASSESSMENT

General Treatment

Earthquake hazard assessment, conducted in connection with risk analyses in metropolitan areas have usually been linked to scenario earthquakes in a deterministic manner.Deterministic earthquake analysis can be defined simply as the calculation of the effects of a single prescribed earthquake on a region. The main procedure of the analysis encompasses; identification of the earthquakes that may reasonably affect the area and calculation of ground shaking in terms of ground motion parameters. This earthquake, which generally called the scenario earthquake, is not necessarily the maximum event but corresponds to a "credible" event that has a fair chance of occurrence during lifetime. Based on geological and seismologic information, scenario earthquakes are generally prescribed in terms of their size, mechanism and rupture characteristics.

Earthquake damage scenarios are considered useful for disaster mitigation since they give vivid image of disasters to decision-makers, city of officials and public. The scenario consequences illustrate a regional damage pattern that is likely to result from the specific scenario earthquake, which is usually given broad terms, involving rupture length, location and the magnitude. It has also been defined as the largest earthquakes expected in a reasonable period time which is the best 100 years for Istanbul. The Istanbul scenario earthquakes will be associated with local and nearby sources.

Scenario Earthquake and Segmentation For Istanbul

For characteristic earthquake modeling in the Marmara sea region, in consideration of previous damaging earthquakes and geotectonic information, a scenario earthquake of Mw=7.5 associated with the Marmara fault can be prescribed. For such modeling, the fault segmentation it was utilized past earthquakes' fault. The segmentation of the northern branch of the North Anatolian Fault in the Marmara Sea can be seen in (Figure 3.7). For the earthquake scenario a Mw=7.5 event is assumed to take place on segments 5, 6, 7 and 8 as shown in (Figure 5.1). According to the

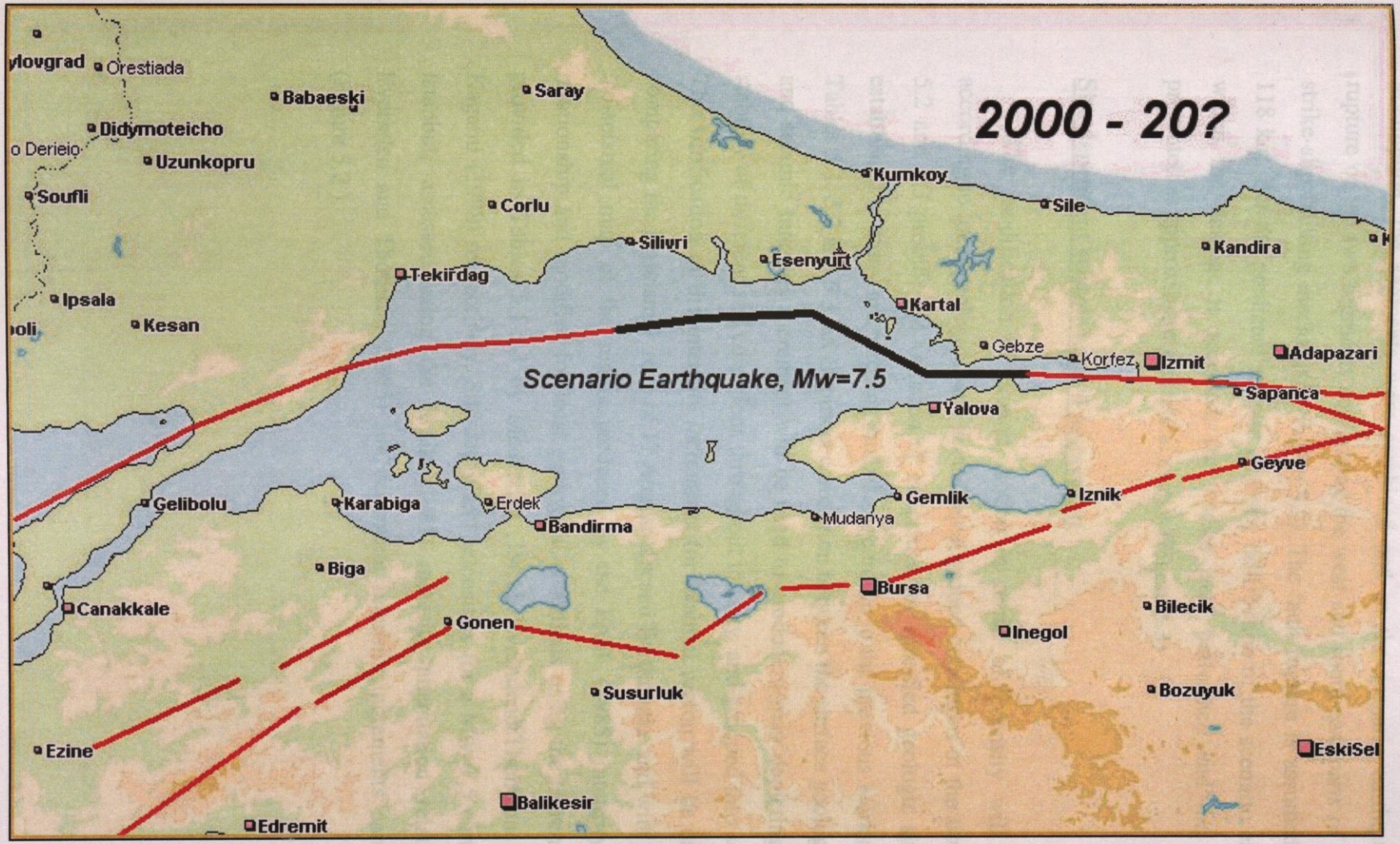

FIGURE 5.1 Mw=7.5 scenario earthquake for Istanbul and vicinity

assumption, the segments were combined and so the scenario earthquake involves rupture of the two segments comprising the west and south-east parts of the Bay with strike-slip faulting mechanism (Figure 5.2). The fault rupture is assumed its length is 118 km. For the predicted seismic intensity distribution of the scenario earthquake for which the damage is assessed, the studies were performed and the results were presented as approximately elliptical shapes (Figure 5.3)

Site dependent seismic hazard assessment

The modification of ground motion in terms of intensity will be supplied according to local geological and geotechnical ground conditions of the sites. Table 5.1, 5.2 and 5.3 provide the variation of intensities for specified geologic site conditions established in many microzoning studies. According to the previous works presented in Tables 5.1, 5.2 and 5.3, an empirical correlation between the surface geology of Istanbul and seismic intensity increment will be used to produce a map depicting the relative stability of different soil conditions throughout the city, and grouped into several zones. The verification of the intensity increments for Istanbul region will be carried out by comparing the isoseismal map of 17 August Kocaeli Earthquake and with the synthetic iso-seismal map of the region produced by the Erdik (1985) intensity attenuation relationship and modified for local geological conditions using the incremental values provided in Tables 5.1-5.3 by Medvedev (1961), Evernden&Thomson (1985) and Kagami (1998) respectively. Site dependent intensities for a Mw=7.5 earthquake near İstanbul, assessed using the Erdik (1985) intensity attenuation relationship and Evernden and Thomson (1985) site dependent intensity increments can be seen in (Figure 5.2)

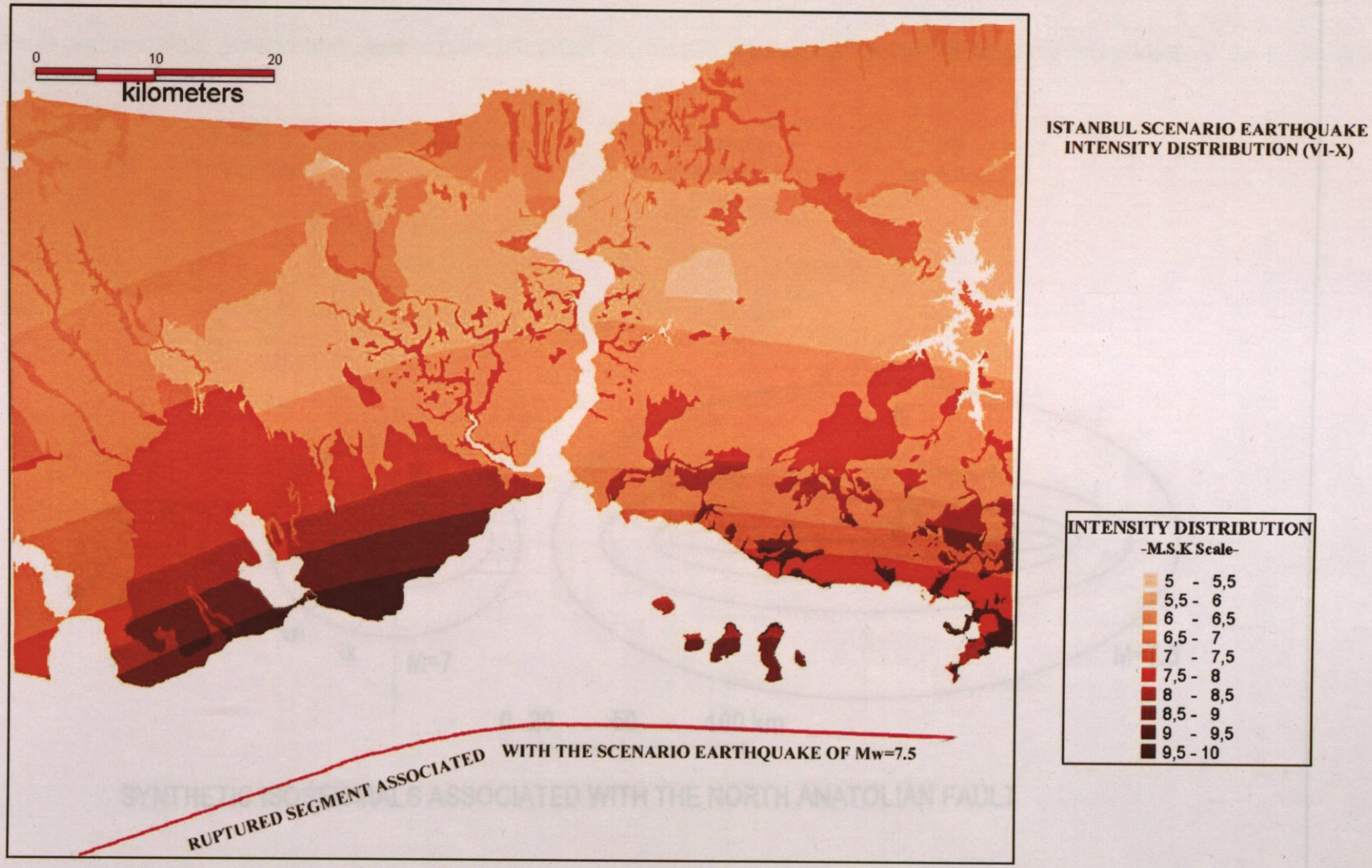

FIGURE 5.2 Site dependent intensity distribution in İstanbul as result of a Mw=7.5 scenario earthquake

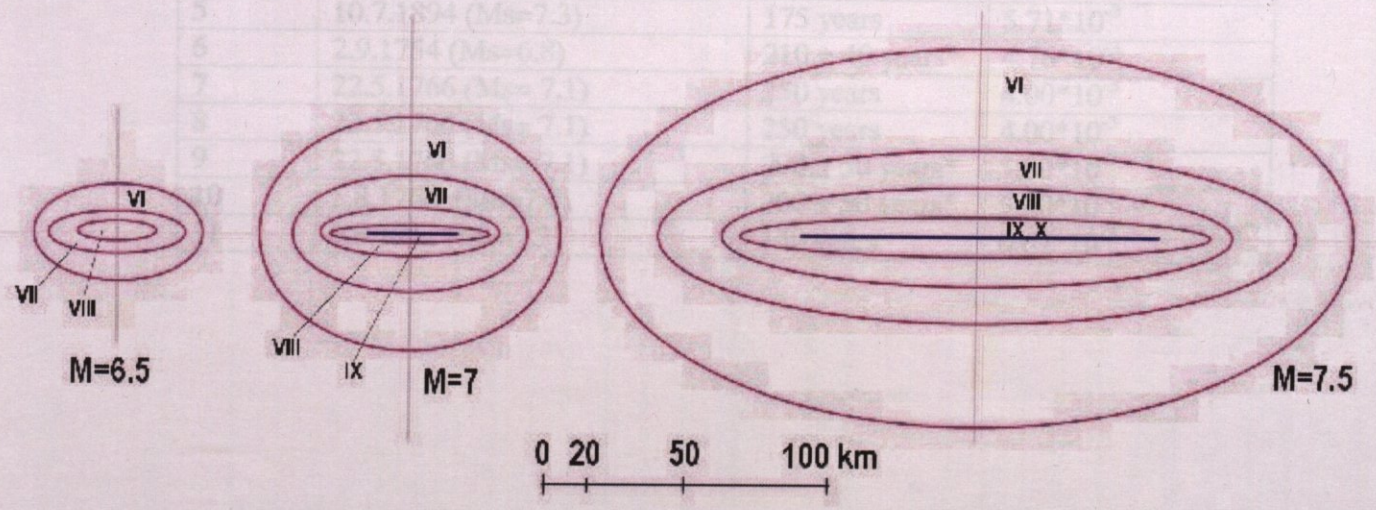

FIGURE 5.3 Synthetic isoseismals associated with the north Anatolian Fault

Table 5.1 Fault segmentation, associated median recurrence times and annual rates of occurrence for the northern portion of the North Anatolian Fault in the Marmara Sea region.

Fault Segment	Last Earthquake	Median Recurrence Time, m	Annual Rate of Occurrence, r
1	12.11.1999(Mw=7.1, Ms=7.3)		
2	17.8.1999 (Mw=7.4, Ms=7.8)	140 ± 35 years*	$7.14*10^{-3}$
3	17.8.1999 (Mw=7.4, Ms=7.8)	140 ± 35 years	$7.14*10^{-3}$
4	17.8.1999 (Mw=7.4, Ms=7.8)	140 ± 35 years	$7.14*10^{-3}$
5	10.7.1894 (Ms=7.3)	175 years	$5.71*10^{-3}$
6	2.9.1754 (Ms=6.8)	210 ± 40 years*	$4.76*10^{-3}$
7	22.5.1766 (Ms= 7.1)	250 years	$4.00*10^{-3}$
8	22.5.1766 (Ms= 7.1)	250 years	$4.00*10^{-3}$
9	22.5.1766 (Ms= 7.1)	200 ± 50 years*	$5.00*10^{-3}$
10	5.8.1766 (Ms=7.4)	200 ± 50 years*	$5.00*10^{-3}$
11	9.8.1912 (Ms=7.3)	150 years	$6.67*10^{-3}$

Table 5.2 Correlation between soil types and intensity increase after Medvedev (1961).

Geological Unit	Intensity Increments
Granites	0
Limestones, sandstones, shales	0.2-1.3
Gypsum, marl	0.6-1.4
Coarse material	1-1.6
Sands	1.2-1.8
Clays	1.2-2.1
Fill	2.3-3.0
Moist Ground (gavel, sand, clay)	1.7-2.8
Moist fill and soil ground (marsh)	3.3-3.9

Table 5.3 Correlation of type of rocks and sediments with intensity increments for California (Evernden&Thomson 1985)

Geological Unit	Intensity Increments
Granitic and metamorphic rocks	0
Paleozoic rocks	0.4
Early Mesozoic rocks	0.8
Cretaceous to Eocene rocks	1.2
Undivided Tertiary rocks	1.3
Oligocene to middle Pliocene rocks	1.5
Pliocene-Pleistocene rocks	2.0
Tertiary volcanic rocks	0.3
Quaternary volcanic rocks	0.3
Alluvium (water table) <10m 10-30 m >30m	 3.0 2.0 1.0

Seismic Intensity Distribution Based On Erdik et. al.,(1985) Attenution Relationship

The assessment of the intensities that would result from the occurrence of the scenario earthquake will be based on intensity attenuation relationship of Erdik (1985). In order to assess the attenuation of intensities for earthquakes associated with the North Anatolian Fault in both parallel and transverse directions Erdik et. al., (1985) proposed a set of attenuation relationships. In the analysis they utilized an iso-seismal data set that covers the earthquakes occurred on the North Anatolian and the East Anatolian Faults.

The attenuation of the intensities in transverse direction to the North Anatolian Fault based on regression analysis is given as;

$$I = -0.34 + 1.545M - 1.237 \ln R - 0.001R \quad \sigma = 0.60$$

where,

I and σ denotes, respectively, the mean intensity at a distance R in transverse direction to the fault and standard deviation.

For three intensity levels, the attenuation of the intensities in parallel direction to the North Anatolian Fault based on regression analysis is given as;

$$\ln D_{VIII} = 2.20\,M - 11.32 \qquad \sigma = 0.47 \qquad r^2 = 0.782$$

$$\ln D_{VII} = 1.80\,M - 8.40 \qquad \sigma = 0.34 \qquad r^2 = 0.829$$

$$\ln D_{VI} = 2.02\,M - 9.55 \qquad \sigma = 0.45 \qquad r^2 = 0.726$$

where,

D = end to end contour interval distances;

σ = standard deviation

r^2 = correlation coefficient

For the scenario earthquake that is assumed to occur on the Marmara Fault, the iso-seismal maps of the region have will have typically elliptical shapes with major axis along the fault as presented in (Figure 5.3)

6. GEOLOGIC AND GEOTECHNICAL CONDITIONS

The surface geology map of İstanbul with a scale of 1/50,000 is prepared by Istanbul Metropolitan Municipality as shown (Figure 6.1A). As it can be seen from (Figure 6.1B), the northern parts of the city are dominated by Sarıyer formation contains marl, mudstone and unweathered Karaburun-Çukurçeşme formation. The Trakya formation including shale and greywacke lie in the middle of the European side of Istanbul. The Paleozoic basement consists of upper Devonian interbedded medium to fine-grained sandstone, siltstone, greywacke and micaceous shale. Upper Miocene sediments and sedimentary rocks including sand and gravel, clay and marl, and limestone overly the Paleozoic basement. Upper Miocene, Bakırköy formation in the south part of the city is comprised of white, porous, chalky, medium to hard limestone with clay interbeds, typically thick-bedded and fine-grained. The Quaternary alluvium and natural fills consist primarily of loose to very loose, medium to fine silty, shelly sand, and dark gray clay and mud. Quaternary alluvium accumulated at a depositional low in the south portion of the city in the European side, and natural continental and marine sediments line the coasts above the bedrock. The late Ordovisian, Kurtköy formation including sandstone, shale and the middle Devonian, Kartal formation contains shale lie in the middle of Asia side. The southern part of Asia side of the city are dominated several formations such as Gözdağ, Aydos, Tuzla and Dolayoba formations. The quaternary alluvium and natural fills consists loose to very loose, medium to fine silty, shelly sand and dark gray clay and mud. The recent manmade fill is dominated along the south coast of Asia side. This artificial fill consists of dense, course to fine sand and gravel mixed silt, clay, cobbles. Most of valleys (basin) and lowlands have been filled for hundreds of years.

The basic approach towards the assessment of the spatial variation of geotechnical conditions include the determination the soil classes to be used. For this purpose we will adopt the NEHRP (1997) soil classification. This classification has international acceptance in earthquake engineering profession and will facilitate the differentiation of

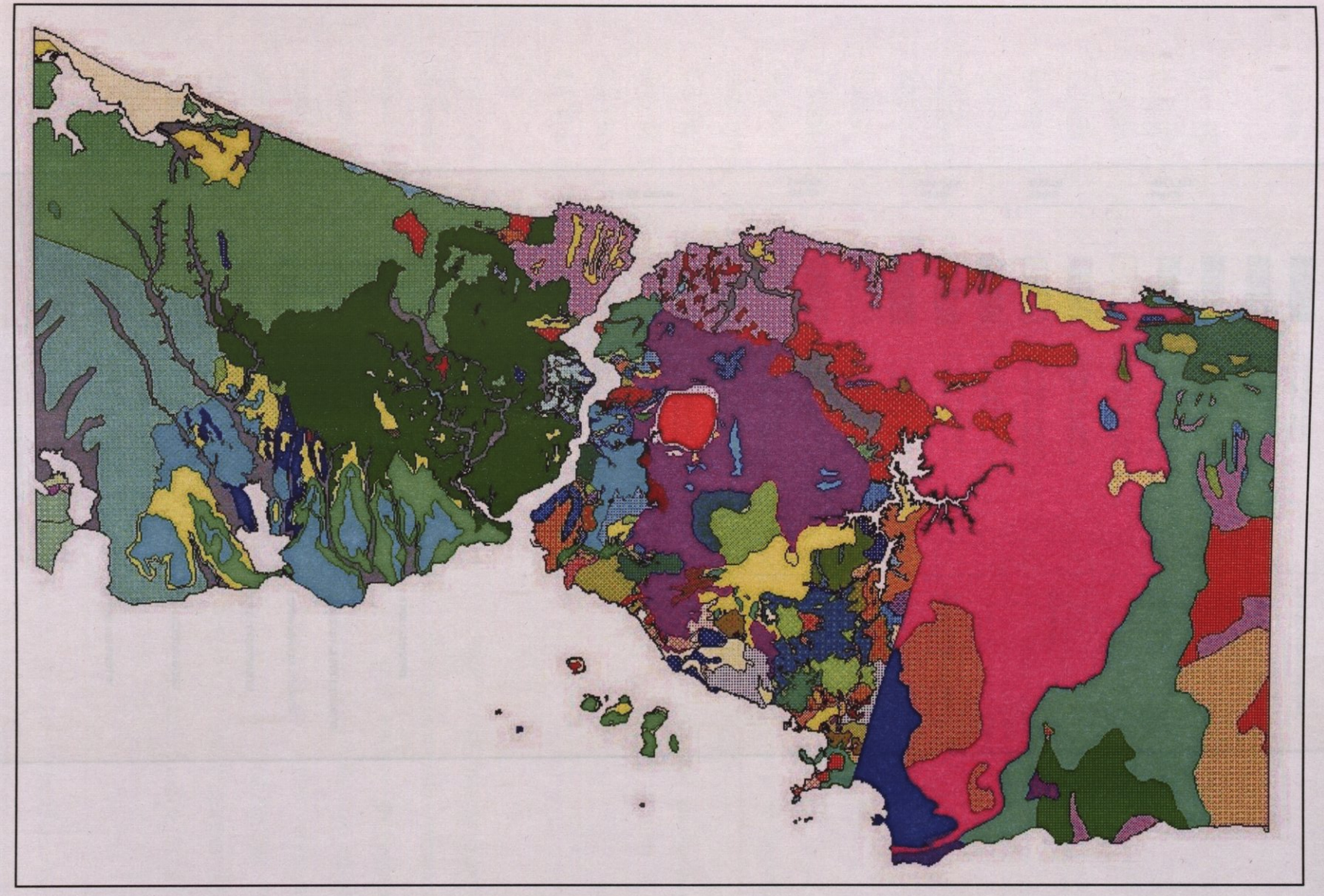

FIGURE 6.1A The surface geology map Istanbul

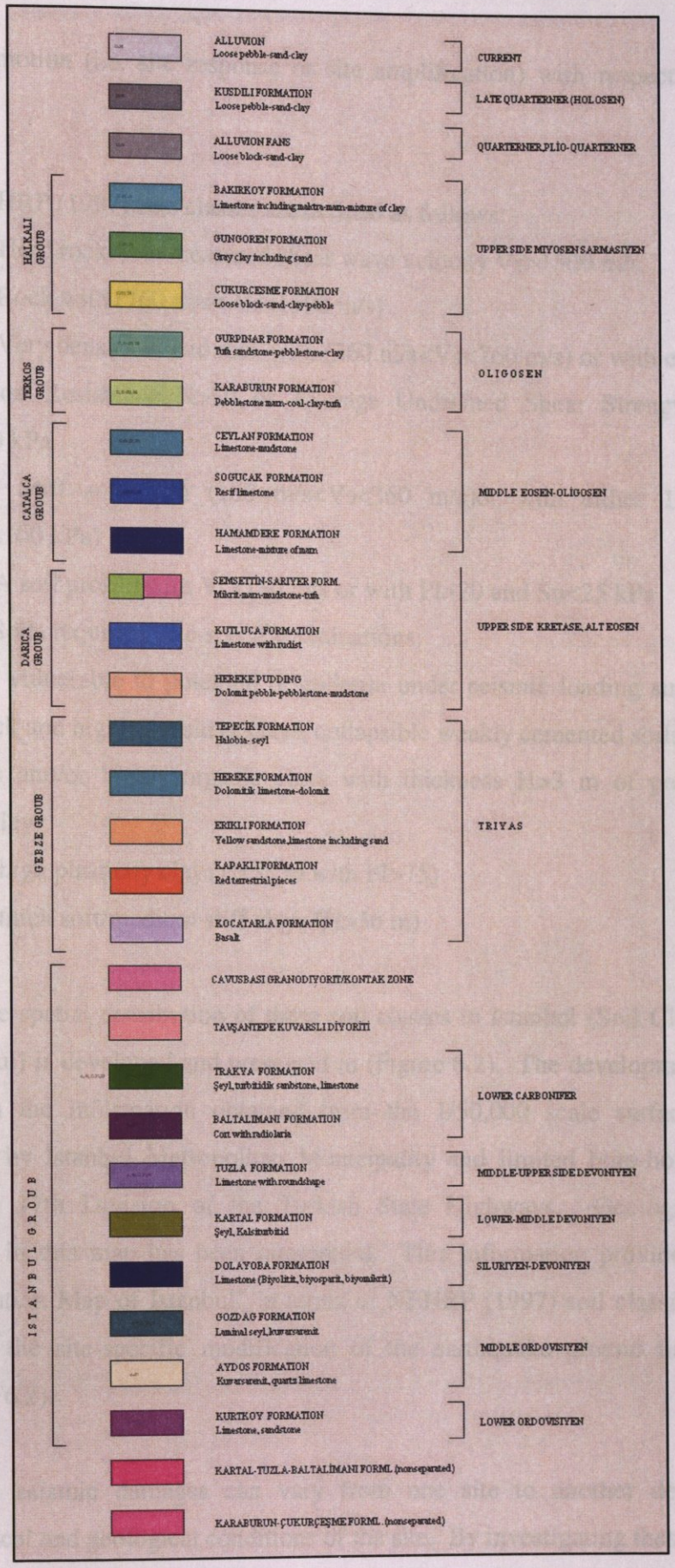

FIGURE 6.1B The surface geology map of İstanbul

ground motion (i.e. site response or site amplification) with respect to different site classes.

The NEHRP (1997) Site classes are defined as follows:

A class: Hard rock with measured shear wave velocity Vs>1500 m/s

B class: Rock with (760 m/s< Vs<1500 m/s)

C class: Very dense soil and rock with (360 m/s<Vs<760 m/s) or with either Standart Penetration Resistance N>50 or Average Undrained Shear Strength at top 30 m Su>=100 kPa

D class: Stiff soil with (180 m/s<Vs<360 m/s)or with either 15<N<50 or (50 kPa<Su<100 kPa)

E class: A soil profile with Vs<180 m/s or with PI>20 and Su<25 kPa

F class: Soils requiring site-specific evaluations:

1-) Soils vulnerable to potential or collapse under seismic loading such as liquefiable soils quick and highly sensitive clays, collapsible weakly cemented soils

2-) Peats and/or highly organic clays with thickness H>3 m of peat and/or highly organic clay

3-) Very high plasticity clays (H>8 m with PI>75)

4-) Very thick soft/medium stiff clays (H>36 m)

The spatial distribution of these soil classes in Istanbul (Soil Classification Map of Istanbul) is developed and presented in (Figure 6.2). The development is essentially based on the information obtained from the 1/50,000 scale surface geology map prepared by Istanbul Metropolitan Municipality and limited bore-hole data obtained from the 17th Division of the Turkish State Highways. Geological information provided in this map has been interpreted. This information provided by the "Soil Classification Map of Istanbul" in terms of NEHRP (1997) soil classifications will be used for the site-specific modification of the earthquake ground motion as shown in(Figure 6.2).

The seismic damages can vary from one site to another depending on the geotechnical and geological conditions of the site. By investigating these conditions of

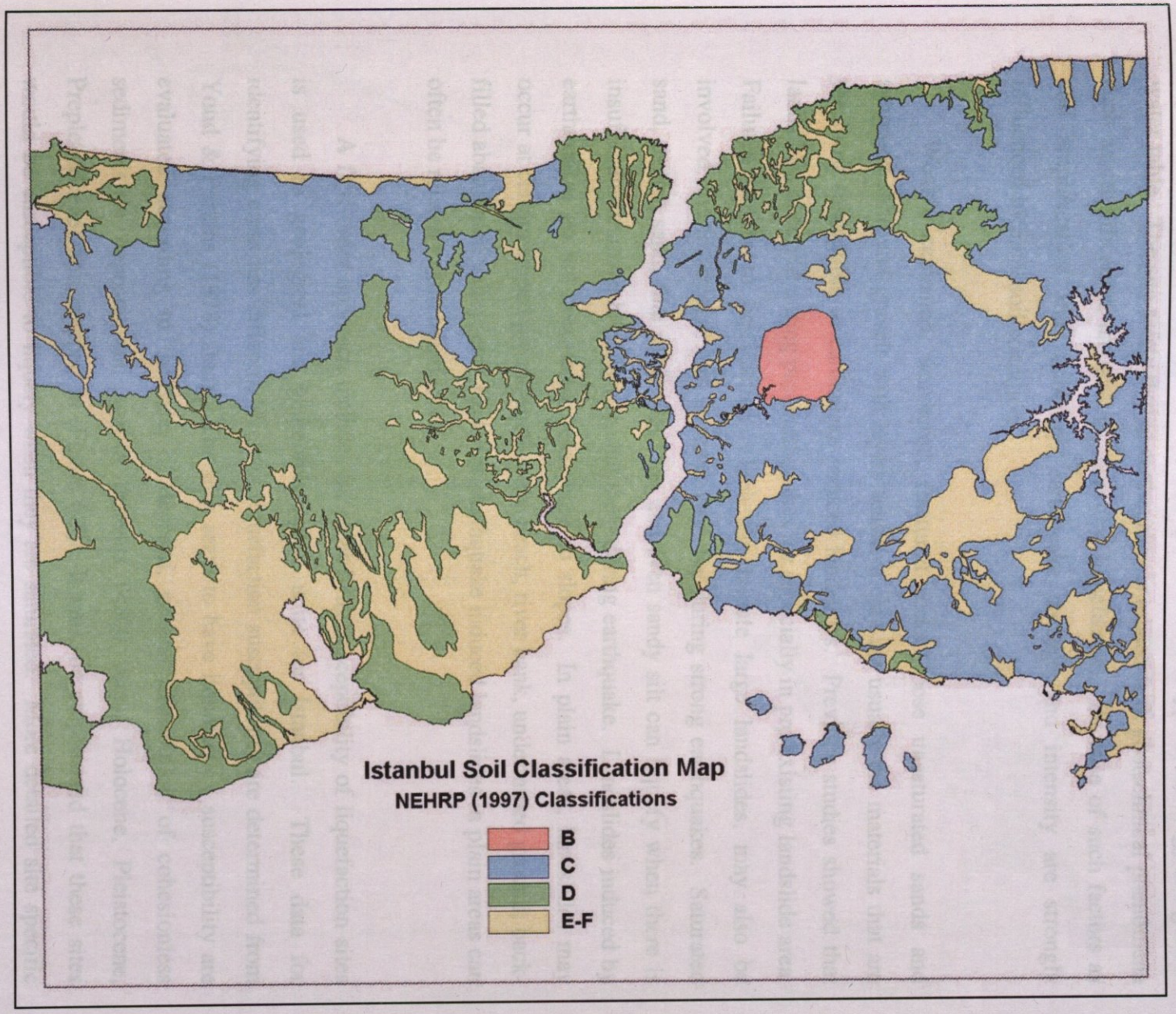

FIGURE 6.2 Soil classification of İstanbul according to NEHRP (1997) soil classes

the sites, it can be possible to estimate damage distribution and to reduce the potential earthquake hazards. The local geotechnical conditions can also be very different due to in thickness and properties of soil layers, depth of bedrock, type of lithology and ground water table. The site safety during earthquakes is related with geotechnical phenomena such as amplification, landsliding, mudflow, liquefaction. Because of such factors as soil amplification and instability, earthquake damage and intensity are strongly influenced by local soil conditions.

Weakly cemented, weathered, fractured rocks, loose unsaturated sands and saturated sand and gravels with layers sensitive clay are usually the materials that are the most susceptible to earthquake induced landslides. Previous studies showed that landslides occurred during past earthquakes are especially in pre-existing landslide area. Failures similar to liquefaction, which can initiate large landslides, may also be involved due to strength loss in sensitivity clay during strong earthquakes. Saturated sand, coarse sand, fine sand, silty sand and even sandy silt can liquefy when there is insufficient drainage boundary around them during earthquake. Landslides induced by earthquakes do not necessarily occur only on slopes. In plain areas, landslides may occur at certain sloped ground such as sea beach, river bank, undermined ground, back-filled abandoned valley, etc. However, earthquake induced landslides in plain areas can often be related to soil liquefaction.

A first-order approach includes for identifying susceptibility of liquefaction sites is used to geological and geomorphological units for Istanbul. These data for identifying areas has different levels of liquefaction susceptibility are determined from Youd & Perkins (1978) study. The sites seem to have liquefaction susceptibility are evaluated according to the type of deposits, general distribution of cohesionless sediments in deposits and age of deposits (<500 years, Holocene, Pleistocene, Prepleistocene) and mapped in (Figure 6.3). It must be emphasized that these sites would be susceptible to liquefy when they are saturated. More detailed site specific investigations includes ground water table and subsurface soil conditions have to be developed in these sites for carrying out some liquefaction analysis. The assessment of potential for landslide is one of the important considerations in the task of earthquake

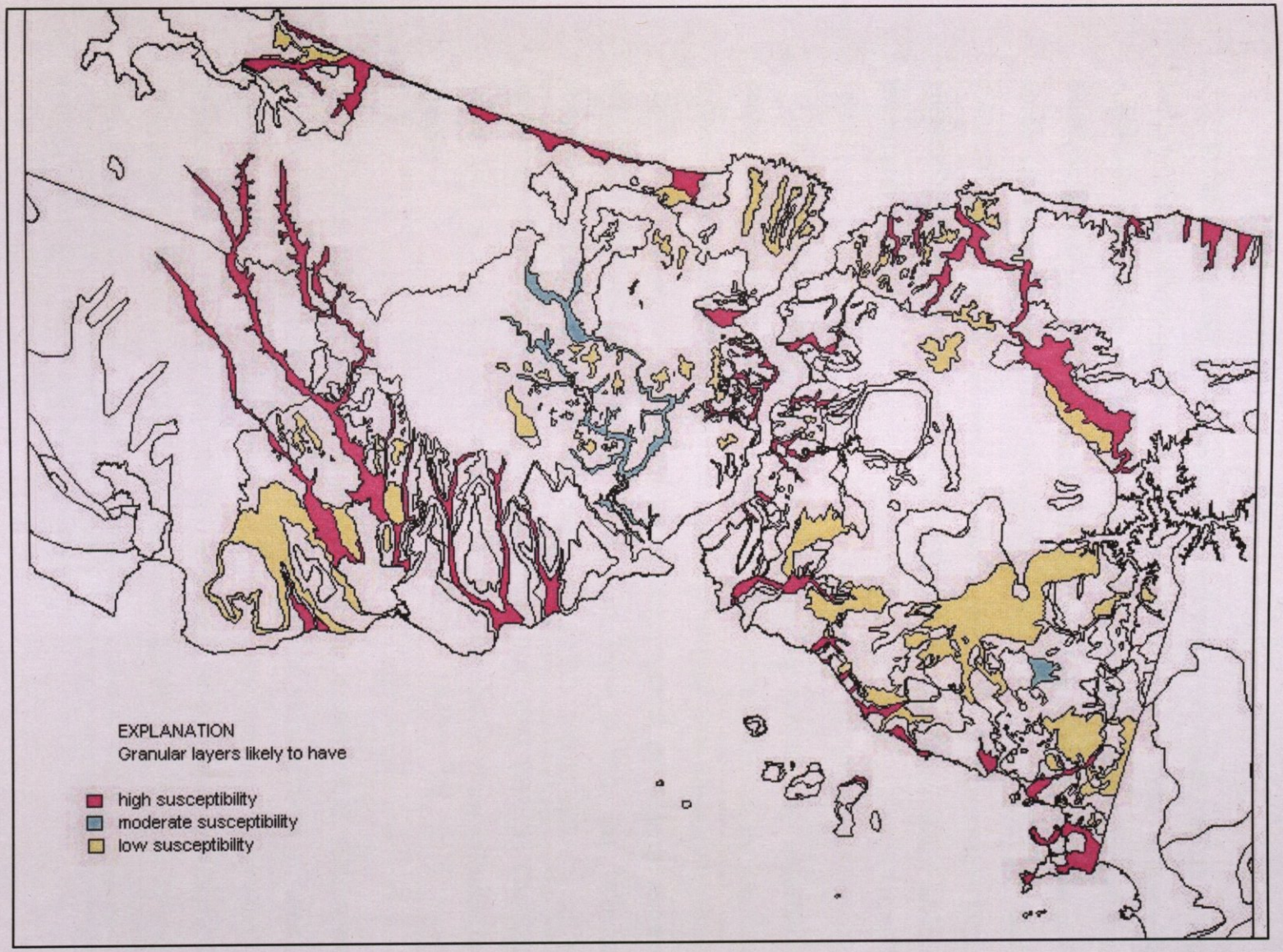

FIGURE 6.3 Liquefaction susceptibility map of İstanbul

risk assessment. Consequently, to find out pre-existing landslides, and more detailed information of these sites have to be need additional surveys for Istanbul.

7. ELEMENTS AT RISK AND VULNERABILITY

Vulnerability is defined as the degree of loss to a given element at risk, or a set of such elements, resulting from the occurrence of a hazard. The vulnerability is commonly expressed by matrices, that can be obtained by statistical studies of damaged structures in earthquake-striken areas (observed vulnerability) or by simulations using numerical models of structures or engineering calculations (predicted or calculated vulnerability) as a function of some parameter describing the earthquake size. Observed vulnerability is valid in a broad probabilistic sense. Calculated vulnerability is available the existing building.

As observed lifeline vulnerability functions are not directly available from earthquake damage patterns in Turkey; the damage ratios of the lifeline structures in İstanbul were assessed from functions that were adopted from studies on worldwide earthquakes. Almost the entire recent infrastructure in general, are designed and built to satisfy the international standards. Thus, it is believed that, the vulnerability observations acquired from world-wide earthquakes (ATC-13, 1985 and ATC-25, 1991) supplemented with the Turkish experience (mostly from 1992 Erzincan Earthquakes) can be used as a guide to describe the physical vulnerabilities of the infrastructure in İstanbul

In urban areas, buildings, population, lifeline systems and socio-economic activities constitute the "elements at risk". The physical vulnerabilities of elements at risk that result from a specified earthquake scenario necessitates extensive collection of an accurate inventory. Since currently, this inventory is not complete, the vulnerabilities were broadly studied in the following categories: buildings, transportation systems, telecommunication systems, electrical distribution systems, water and waste water system, natural gas systems and building content.

Building Inventory

Building inventory in terms of footprints exist in MapInfo format based on aerial photos from 1995 and 1998 for the greater Istanbul area. The existing inventory however lacks data such as number storeys, construction date, and construction type. However, another data source, State Statistical Institute, (SSI, Devlet Istatistik Enstitüsü), has done an inventory of buildings in 2000 and it has been supplied from the institute however it lacks of street address data. The data includes the construction year, the purpase of usage, the construction type, and the storey number of the building. The complete SSI building inventory data will be published in the near future. The data that comes from different sources has been and will be correlated between each other in different techniques. In the correlations produced in this study, lowrise (1-3 storey), midrise (4-8 storey) and highrise (9 or more storey) buildings in İstanbul were analyzed as reinforced concrete also masonry buildings was included in such analysis. Density of such buildings count were shown respectively in (Figure 7.1 - 7.2 - 7.3 - 7.4)

Infrastructure Inventory

The infrastructure facilities in Istanbul that has been studied following includes:
Electric system: Electric power transmission substations
Water System: Waste water reservoir, pumping stations and distribution lines
Transportation: Highway and bridges, viaducts and overpasses
Natural Gas: Distribution system
Telecommunication Systems: Distribution of administrative buildings and switchboards

Links have been established with the following institutions: Istanbul Metropolitan Municipality, ISKI (Istanbul Water and Sewer Administration), Turkish Telecommunication Administration, IGDAS (Istanbul Natural Gas Distribution Association), BEDAS (Beyazid Electricity Distribution Association) and General Directorate of Highways.

Data, obtained from these institutions in digital format and most of the time in raw form, have been transferred into GIS (Geographic Information System). The existing

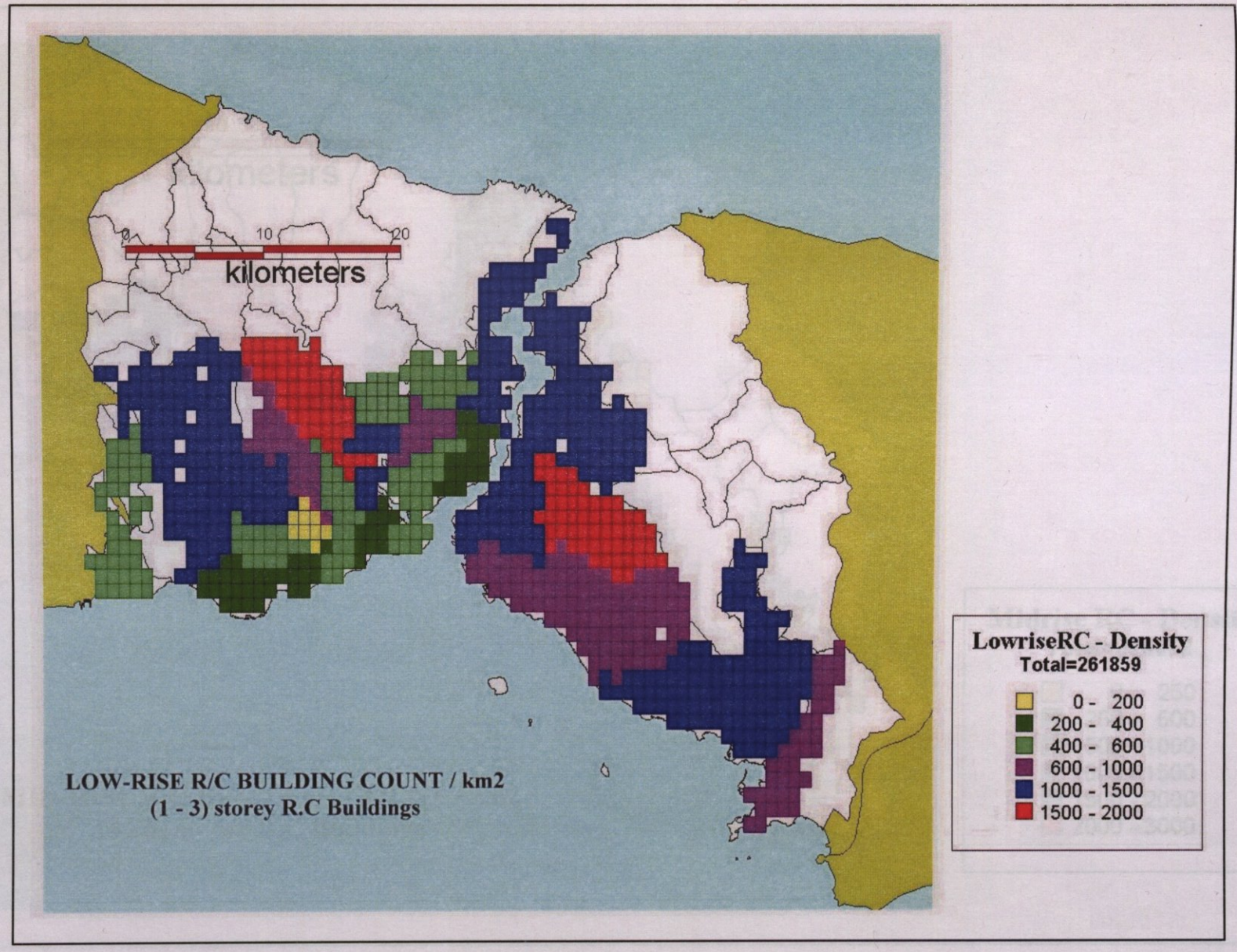

FIGURE 7.1 Low-Rise (1-3 storey) R/C building density (SSI,2000)

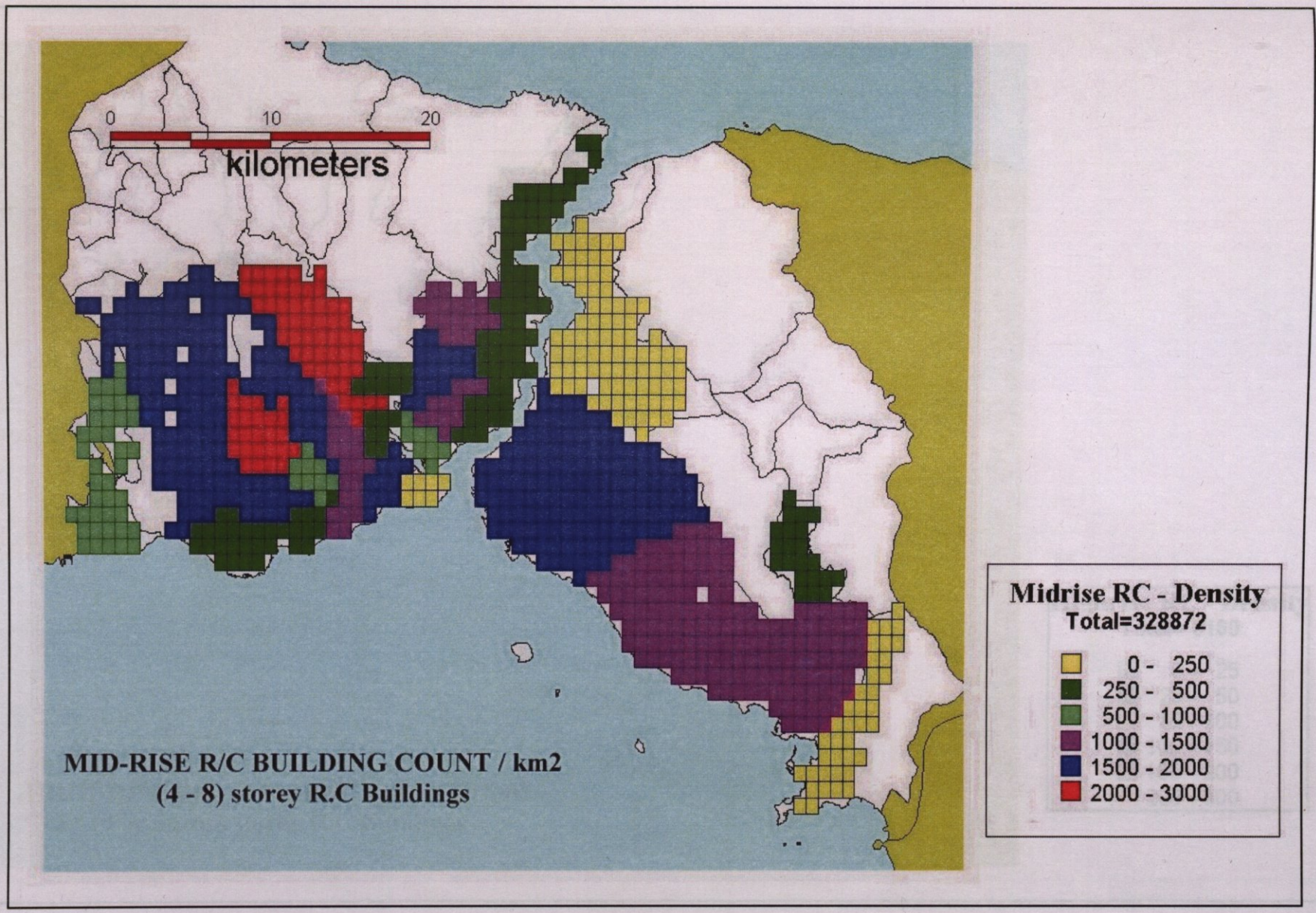

FIGURE 7.2 Mid-Rise (4-8 storey) R/C building density (SSI,2000)

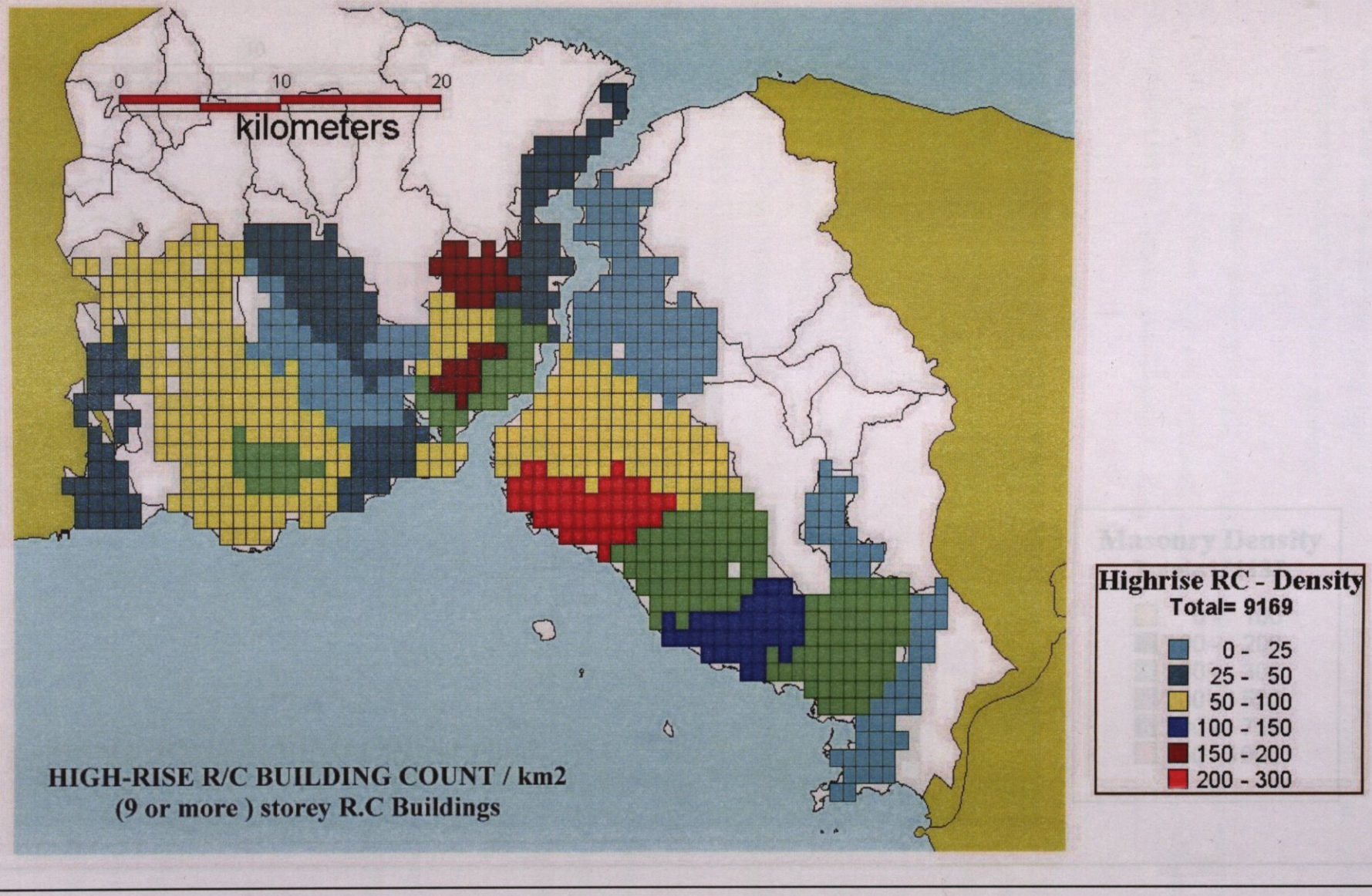

FIGURE 7.3 High-Rise (9 or more storey) R/C building density (SSI,2000)

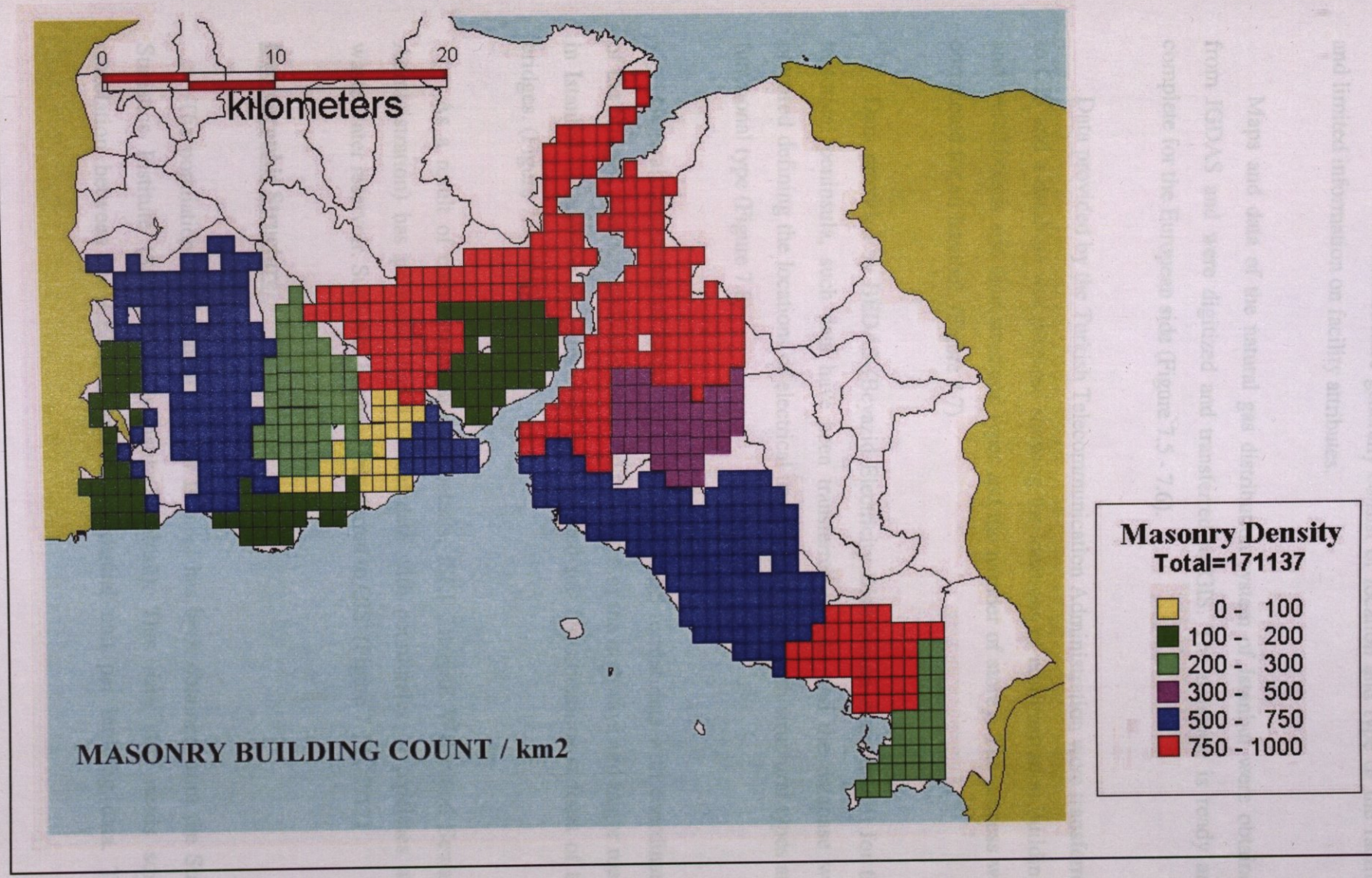

FIGURE 7.4 Masonry building density (SSI,2000)

GIS data about the infrastructure generally consist of location and type of the facility and limited information on facility attributes.

Maps and data of the natural gas distribution system of Istanbul were obtained from IGDAS and were digitized and transferred to GIS. The database is ready and complete for the European side (Figure 7.5 - 7.6).

Data provided by the Turkish Telecommunication Administration were transferred to GIS and a database was prepared showing the locations of administration buildings and switchboards and their structural types and the number of storey. The process was completed for all Istanbul. (Figure 7.7)

Data provided by BEDAS (Beyazid Electricity Distribution Association) for the historical peninsula, such data have been transferred to GIS and the database was prepared defining the locations of electrical transformers their both structural types and functional type (Figure 7.8)

General Directorate of Highways has provided GIS format data with coordinates of the bridges, viaducts and overpasses and the routes of the highways and major roads in Istanbul. In addition the directorate has provided soil classifications at foots of the bridges. (Figure 7.9 - 7.10)

As a result of communication and contacts, ISKI (Istanbul Water and Sewage Administration) has provided digital format data with coordinates of pipelines and waste water reservoir. Such data has been transferred to GIS (Figure 7.11 - 7.12)

Demographic Structure

The population and building data for Istanbul has been obtained from the State Statistics Institute (SSI, Devlet Istatistik Enstitüsü). This data also needs some correlation between the CENSUS and the residential unit per building data. The

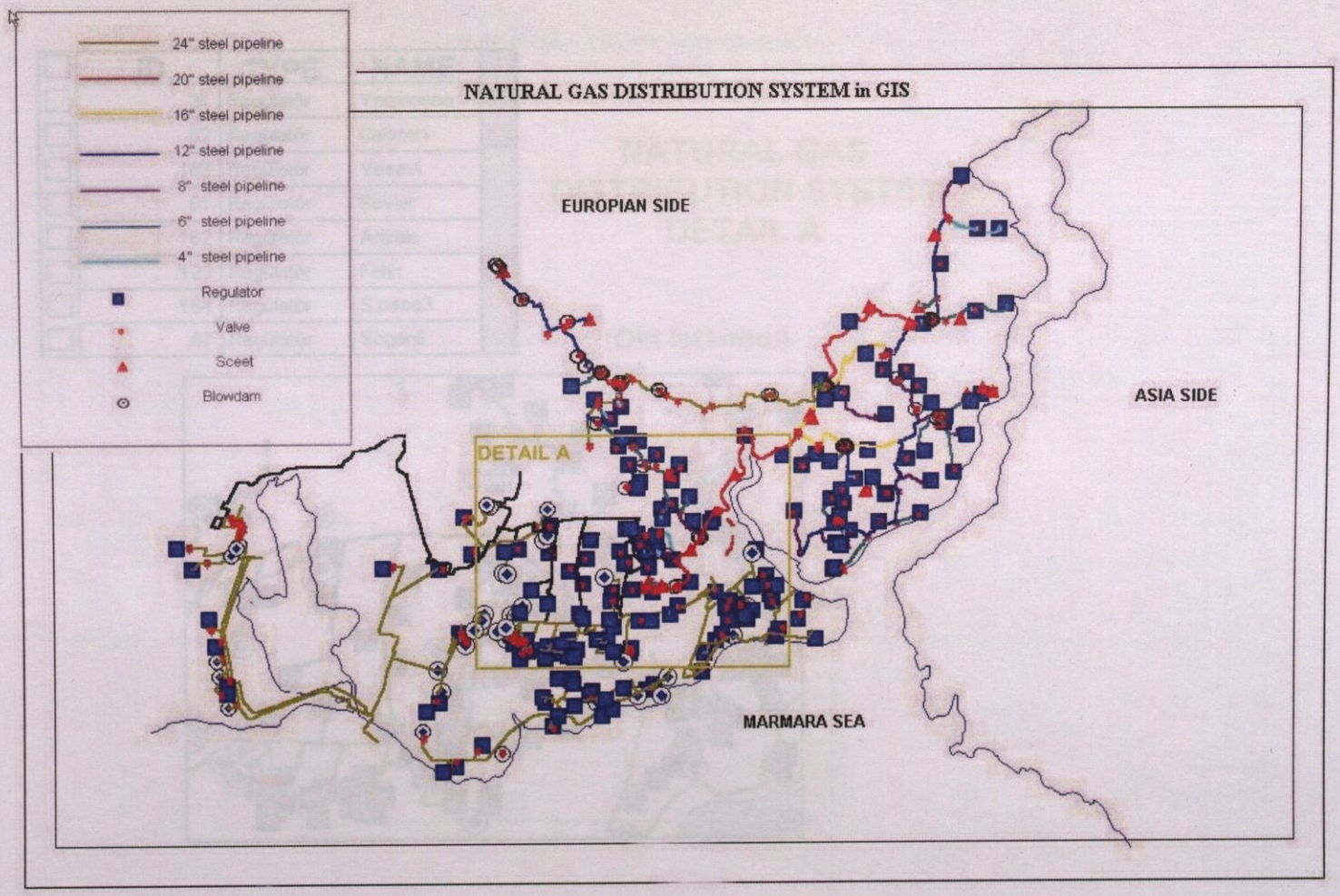

FIGURE 7.5 Natural gas system of İstanbul in GIS

ID	TYPE	NAME
31	Regülatör	Yenibosna
62	Regülatör	Cakmak
163	Regülatör	Yesevi
61	Regülatör	Sevler
162	Regülatör	Askale
123	Regülatör	Fetih
164	Regülatör	S.pasa3
57	Regülatör	Soganli

NATURAL GAS
DISTRIBUTION SYSTEM
DETAIL A

(Old Istanbul)

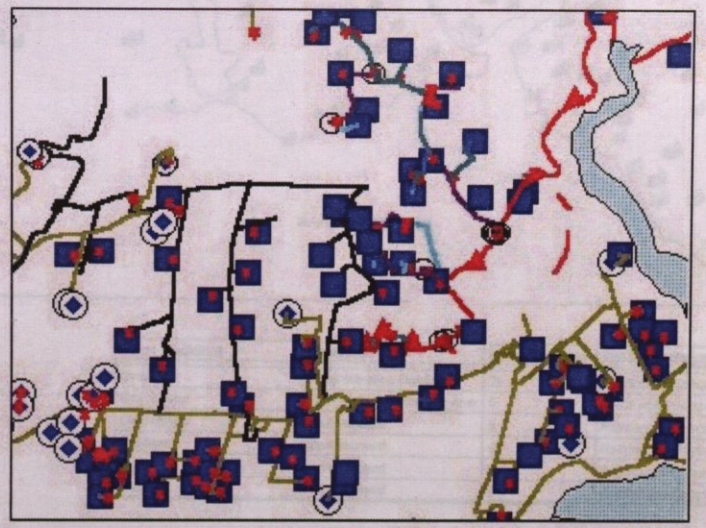

FIGURE 7.6 Detail "A" of natural gas system in GIS

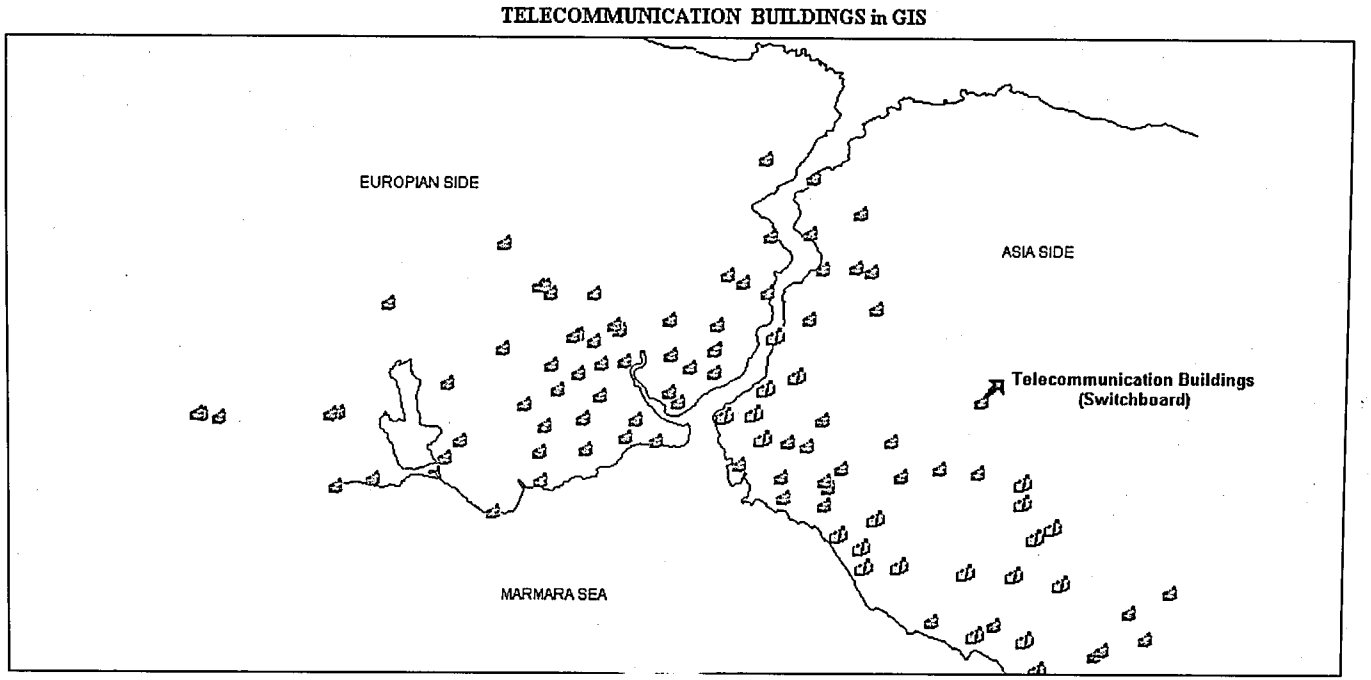

Name_Building	Function	Story_Building	Type_Structure
Besiktas	Administration Building	22	Reinforced Concrete
Gayrettepe	Telecommunication Service:	5	Reinforced Concrete
Gayrettepe	Switchboard	5	Reinforced Concrete
Besiktas	Switchboard	4	Reinforced Concrete
Levent	Switchboard	4	Reinforced Concrete
Bebek	Switchboard	4	Reinforced Concrete

FIGURE 7.7 Telecommunication system of İstanbul in GIS

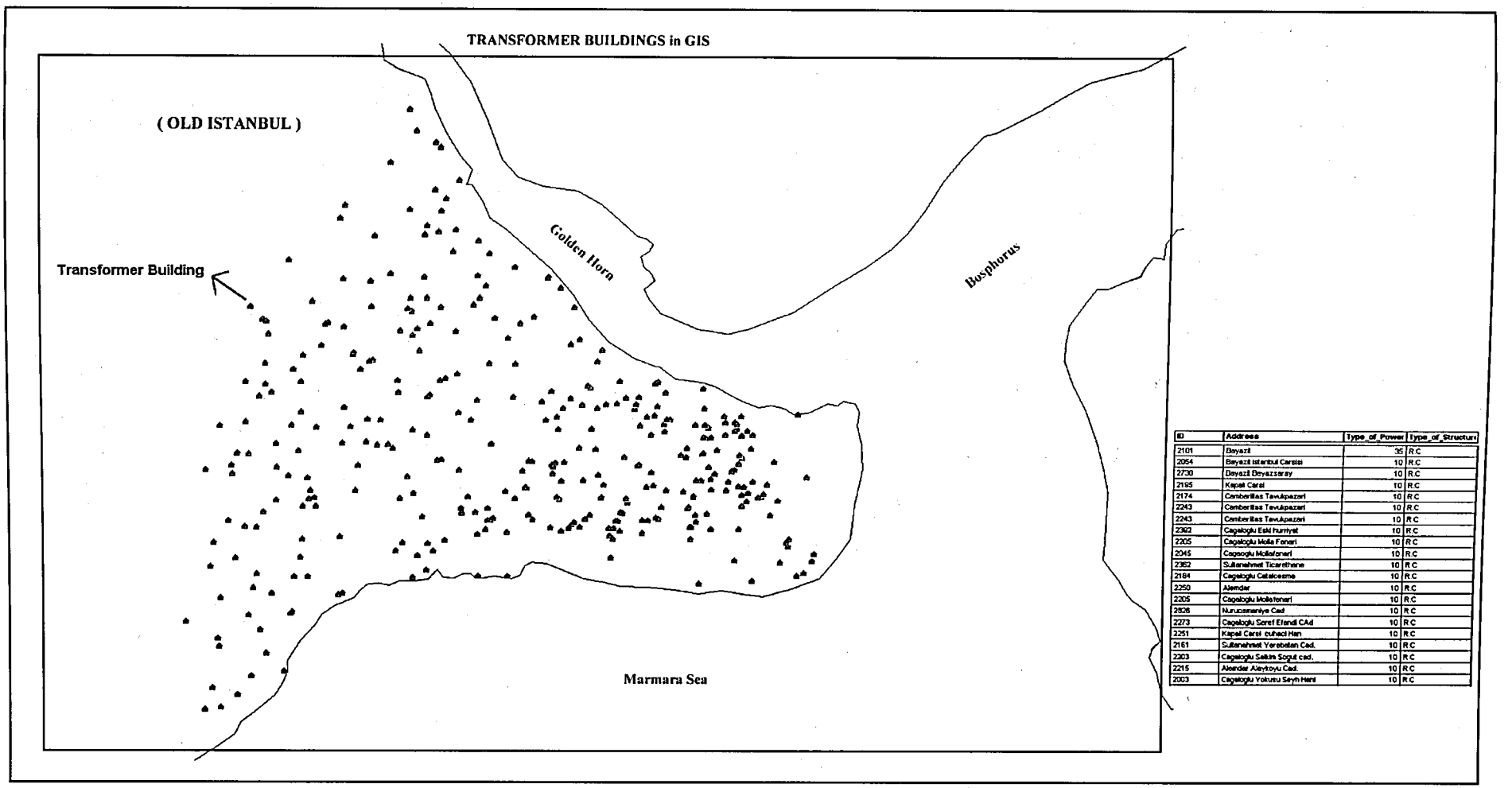

ID	Address	Type_of_Power	Type_of_Structure
2101	Bayazit	35	R C
2054	Bayazit istanbul Carsisi	10	R C
2730	Bayazit Beyazsaray	10	R C
2195	Kapali Carsi	10	R C
2174	Camberlitas Tevkipazari	10	R C
2243	Camberlitas Tevkipazari	10	R C
2243	Camberlitas Tevkipazari	10	R C
2302	Cagaloglu Eski hurriyet	10	R C
2205	Cagaloglu Molla Fenari	10	R C
2045	Cagaoglu Mollafenari	10	R C
2352	Sultanahmet Ticarethane	10	R C
2184	Cagaloglu Cataleesma	10	R C
2250	Alemdar	10	R C
2205	Cagaloglu Mollafenari	10	R C
2826	Nurucsmaniye Cad	10	R C
2273	Cagaloglu Soref Efendi CAd	10	R C
2251	Kapal Carsi cuhaci Han	10	R C
2161	Sultanahmet Yerebatan Cad.	10	R C
2303	Cagaloglu Sakirs Sogut cad.	10	R C
2215	Alemdar Aleykoyu Cad	10	R C
2003	Cagaloglu Yokusu Seyh Heni	10	R C

FIGURE 7.8 Electrical transformers of Old Istanbul in GIS

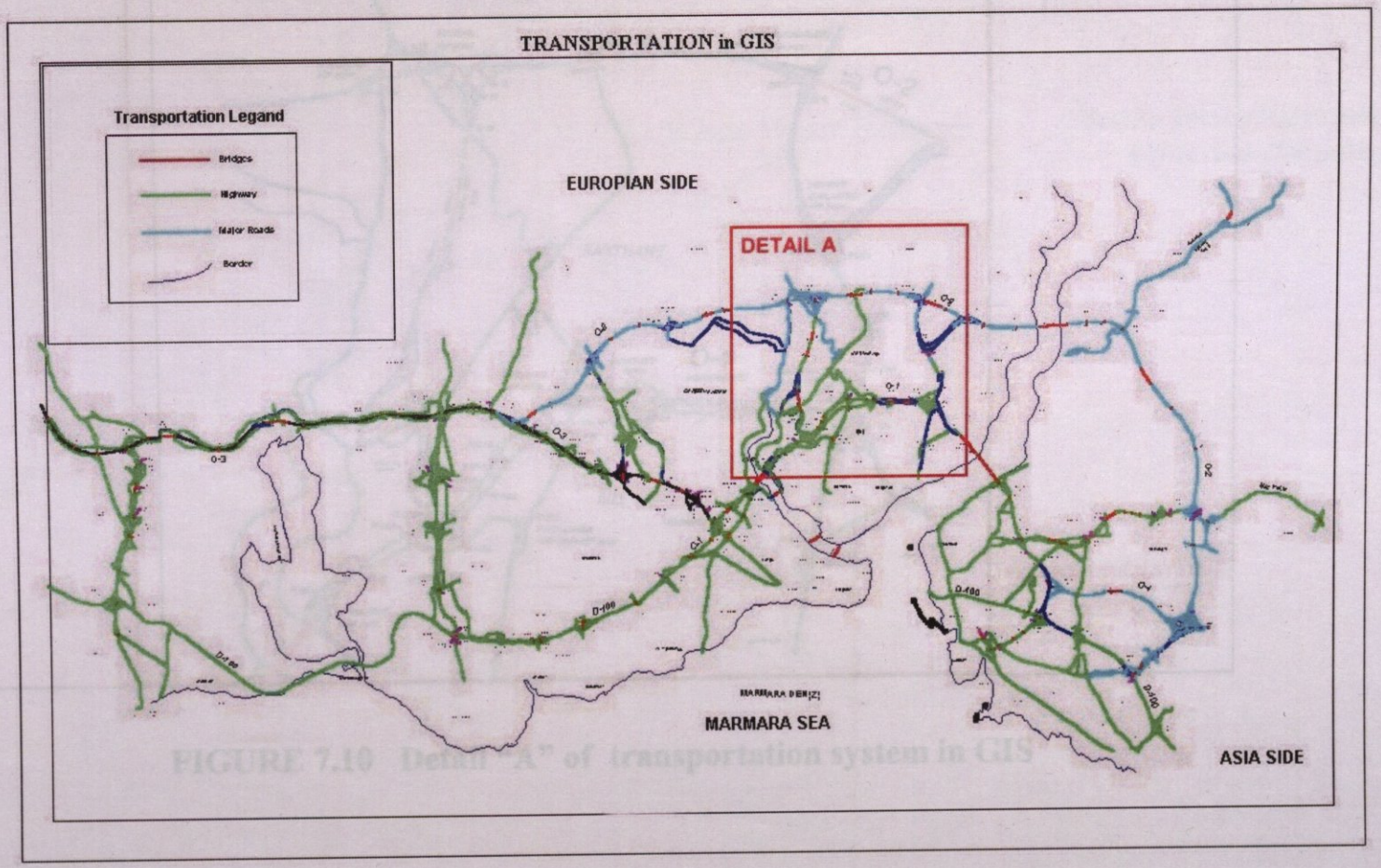

FIGURE 7.9 Transportation system of Istanbul in GIS

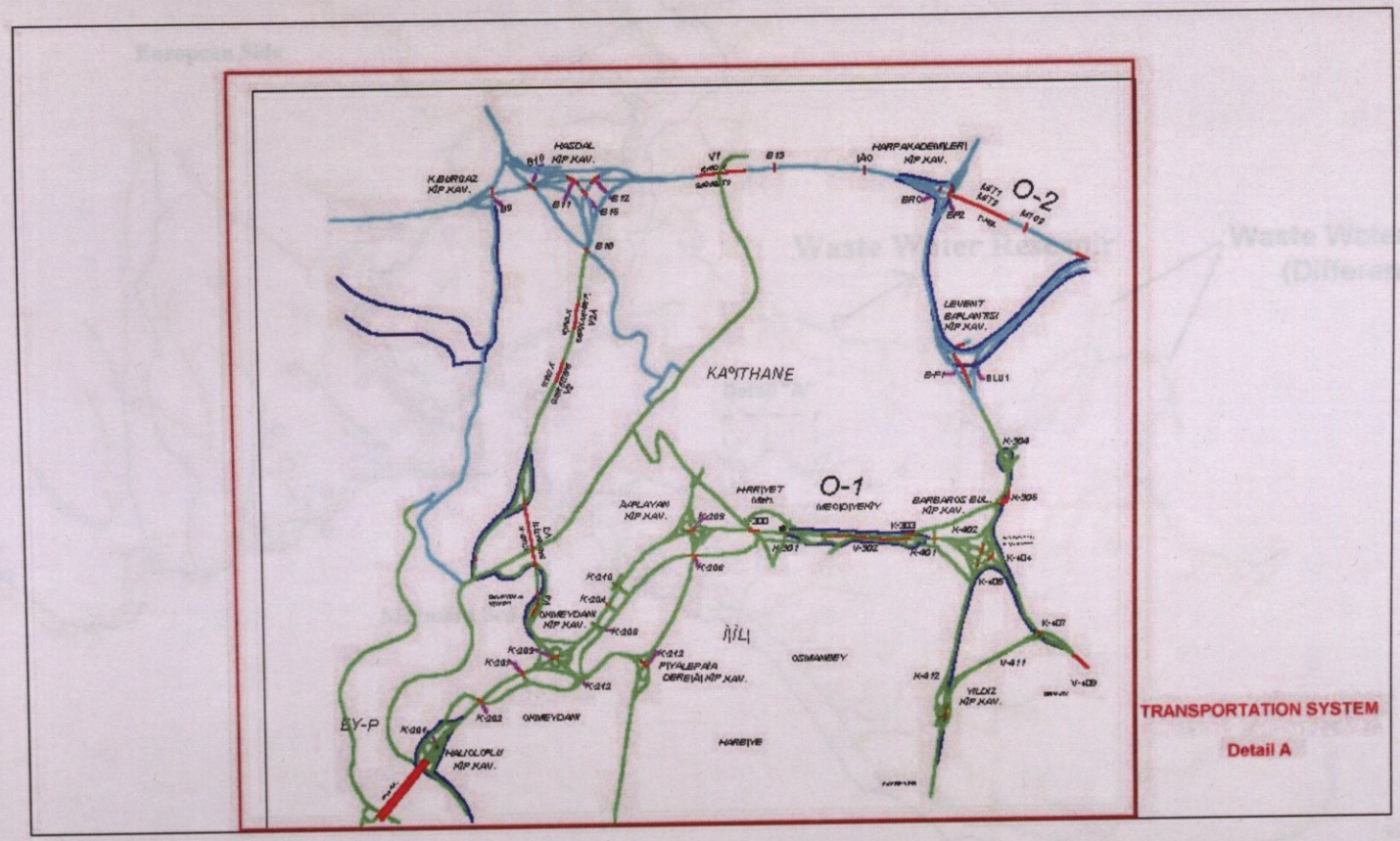

FIGURE 7.10 Detail "A" of transportation system in GIS

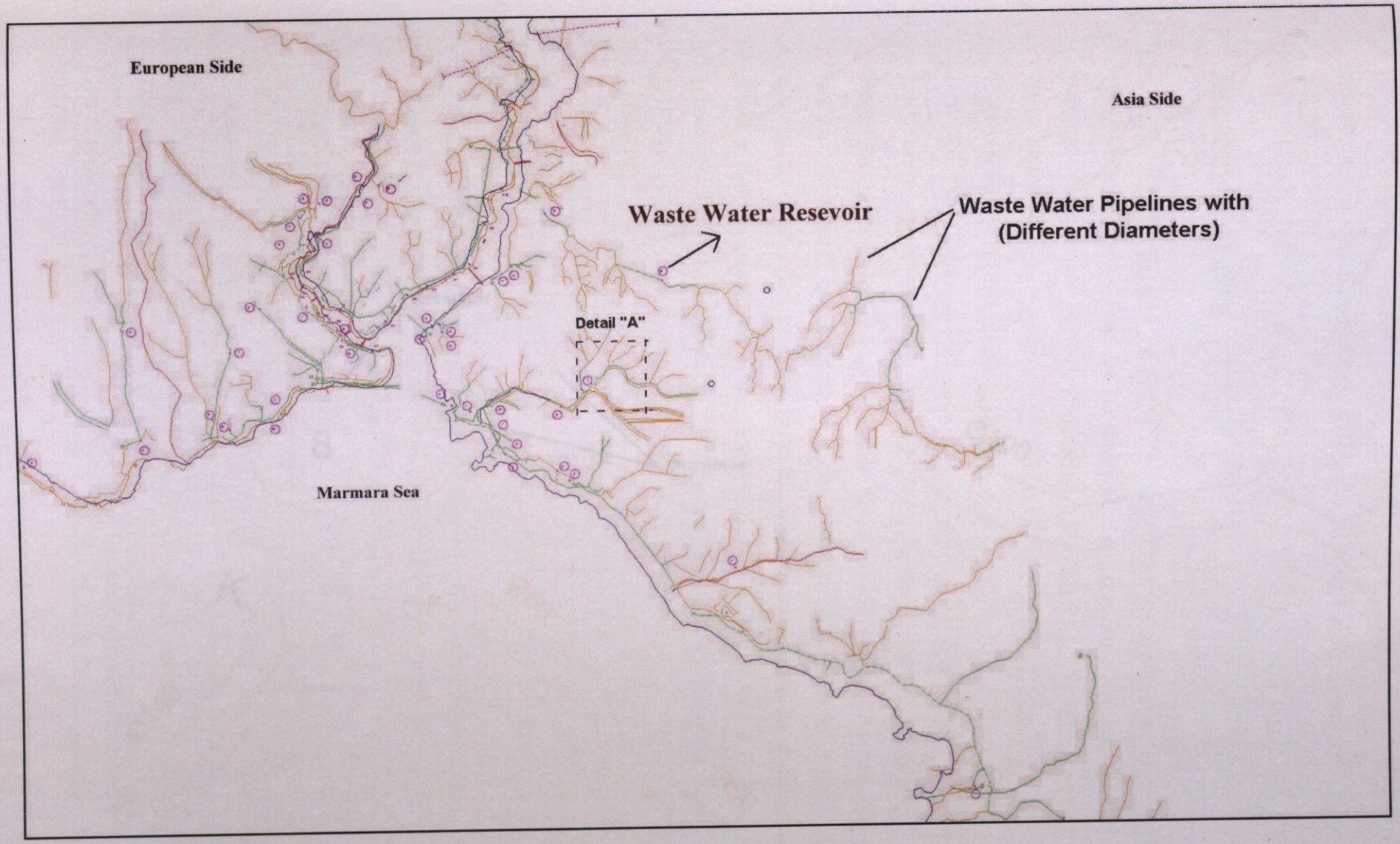

FIGURE 7.11 Waste water distribution of Istanbul in GIS

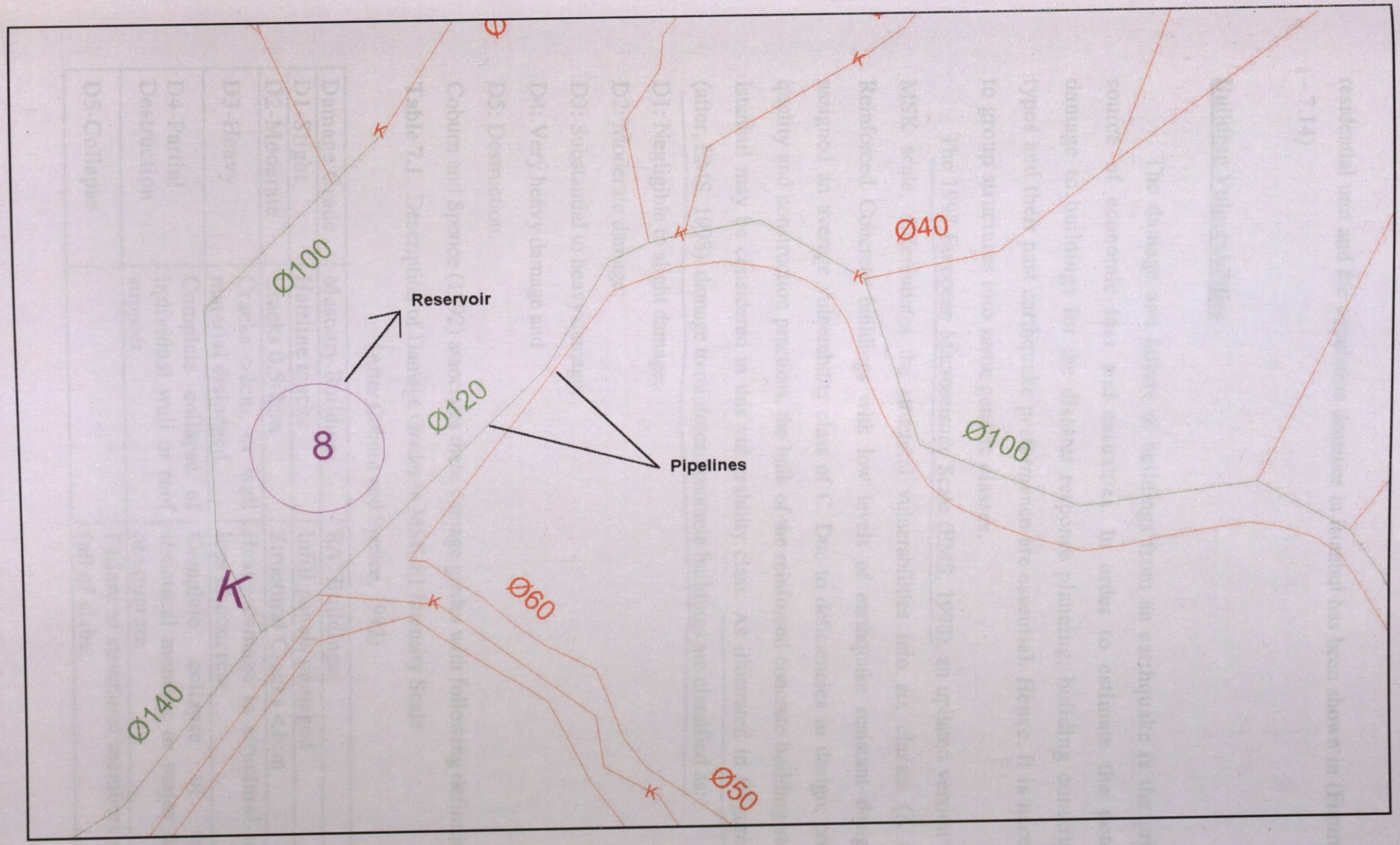

FIGURE 7.12 Detail "A" of waste water distribution system in GIS

residential unit and the population densities in Istanbul has been shown in (Figure 7.13 – 7.14)

Building Vulnerabilities

The damage and failure of buildings from an earthquake is the primary source of economic loss and casualties. In order to estimate the potential damage to buildings for the disaster response planning, building construction types and their past earthquake performance are essential. Hence, it is necessary to group structures into some generic classes.

The 1998 European Macroseismic Scale (EMS, 1998), an updated version of the MSK scale, differentiates the structural vulnerabilities into six classes (A to F). Reinforced Concrete buildings with low levels of earthquake resistant design are assigned an average vulnerability class of C. Due to deficiencies in design; concrete quality and construction practices, the bulk of the reinforced concrete building stock in Istanbul may be considered in this vulnerability class. As illustrated in (Figure 7.15) (after, EMS, 1998), damage to reinforced concrete buildings are classified as:

D1: Negligible to slight damage;

D2: Moderate damage;

D3: Substantial to heavy damage;

D4: Very heavy damage and

D5: Destruction.

Coburn and Spence (1992) associates these damage grades with following definitions:

Table 7.1 Description of Damage Grades in MSK-81 Intensity Scale

(After Coburn and Spence, 1992)

Damage Grade	Masonry Buildings	R/C Buildings
D1-Slight	Hairline cracks	Infill panels damaged
D2-Moderate	Cracks 0.5-2cm	Structural Cracks <1cm
D3-Heavy	Cracks >2cm. or wall material dislodged	Heavy damage to structural members, loss of concrete
D4-Partial Destruction	Complete collapse of individual wall or roof support	Complete collapse of individual structural member or major deflection of structure
D5-Collapse		Failure of structural members to allow fall of slabs.

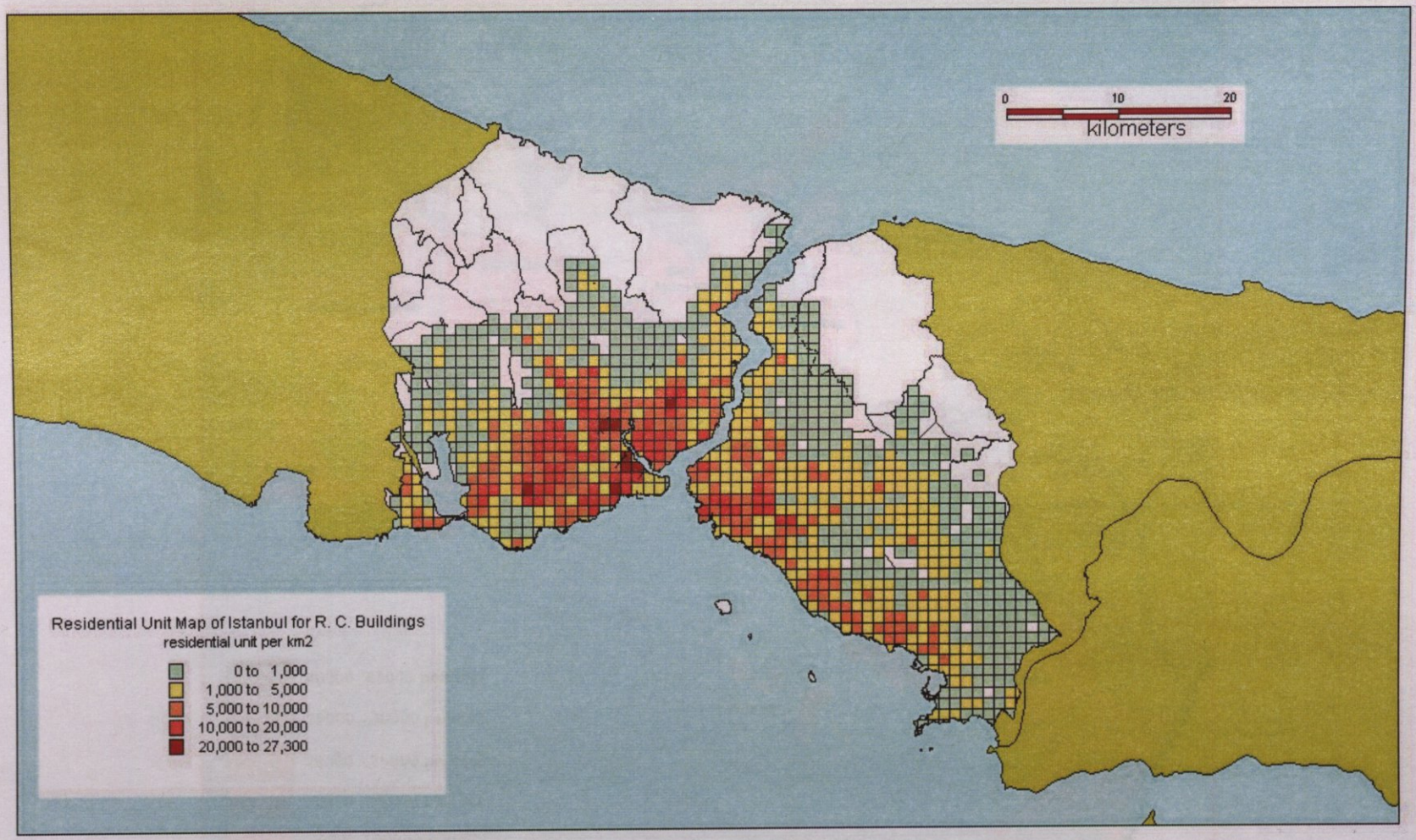

FIGURE 7.13 Density of residential units in reinforced concrete structures in Istanbul

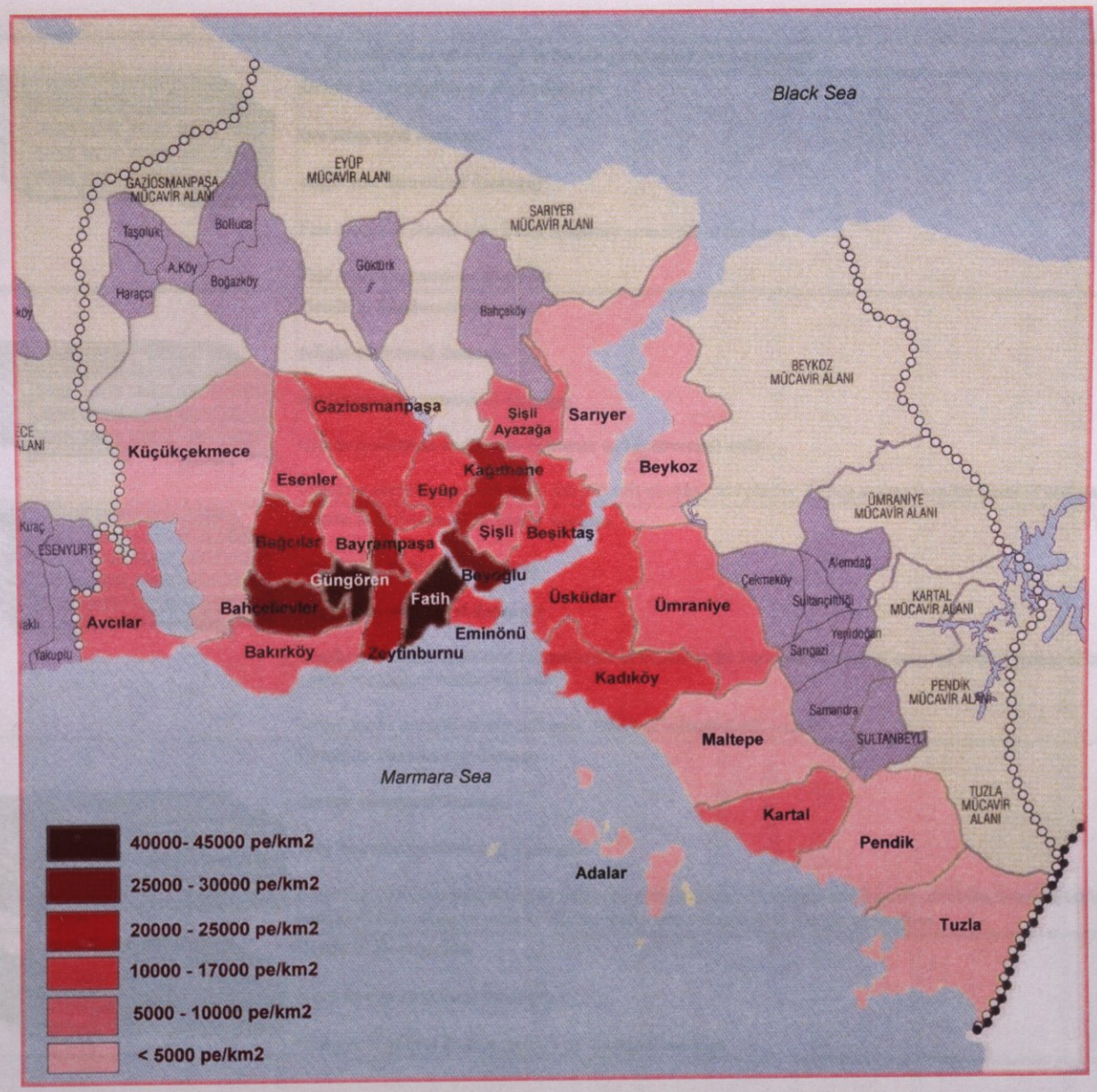

FIGURE 7.14 Population density in Istanbul

Classification of damage to buildings of reinforced concrete	
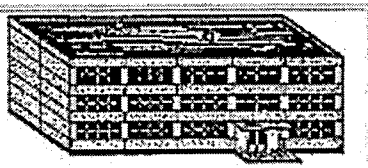	**Grade 1: Negligible to slight damage** **(no structural damage,** **slight non-structural damage)** Fine cracks in plaster over frame members or in walls at the base. Fine cracks in partitions and infills.
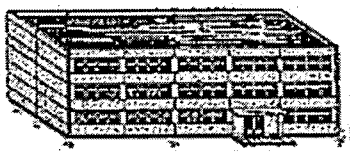	**Grade 2: Moderate damage** **(slight structural damage,** **moderate non-structural damage)** Cracks in columns and beams of frames and in structural walls. Cracks in partition and infill walls, fall of brittle cladding and plaster. Falling mortar from the joints of wall panels.
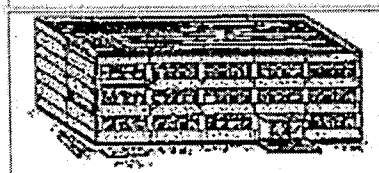	**Grade 3: Substantial to heavy damage** **(moderate structural damage,** **heavy non-structural damage)** Cracks in columns and beam column joints of frames at the base and at joints of coupled walls. Spalling of concrete cover, buckling of reinforced rods. Large cracks in partition and infill walls, failure of individual infill panels.
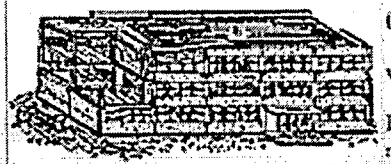	**Grade 4: Very heavy damage** **(heavy structural damage,** **very heavy non-structural damage)** Large cracks in structural elements with compression failure of concrete and fracture of rebars; bond failure of beam reinforced bars; tilting of columns. Collapse of a few columns or of a single upper floor.
	**Grade 5: Destruction** **(very heavy structural damage)** Collapse of ground floor or parts (e. g. wings) of buildings.

FIGURE 7.15 Damage grades for reinforced concrete buildings, EMS 1998

The ratio of the cost of repair of the damage to the cost of reconstruction, expressed as the Repair-Cost Ratio, corresponding to the damage grades D1 through D5 can be approximately given as 0.05, 0.20, 0.50, 0.80 and 1.0. Damage levels encompassing damages D3, D4 and D5 (i.e. D>=D3) is an important descriptor of the earthquake damage since D3 represents an approximate borderline between repair and replacement of the building stock exposed to an earthquake.

For the vulnerability class C EMS (1998) provides the following definitions of intensity:

Intensity VI: A few buildings of vulnerability class C sustain Damage of grade 1.

Intensity VII: A few buildings of vulnerability class C sustain damage of grade 2.

Intensity VIII: Many buildings of vulnerability class C suffer damage of grade 2;
a few of grade 3.

Intensity IX: Many buildings of vulnerability class C suffer damage of grade 3;
a few of grade 4.

Intensity X: Many buildings of vulnerability class C suffer damage of grade 4;
a few of grade 5.

Where "Few" describes less than 20% and "Many" describes between 20% and 60%.

The vulnerabilities of Turkish building stock are at least an order of magnitude higher than their counterparts in California. The reasons for this high vulnerability can be traced back to several reasons. Essentially the building development system was conducive to poor construction due to high (chronic) rate of inflation (consequently very limited mortgage and insurance, impediment to large scale development and industrialization of the construction sector), high rate of urbanization (which created the demand for inexpensive housing), ineffective control/supervision of design/construction, regulations with limited enforcement and no accountability and government acting as a free insurer of earthquake risk

Istanbul is the most crowded city in Turkey with a total population about 15 million. Following types of buildings dominate the building stock in Istanbul. An inventory of the different types of buildings and their potential risks is beyond the scope of this study. Therefore, the building classification was mainly performed based on visual inspection. On the basis of earthquake performance of the buildings in İstanbul, the rural and urban building stock can be classified under the groups of; 1) Unreinforced brick masonry, dressed stone and concrete block masonry (no ring beam), 2)Reinforced Concrete Frame with Unreinforced Masonry Infill, 3)Dual Reinforced Concrete Frame and RC Shear Wall System, 4) Precast Concrete Frame

Unreinforced Brick Masonry

They are usually low rise (up to three storeys) buildings. The structure consists of load-bearing fired brick in a cement or lime mortar. Horizontal structure is commonly timber beams, or reinforced concrete slabs. The use of timber or reinforced concrete lintels and ring-beam is more common in the better-built houses. Roofs with timber trusses covered by tiles or flat reinforced concrete slabs are common. Many of the older buildings are of this type, often ornate and sometimes with stone masonry quoins or stone masonry facades. Some monumental buildings (mosques, old public buildings etc.) are in load-bearing brick, but their massive construction would be expected to have a different vulnerability function to the residential structures described here.

In Table 7.2 and 7.3 vulnerability rates proposed by different authors are provided.

Table 7.2 Vulnerability Ratios for Brick, Dressed Stone and Concrete Block Masonry (No Ring Beam) Buildings. Percent Damage (Heavy Damage to Collapse, D>=D3)

MSK INTENSITY LEVEL

Source	MSK-Intensity					
	V	VI	VII	VIII	IX	X
Ergünay and Erdik(1984)	2	5	25	40	80	
Coburn and Spence (1992)						
Concrete Block Masonry			5-15	15-35	35-60	60-80
Dressed Stone Masonry			15-35	35-60	60-80	80-92
Brick Masonry			10-25	25-50	50-75	75-90

Table 7.3 Vulnerability Ratios for Good Quality Masonry (with ring beam) Buildings

Percent Damage (Heavy Damage to Collapse, D>=D3)

MSK INTENSITY LEVEL

Source	MSK-Intensity					
	V	VI	VII	VIII	IX	X
Ergünay and Erdik (1984)			10	20	75	
Coburn and Spence (1992)			2-8	8-20	20-50	70-70

The empirical damage ratios for the Unreinforced Brick Masonry buildings for different intensities are provided in Table 7.4 (after, CAR and BU, 2000). The damage distribution figure for masonry buildings in İstanbul was shown in (Figure 7.16) concerning to Table 7.4

Table 7.4 Vulnerability Functions for Unreinforced Brick Masonry

Expected Damage Ratio MDR(%) for MSK Intensity Levels

Following values were found utilizing from (Figure 7.17)

I-MSK	**5.0**	**5.5**	**6.0**	**6.5**	**7.0**	**7.5**	**8.0**	**8.5**	**9.0**	**9.5**	**10.0**	**10.5**	**11.0**
MDR	-	-	-	-	2.5	5	10.8	19.2	30.8	43.3	55	66.7	79.2

Reinforced Concrete Frame with Unreinforced Masonry Infill

This is the most common building type in Istanbul. The most common type of reinforced concrete structure is the cast-in-situ reinforced concrete frame with masonry infill walls. The height of most of these buildings is 1 to 8 storeys, but in Istanbul and other major cities, high-rise structures of 10 to 20 storeys are now numerous. Ground floors are often left open for shops. Buildings with irregular plan shape are common due to irregular land lots and urban congestion. For infill walls 20-30 cm thick horizontally perforated burned clay bricks or concrete blocks are used with no reinforcement.

In this century only a limited number earthquakes in Turkey have affected urban areas. The following vulnerability matrices for non-engineered multistory reinforced concrete frame buildings. The vulnerability data obtained from 1976 Denizli, 1971 Bingöl, 1992 Erzincan earthquakes (Bayülke, 1982; Şengezer, 1993; Kandilli, 1992) are presented in Table 7.5.

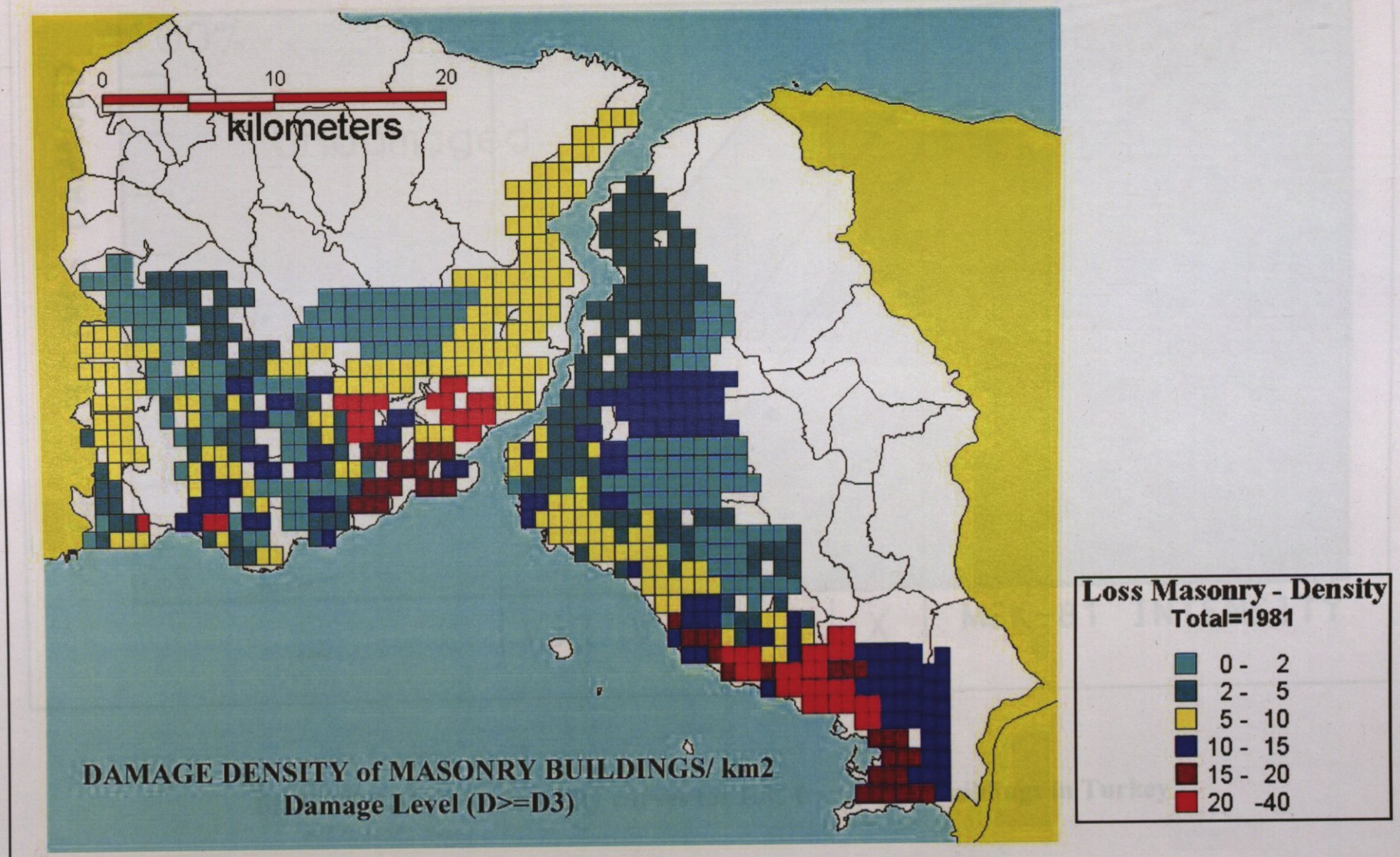

FIGURE 7.16 Damage density of masonry building

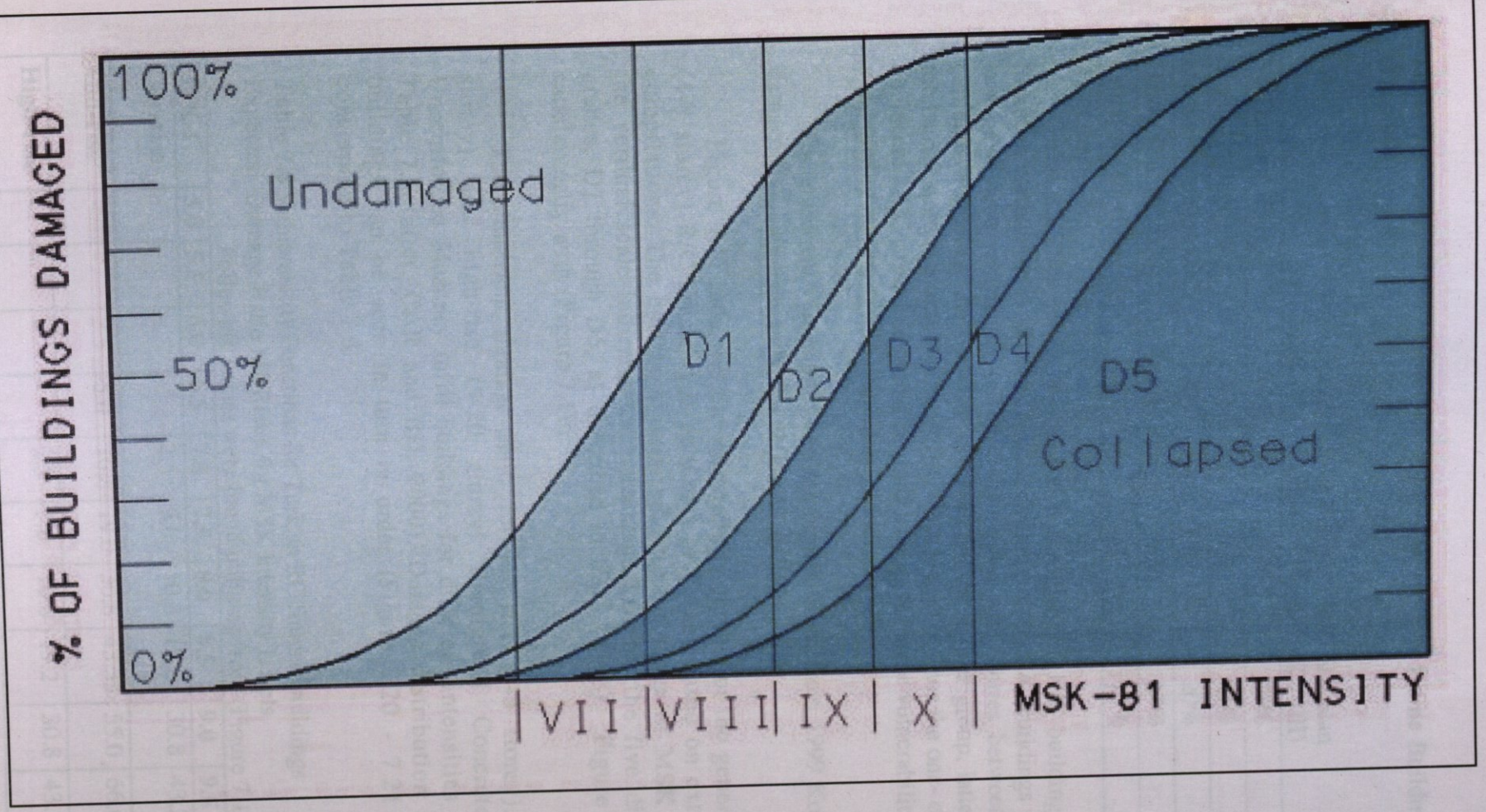

FIGURE 7.17 Vulnerability curves for R/C frame type buildings in Turkey

Table 7.5 Vulnerability Matrix for Non-Engineered R/C Frame Buildings (Percentage of the total stock)

	1976 Denizli (I-MSK=VI)	1971 Bingöl (I-MSK=VIII)	1992 Erzincan (I-MSK=VIII)
No Damage (D0)	40%	16%	25%
Slight Damage (D1)	38%	27%	25%
Medium Damage (D2)	17%	36%	20%
Heavy Damage (D3)	5%	15%	17%
Collapse (D4+D5)	-	6%	13%

These statistics belong to the total non-engineered R/C building stock. In 1992 Erzincan earthquake (I-MSK=VIII) the behaviour of the R/C buildings with 2 stories or less have been remarkably different than those with stories between 3 and 6. The cumulative damage rate (D>=D3) observed for the former group, latter group and the total stock were respectively about 10%, 40% and 30%. Thus the one- or two-story non-engineered R/C structures should be considered in the same vulnerability group with the good quality masonry (with ring beams) buildings.

The empirical vulnerability relationships obtained from 1999 Kocaeli earthquake damage distribution are provided in (Figure 7.18 and 7.19)

Figure 7.17 indicates the vulnerability curves for the general medium-rise (4-8 storey) R/C Frame type buildings in Turkey based on extensive data set compilations. The horizontal axis indicates the range of MSK intensities and the vertical scale indicates the percentage loss for the five different damage grades, D1 through D5, as described in EMS (1998). Figure 7.15 compares satisfactorily with (Figure 7.19)

The empirical damage ratio for low-rise (1-3 storey), mid-rise (4-8 storey) and high-rise (9-20 storey) Reinforced Concrete Frame with Unreinforced Masonry Infill buildings for different intensities were plotted in Table 7.6 (after, CAR and BU, 2000). Damage distribution figures of such buildings can be seen in turn in order (Figure 7.20 - 7.21 - 7.22 - 7.23) concerning to Table 7.6.

Table 7.6 Vulnerability Functions for Turkish RC framed buildings
Expected Damage Ratio MDR(%) for MSK Intensity Levels
Following values were found utilizing from (Figure 7.17)

MSK-I	**5.0**	**5.5**	**6.0**	**6.5**	**7.0**	**7.5**	**8.0**	**8.5**	**9.0**	**9.5**	**10.0**	**10.5**	**11.0**
Low-rise	-	-	-	-	2.5	5.0	10.8	19.2	30.8	43.3	55.0	66.7	79.0
Mid-rise	-	-	2.5	5.0	10.8	19.0	30.8	43.33	55.0	66.6	79.2	87.5	92.0
High-rise	-	-	-	-	2.5	5.0	10.8	19.2	30.8	43.3	55.0	66.7	79.0

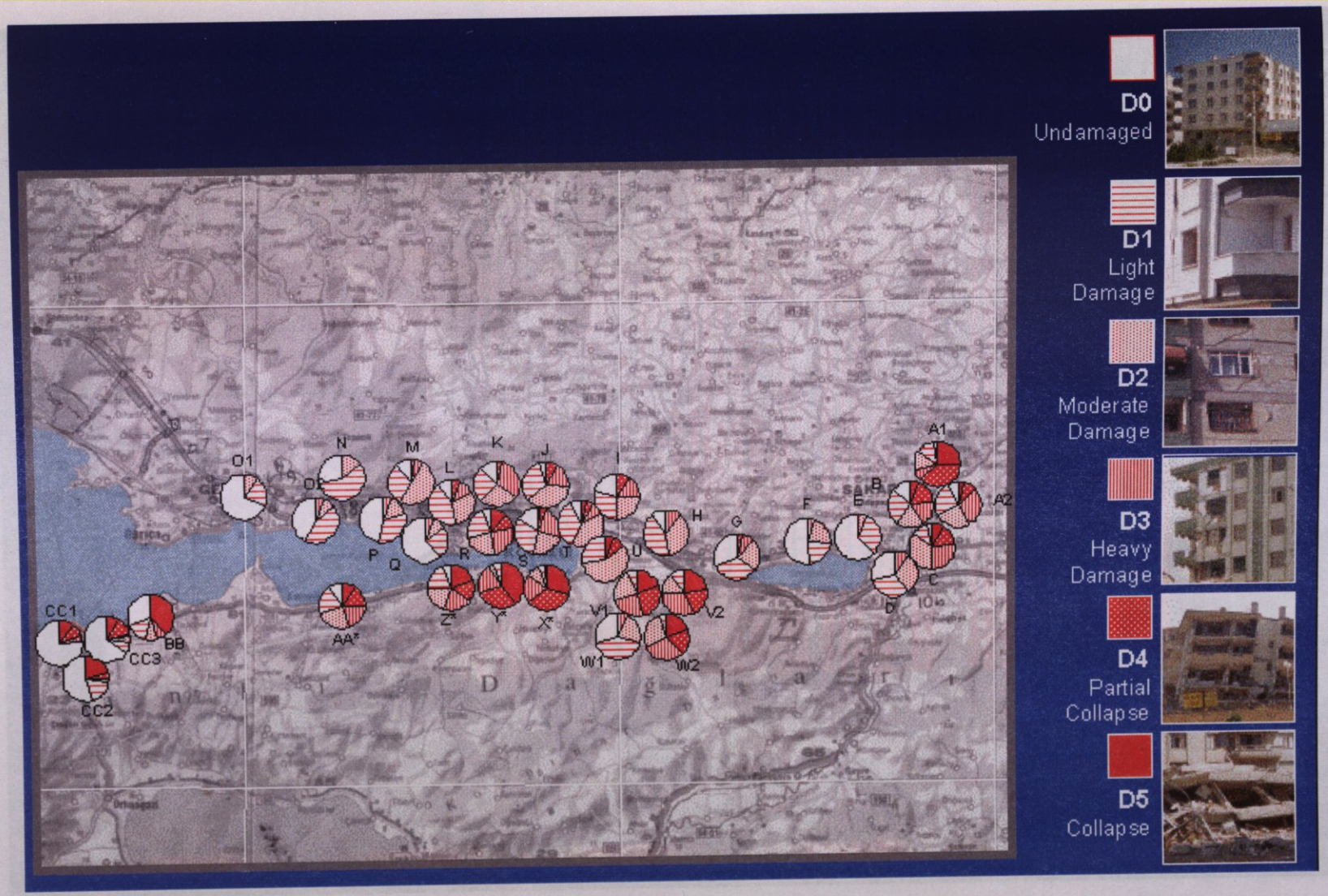

FIGURE 7.18 Damage statistics obtained from Kocaeli earthquake damage distribution (After A. Coburn,RMS)

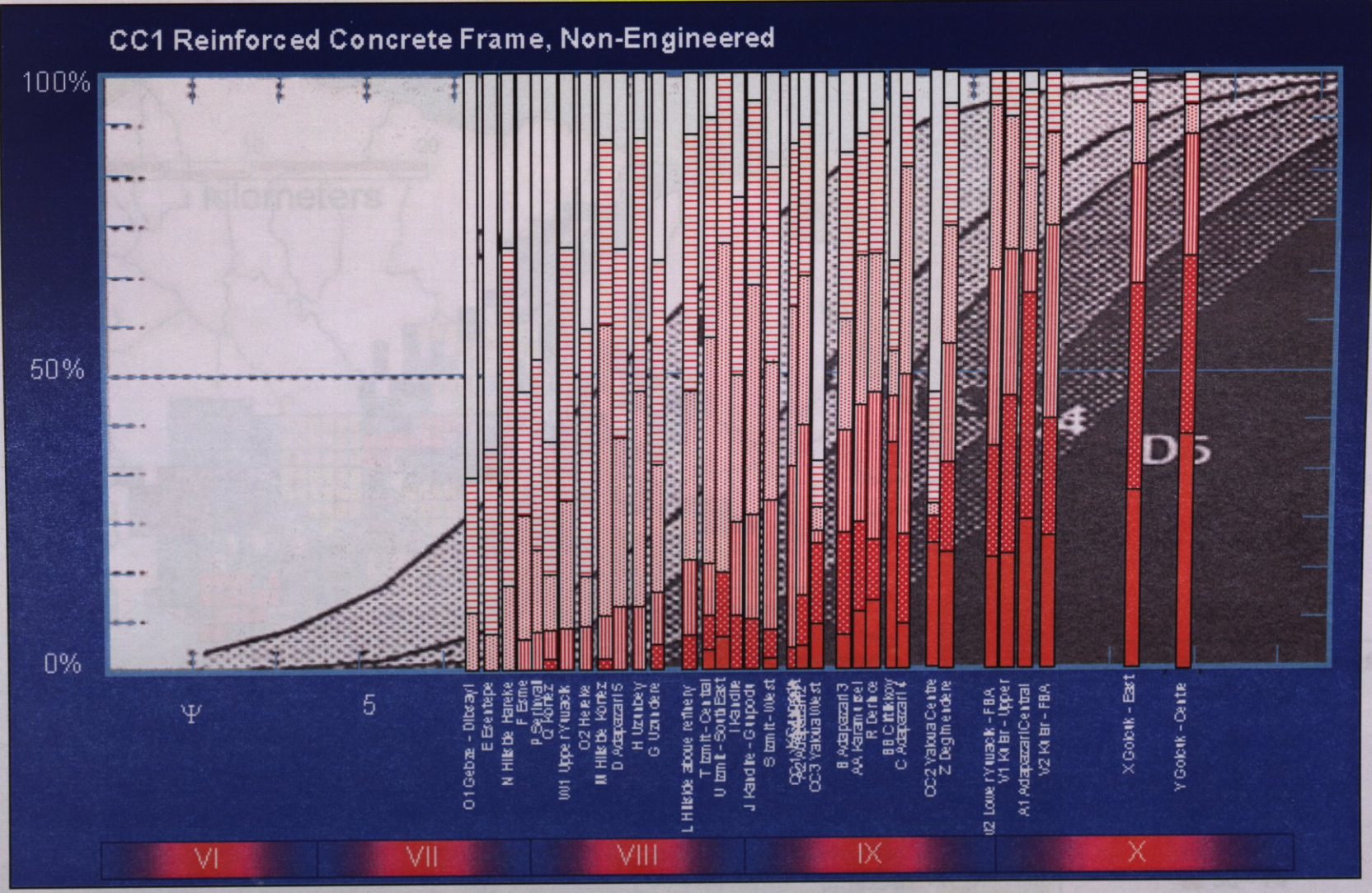

FIGURE 7.19 The empirical vulnerability relationships obtained from 1999 Kocaeli earthquake damage distribution
(After A. Coburn,RMS)

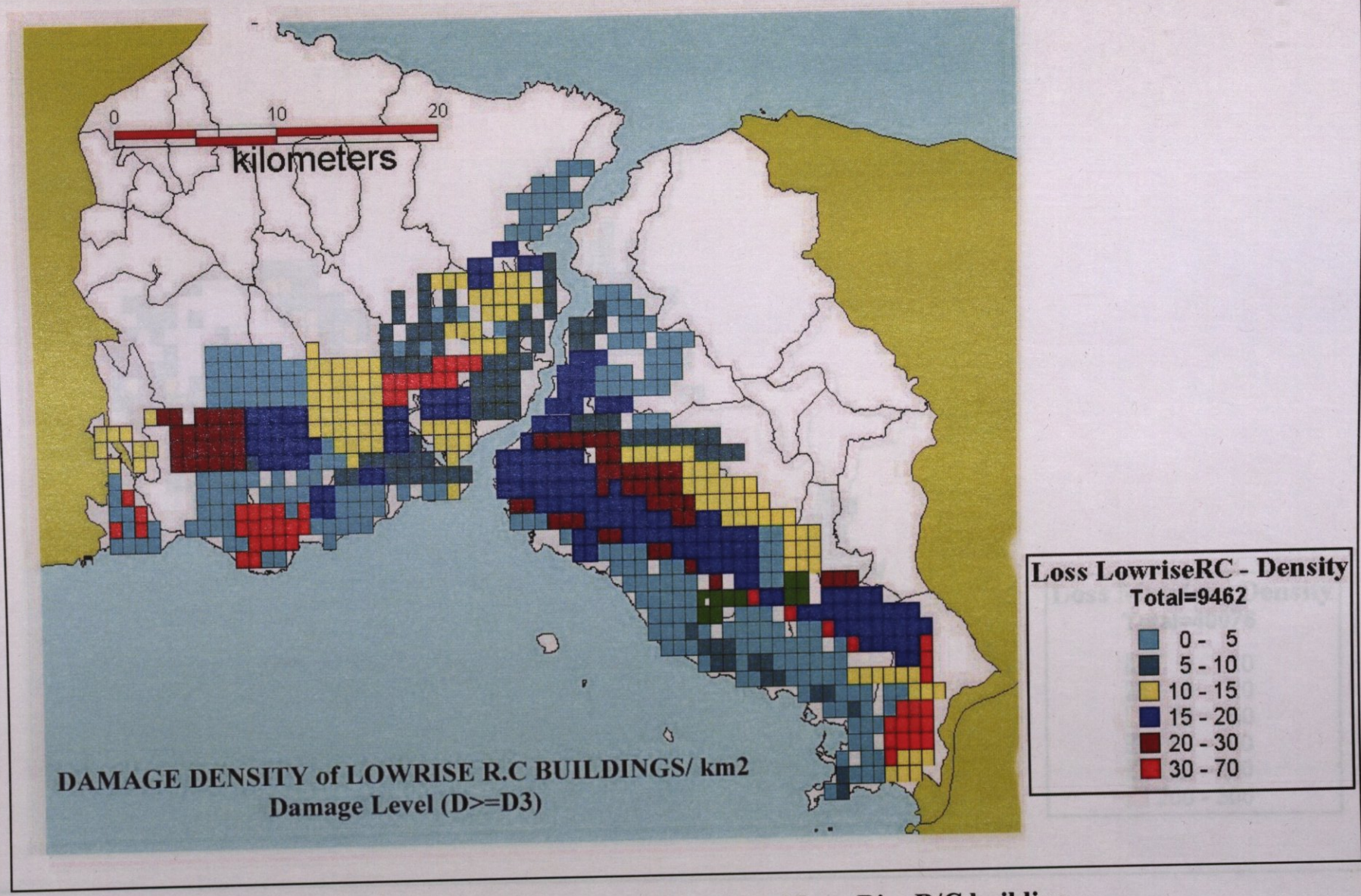

FIGURE 7.20 Damage distribution of Low-Rise R/C building

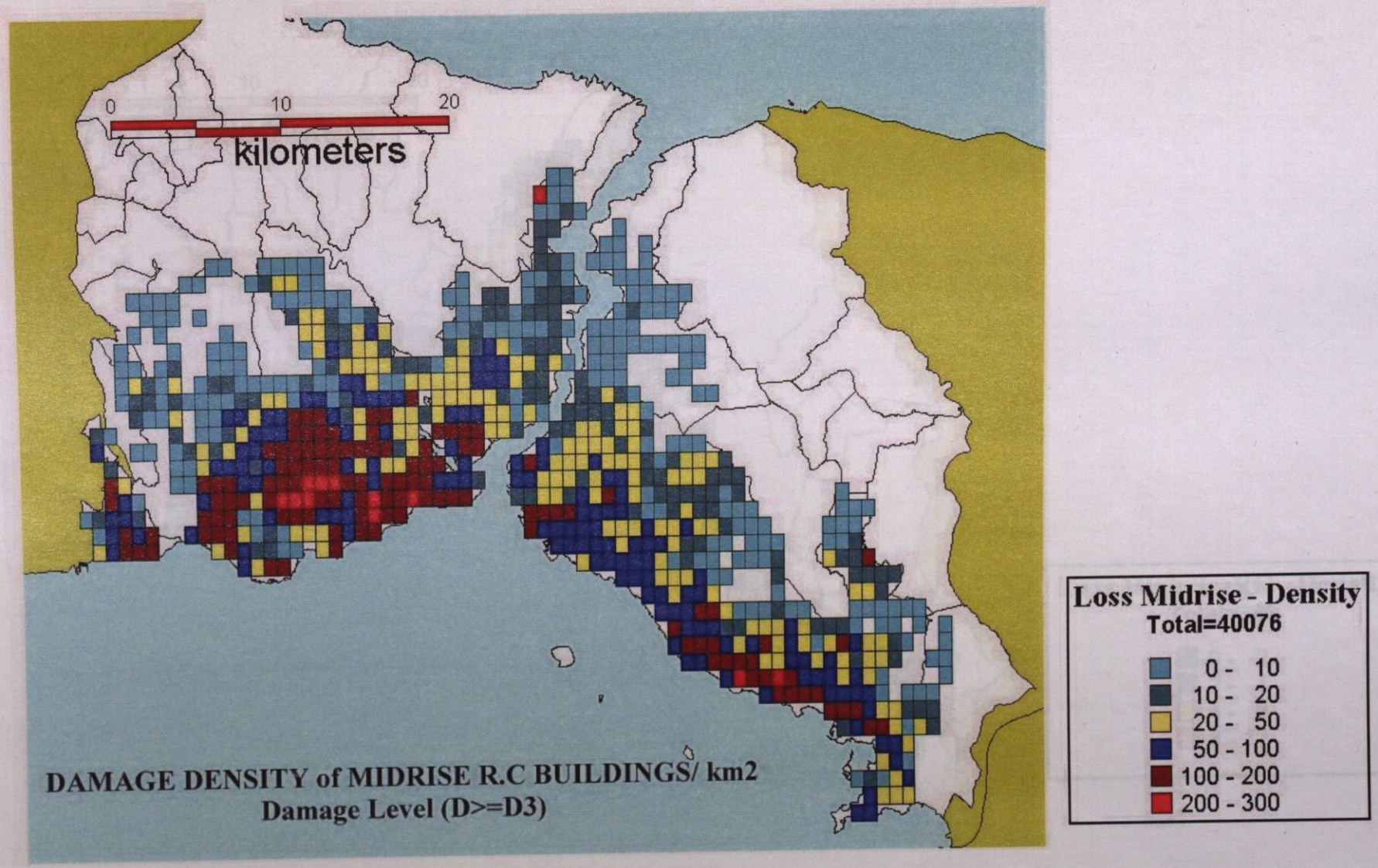

FIGURE 7.21 Damage distribution of Mid-Rise R/C building

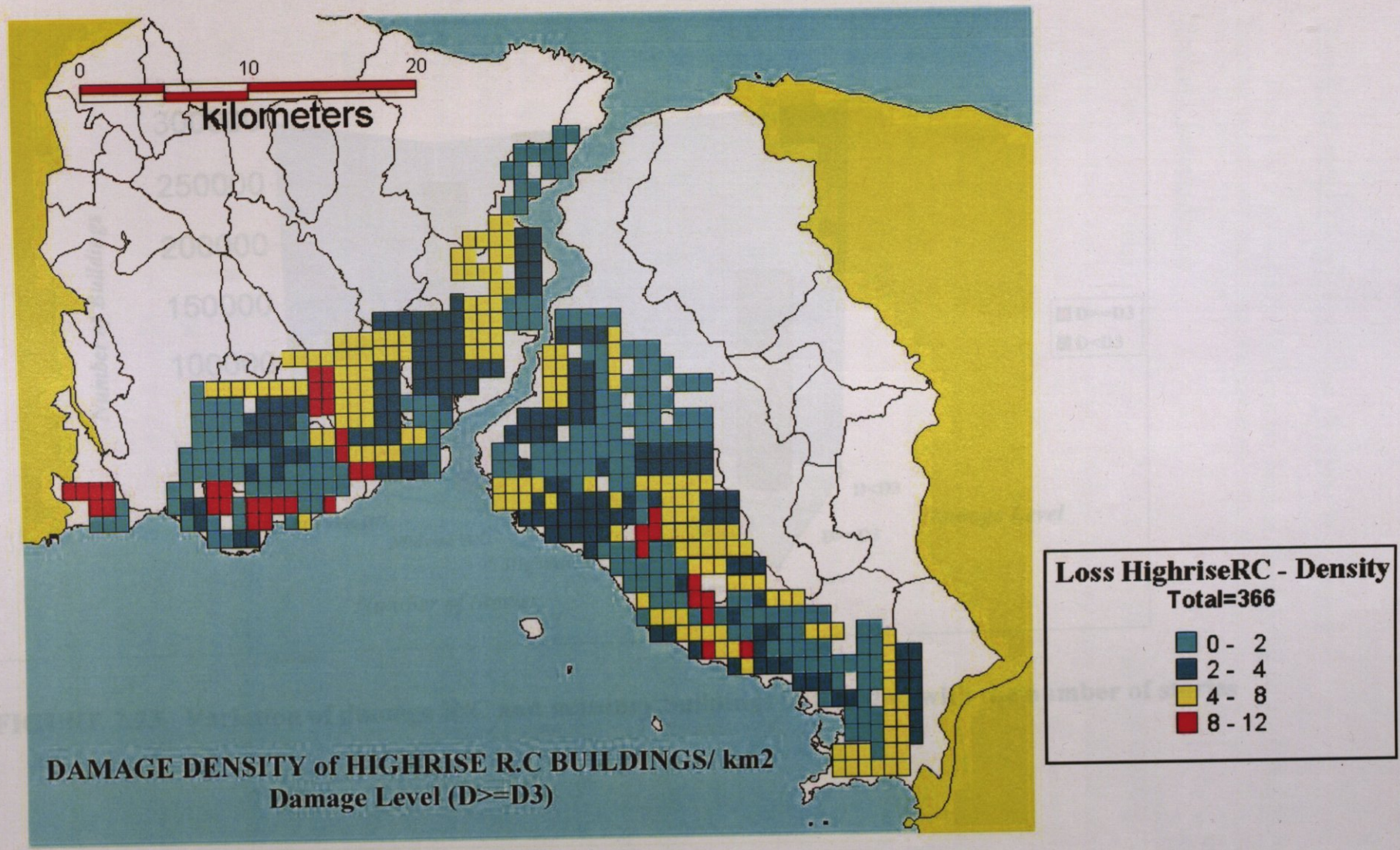

FIGURE 7.22 Damage distribution of High-Rise R/C building

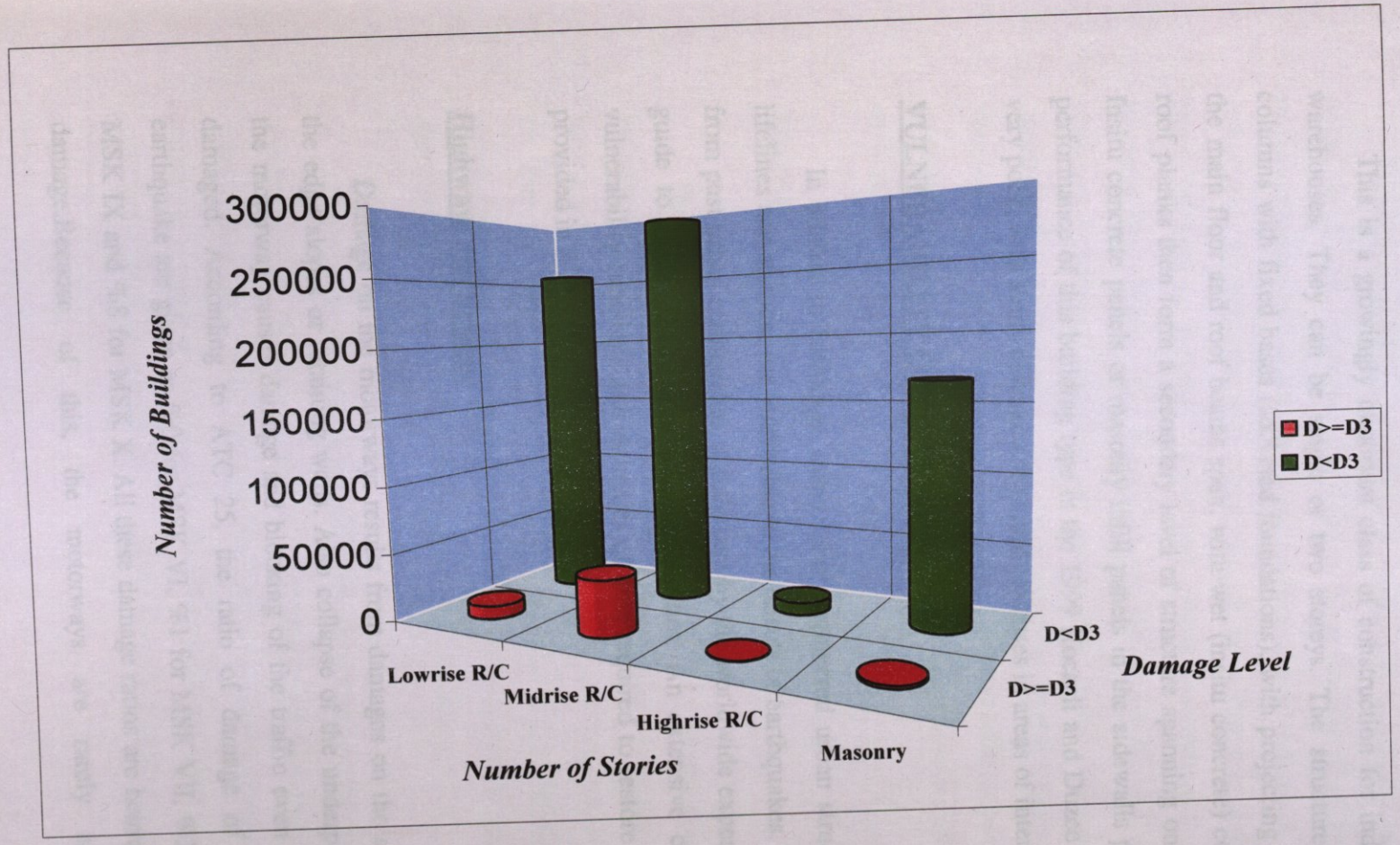

FIGURE 7.23 Variation of damage R/C and masonry buildings in İstanbul with the number of stories

Dual Reinforced Concrete Frame and RC Shear Wall System

This is not very common yet, however many of the high-rise concrete buildings in Istanbul use this system for increased strength in the structure.

Precast Concrete Frame

This is a growingly important class of construction for industrial buildings and warehouses. They can be single or two storeys. The structure consists of vertical columns with fixed bases (socketed foundations), with projecting brackets on to which the main floor and roof beams span, with wet (insitu concrete) connections. Floor and roof planks then form a secondary level of structure spanning onto these main beams. Insitu concrete panels or masonry infill panels in the sidewalls provide bracing. The performance of this building type in the 1999 Kocaeli and Duzce earthquakes has been very poor, with many collapses or partial collapses in areas of intensity VIII-IX

VULNERABILITY OF LIFELINES

In adition to buildings, many other engineered urban structures, infrastructures, lifelines and services are vulnerable to the effects of earthquakes. Observations acquired from past urban earthquakes, supplement by the worldwide experience can be used as a guide to assess their physical vulnerabilities. An extensive compilation of lifeline vulnerability functions and estimates of time required to restore damaged facilities are provided in ATC-25.

Highways and Bridges

Damage on the motorways results from damages on the surfacing or collapse of the edge slopes or retaining walls. Also collapse of the underpasses or buildings onto the motorway causes damage and blocking of the traffic even if the motorway is not damaged. According to ATC 25, the ratio of damage of motorways during an earthquake are given as %0 for MSK VI, %1 for MSK VII, %2 for MSK VIII, %4 for MSK IX and %8 for MSK X. All these damage ratios are below the upper limit of low damage.Because of this, the motorways are rarely affected directly from

earthquake.(Figure 7.24 – 7.25) show transportation system in İstanbul overlain with the scenario earthquake intensity distribution.

Telecommunication Systems

Disruption of the communication systems is mainly due to falling buildings or poles. In Turkey previous earthquakes have showed that main damages on the telecommunication system arise mostly from the weakness of the structural system rather than the behavior of the system equipment. Based on the information supplied from Telekom in İstanbul, 139 central offices (switchboard) were observed in the scenario area (Figure 7.26). Most of the central offices are two to five story reinforced concrete buildings. Assuming all the central office buildings are designed and constructed according to the requirements of the Turkish Earthquake Code, it can be concluded that the main damage to the telecommunication system are caused by the fall of equipment inside the central offices. Telephone services could be interrupted after the earthquake.

Electrical Transmission and Distribution Systems

The performance of most power system components and overall system performance have been good in response to a moderate or big earthquake. However a large earthquake may cause long duration power outages over a large area. The damage on the electrical system directly affects all power dependent systems such as communications, water supply and waste water treatment systems. Therefore, these systems should be planned for an extended power outage.

Substations are the most vulnerable elements in the electrical power delivery system. Major substations contain switches, porcelain insulators, circuit breakers, transformers, and control equipment. Damage generally occurs in improperly anchored electrical equipment. For non-upgraded electrical transmission substations in California, ATC-25 (1991) assigns 16, 26, 42 and 70 per cent damage values, spectively or

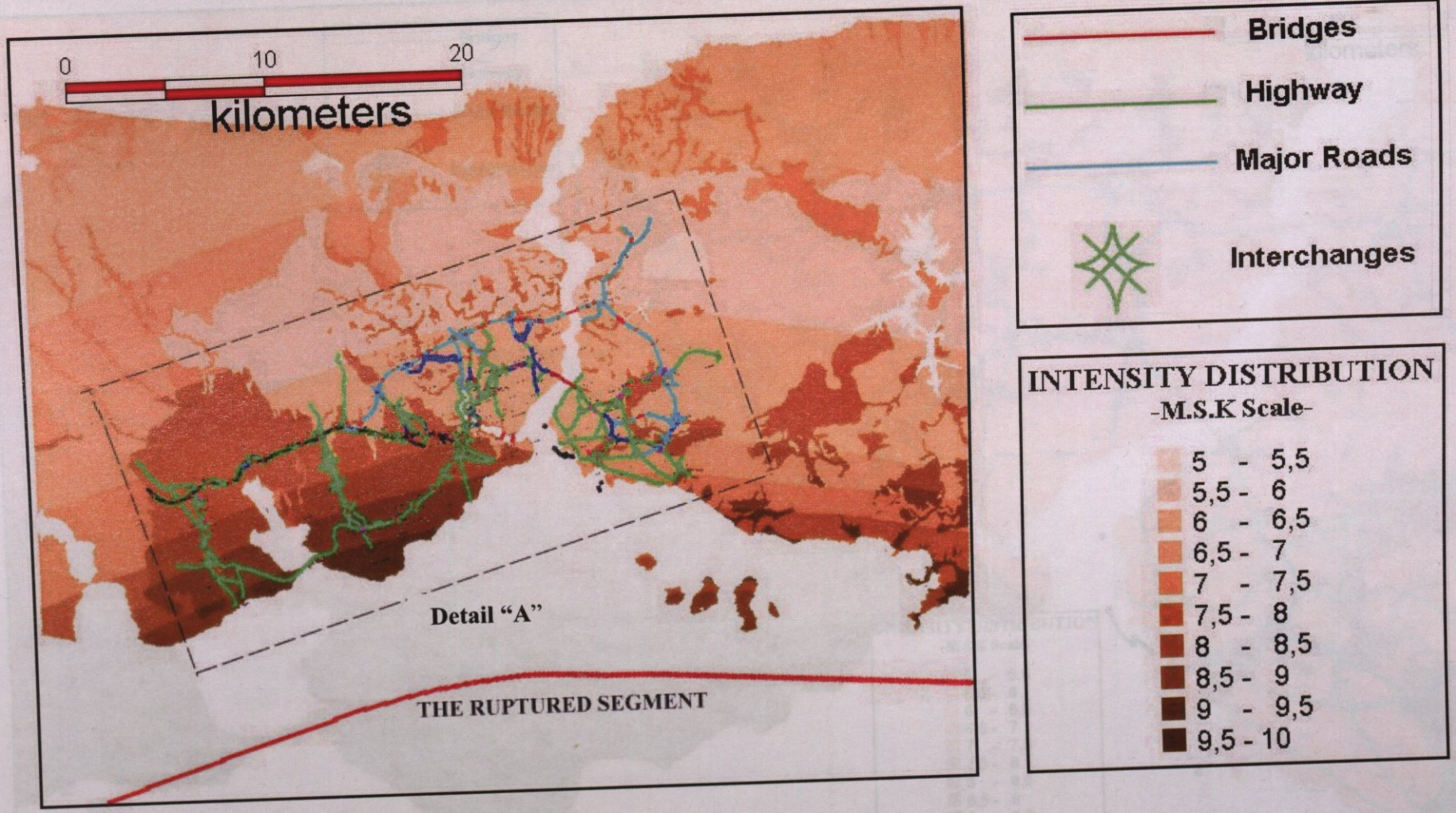

FIGURE 7.24 Transportation system in İstanbul overlain with the scenario earthquake intensity distribution

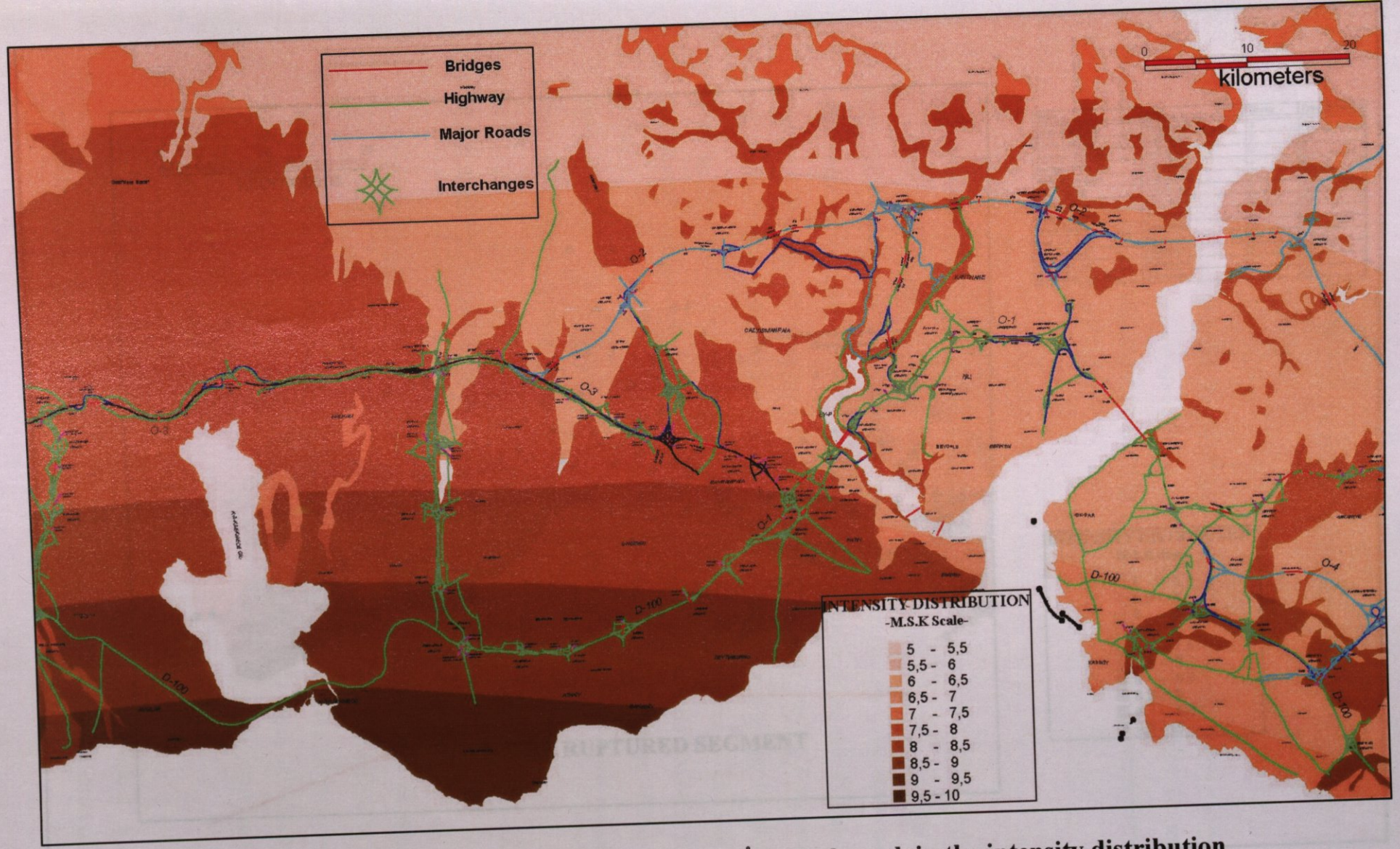

FIGURE 7.25 Detail "A" of transportation system in İstanbul overlain the intensity distribution

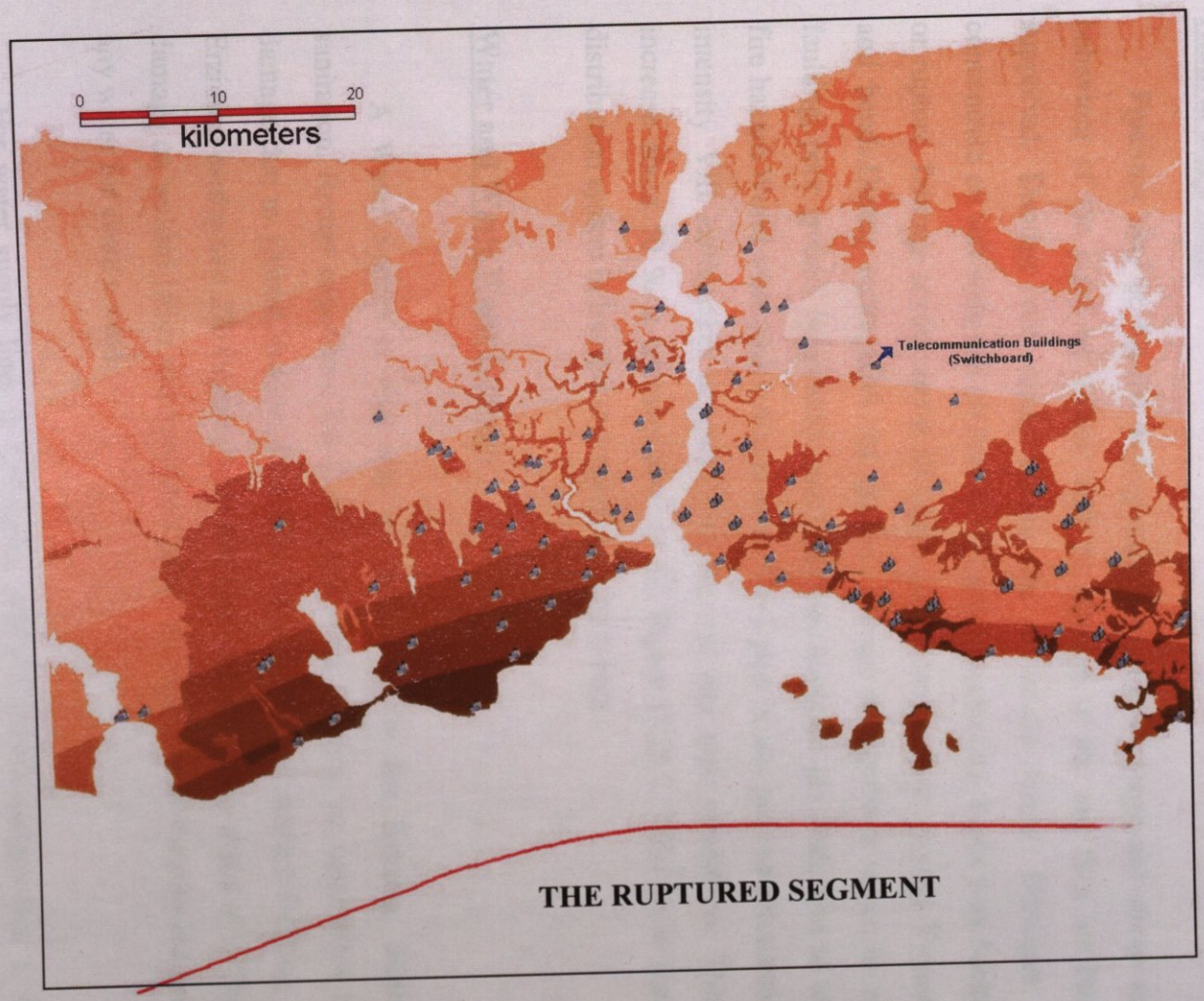

Name	Type	Storey	Type_Structure
Terabya Sant. Amr	Switchboard	3	R.C
B.Dere Sant. Amr	Switchboard	3	R.C
Ayazaga-I Sant. Amr	Switchboard	2	R.C
Ayazaga-II Sant. Amr	Switchboard	4	R.C
Beybi Giz Sant.Amr	Switchboard	1	R.C
Polaris Santrali	Switchboard	1	R.C
Park Plaza Sant.	Switchboard	1	R.C
Borsa Sant. Amr	Switchboard	1	R.C
Sinpas Santrali	Switchboard	1	R.C
Dost Sant. Amr	Switchboard	2	R.C
Etiler Sant. Amr	Switchboard	6	R.C
Kilyos Sant. Amr	Switchboard	4	R.C
RumeliFeneri Sant. Amr.	Switchboard	1	R.C

FIGURE 7.26 Telecommunication system in İstanbul overlain with the scenario earthquake intensity distribution

earthquake intensities of VII, VIII, IX and X. The respective damage percentages are 8, 13,25, 52 for distribution substations.

Based on the information supplied from BEDAS in İstanbul, 147 transformers were observed in the scenario area (Figure 7.27). Most of the transformers in İstanbul are exposed to ground shaking of IX and VIII. Transformers could be damaged and this may cause extensive power failure.

Natural Gas System

Pipelines may be burried underground, on grade or supported above soil. The behaviour of the pipes are related with the damage of the soil they are burried or supported. Damage very rarely occurs due to inertia forces. Damages usually concentrate on soft soils and on lines where soil type changes. Pipes may buckle, bend or rupture. Damage occurs almost all supporting elements above ground, T-connections and bends.During earthquakes the greatest damage to pipelines occur in zones of faulting, poor ground, liquefaction and landslide. Ruptured gas lines lead to leaks and fire hazard.World wide data indicates about 0.5-1 pipe breaks per one kilometer pipe in intensity VIII earthquakes depending on the soil and pipe conditions. These rates increase about 50 % at intensity level of IX. Figure (7.28 – 7.29) show natural gas distribution system in İstanbul overlain the intensity map.

Water and Waste Water Systems

A Water System is vital after an earthquake for fire fighting, drinking and sanitation. Recent experience has shown that water systems are susceptible to severe damage due to ground shaking, landslides, liquefaction and surface faulting. In 1992 Erzincan earthquake 270 ruptures were reported on the laid city pipes of 272km due to damage on welded joints and separation joints. A large part of the city did not receive any water for about a week.

For water supply lines in California, ATC-25 (1991) assigns 0.5, 1, 4 and 12 breaks/km, respectively for earthquake intensities of VII, VIII, IX and X. damage rates

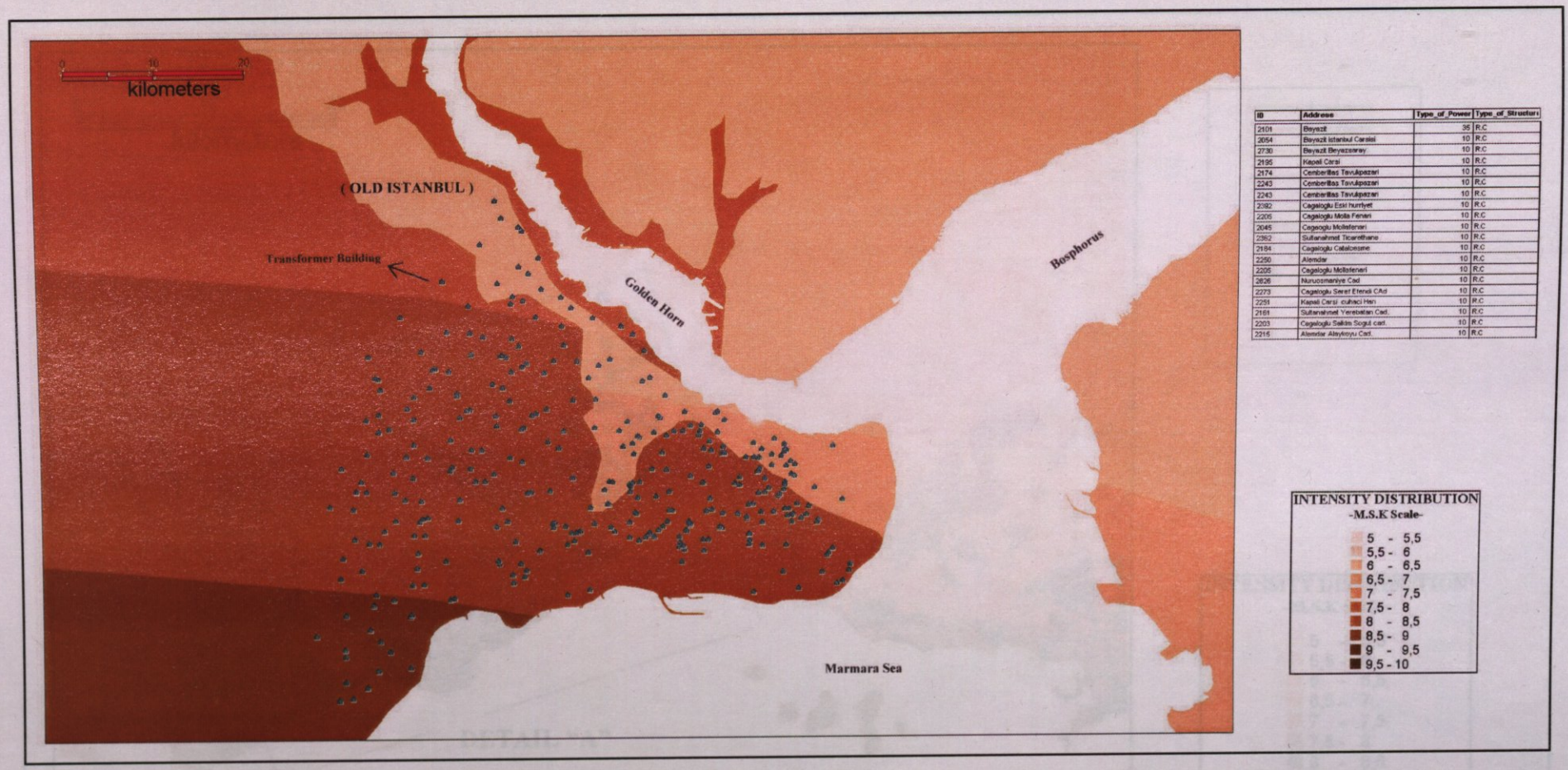

ID	Address	Type_of_Power	Type_of_Structure
2101	Beyazit	35	R.C
2054	Beyazit Istanbul Carsisi	10	R.C
2730	Beyazit Beyazsaray	10	R.C
2195	Kapali Carsi	10	R.C
2174	Cemberlitas Tavukpazari	10	R.C
2243	Cemberlitas Tavukpazari	10	R.C
2243	Cemberlitas Tavukpazari	10	R.C
2382	Cagaloglu Eski hurriyet	10	R.C
2205	Cagaloglu Molla Fenari	10	R.C
2045	Cagaoglu Mollafenari	10	R.C
2362	Sultanahmet Ticarethane	10	R.C
2184	Cagaloglu Cakalcesme	10	R.C
2250	Alemdar	10	R.C
2205	Cagaloglu Mollafenari	10	R.C
2826	Nuruosmaniye Cad	10	R.C
2273	Cagaloglu Seref Efendi CAd	10	R.C
2251	Kapali Carsi cuhaci Han	10	R.C
2161	Sultanahmet Yerebatan Cad.	10	R.C
2203	Cagaloglu Salim Sogut cad.	10	R.C
2215	Alemdar Alaykoyu Cad.	10	R.C

FIGURE 7.27 Electrical transmission system in Old Istanbul overlain with the scenario earthquake intensity distribution

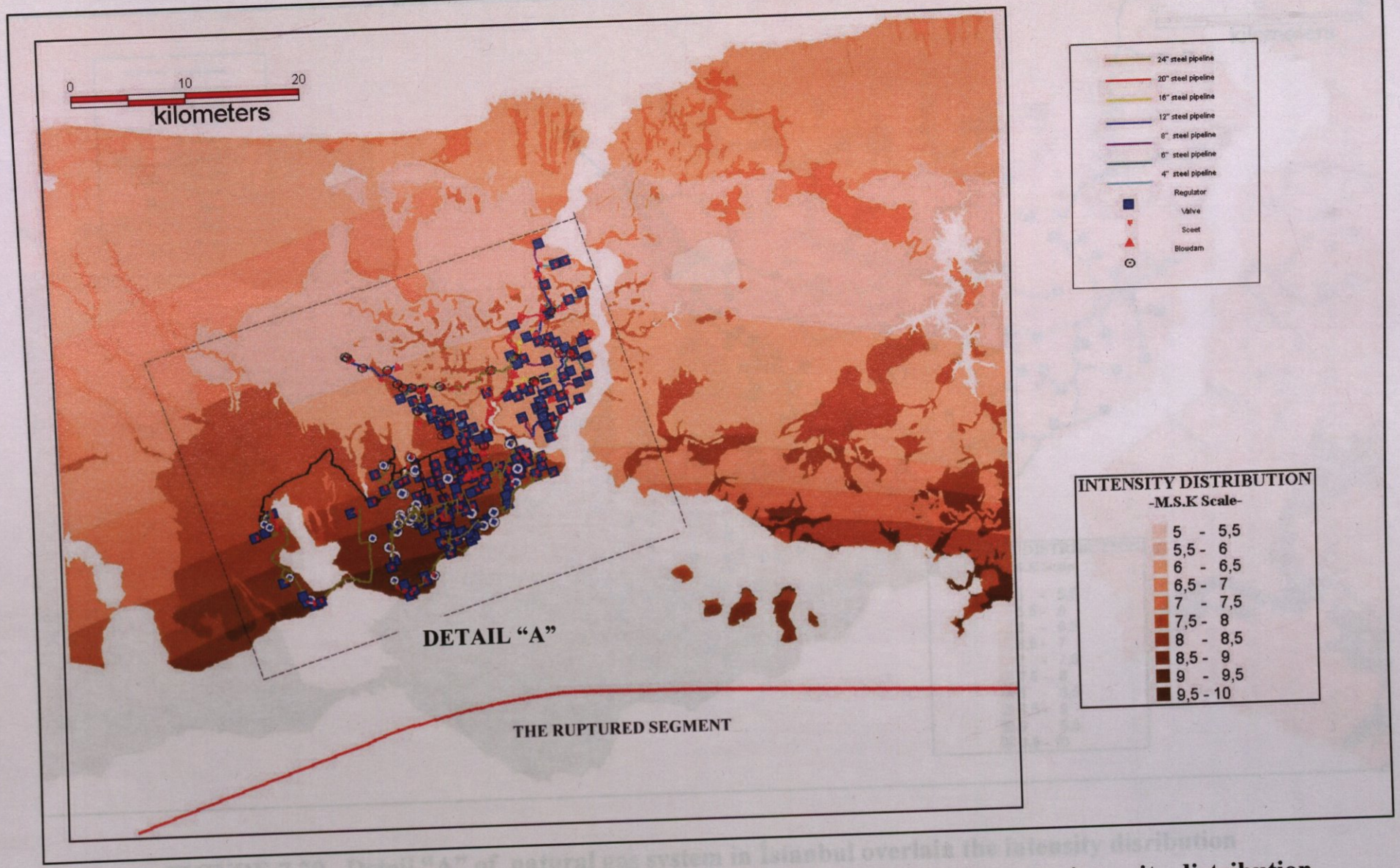

FIGURE 7.28 Natural gas system in İstanbul overlain with the scenario earthquake intensity distribution

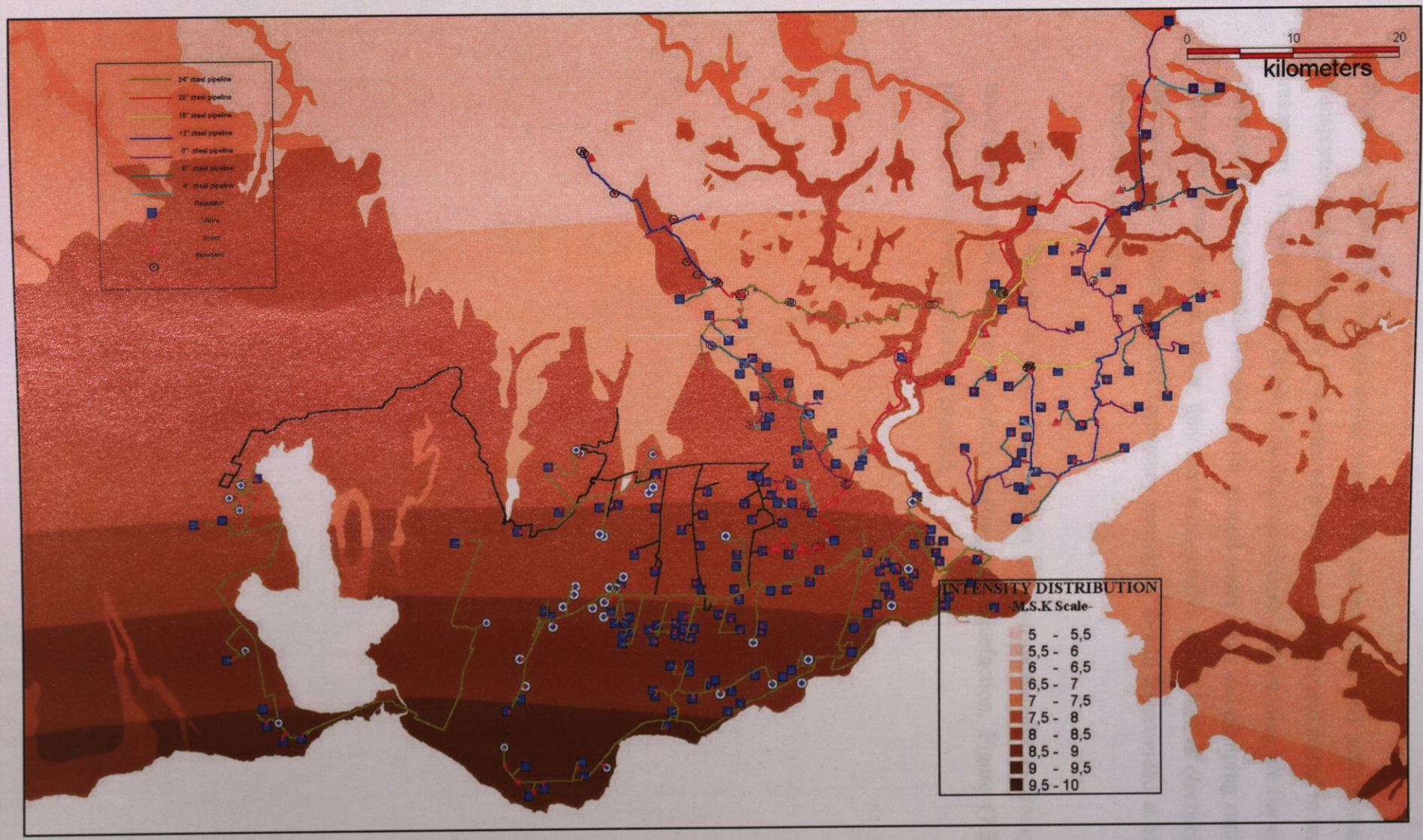

FIGURE 7.29 Detail "A" of natural gas system in İstanbul overlain the intensity disribution

should be doubled for sanitary sewer mains. The underground and surface waters are transported from their source by a series of pipeline and flumes and stored in tanks and reservoirs. The line breaks, failure of piping connections and buckling are the expected damages for storage tanks. Because all the ground water wells and pumping stations are dependent upon electrical power, they can be inoperative due to lack of electricity after the earthquake. Hence, portable emergency generators should be provided at all water production facilities.

The most damage to waste water system from an earthquake is from broken underground pipes in areas of surface faulting and liquefaction. Figure (7.30-7.31) illustrate waste water facilities in İstanbul.

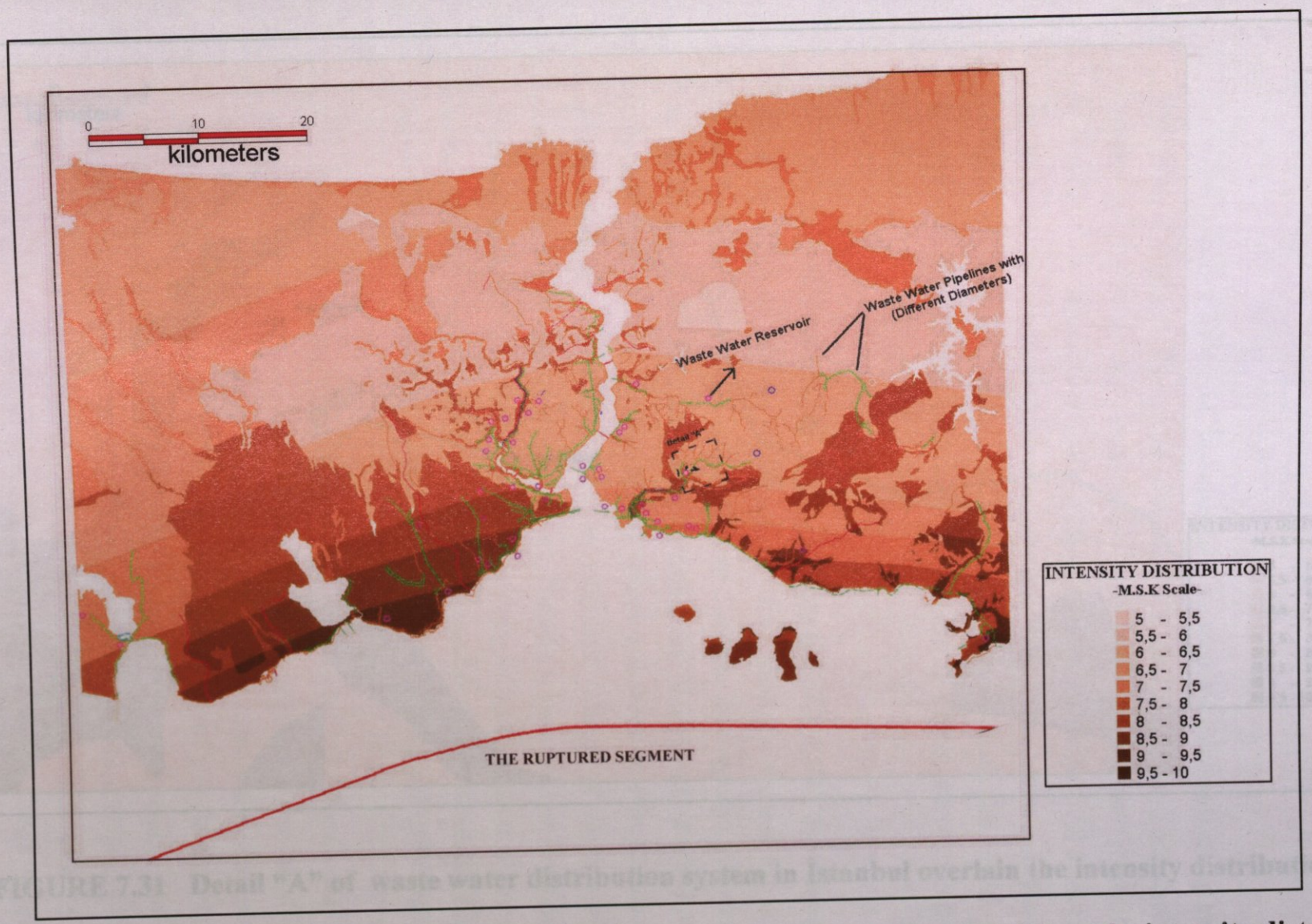

FIGURE 7.30 Waste water distribution system in İstanbul overlain with the scenario earthquake intensity distribution

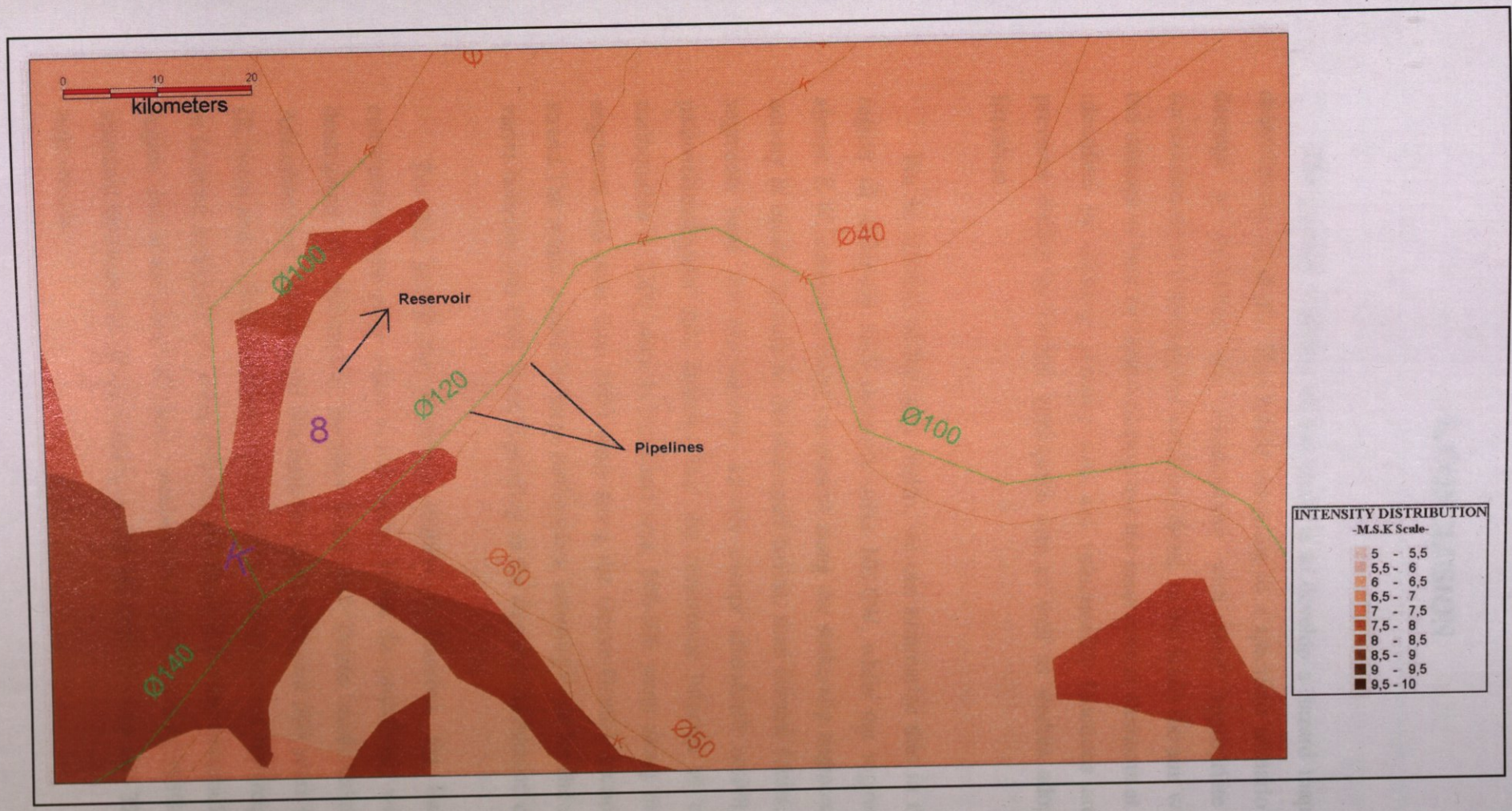

FIGURE 7.31 Detail "A" of waste water distribution system in İstanbul overlain the intensity distribution

8. CONCLUSION

The primary objective of this study is to develop a hazard map of İstanbul by deterministic approach. This means according to a specified scenario earthquake the damage to buildings and infrastructure with their appropriate physical and socioeconomical consequences were considered. In this study the aim was to investigate the damage to both suffered buildings and the most critical elements at risk. They were identified by utilizing intensity map and vulnerability functions are based on the previous studies in Turkish earthquake data as well as studies adopted from other literature.

For he tectonic of Marmara region, we can summarize that in the Marmara sea region all strike-slip fault segments strike NE-SW, while the regional lip vector is almost E-W, causing a thrust component along the strike-slip segments. Microseismic actvity is mostly located to the pull-apart basins, thus normal faults,while strike-slip segments have not microseismic activity except aftershock activity.Historical and paleoseismological data indicate, that the recurrunce interval of clusters of large earthquakes is 1200 years in the İzmit area, 500-800 years along the Gazikoy-Saros segments and more than 2000 years along the Geyve-Gemlik section of the middle strand.The return period for large earthquakes, intensity>VIII for the south of İstanbul varies between 100-1000 years, depending on the size and mechanism of earthquakes.

For the probability of strong shaking in İstanbul, the Barka and Stein's calculations were given place to this study. While the probability was calculated, the description of earthquakes included İzmit and Duzce earthquakes on the North Anatolian fault system in the Marmara Sea during the past 500 years was calculated by (R. Stein and A. Bark) and tested the resulting catalog against the frequency of damage in Istanbul during the preceding millennium. There is a stress accumulation in Marmara region and at the result of these calculations it is found a 62±15% probability (one standard deviation) of strong shaking during the next 30 years and 32±12% during the next decade.

The iso-intensity hazard map presented in deterministic assessments were modified by assigning simplified site categories.The intensity values were corrected utilizing the intensity increments and decrements corresponding to each site category. The seismic damages can vary from one site to another depending on the geotechnical and geological conditions of the site. The local geotechnical conditions can also be very different due to in thickness and properties of soil layers, depth of bedrock, type of lithology and ground water table.

Deterministic hazard assessment was achieved by defining a hypothetical earthquake, which represents a highly significant and reasonably probable event that can affect area, on the basis of the seismic history and neo-tectonic structure of the region. The scenario earthquake of Mw=7.5 was given on the Marmora Fault that contributes the highest risk to İstanbul.

The seismic intensity distribution map of the scenario earthquake was plotted as concentric ellipses centered on İstanbul Fault. The iso-seismal map of the scenario earthquake based on Erdik et al., (1983) attenuation relationship whose ellipses denote VIII intensity and decrease to VI intensity.

The resultant iso-seismal map of the scenario earthquake reaches especially the highest values in the some south parts of İstanbul depending on distance to such fault and amplification factors of ground. With distance from the fault, each successive ellipse is an intensity unit less than the previous one.

All vulnerability assessments were done based on the iso-seismal map of the scenario earthquake because of the fact that the deterministic approach provides an easily understood and transmitted method of estimating site specific hazards. For buildings in İstanbul, at the scope of vulnerability assessment, lowrise (1-3 storey), midrise (4-8 storey), highrise (9 or more storey) reinforcedconcrete buildings and masonry buildins were analyzed. At the resultant such assessment, midrise buildings in

İstanbul are the considerable part of the buildings suffered from the scenario earthquake.

The resulting planning earthquake scenario is intended to contribute to the efforts the local offices with emergency planning responsibilities and private sectors and planners who must understand the scope of the hazard in order to prepare it.

REFERENCES

Aki, K., and K. Irikura, "Characterization and Mapping of Earthquake Shaking for Seismic Zonation," *Proc. of the IV. Int. Conf. on Seismic Zonation*, Vol.1, pp. 61-110, 1991.

Ambraseys, N., N., and C.F. Finkel, 1995. *The seismicity of Turkey and adjacent areas*, a historical review, 1500-1800, 240 pp., Eren, İstanbul.

Ambraseys, N., N., and J.A. Jackson, 2000. Seismicity of the sea of Marmara (Turkey) since 1509, *Geophys.* J. Int., 141, F1-F6

Ambraseys, N.N. and C.F.Finkel (1991), Long-term Seismicity of Istanbul and of he Marmara Sea Region, Terra Nova, 3, 527-539.

Ambraseys, N.N. and Finkel, C.F., 1987, The Saros-Marmara earthquake of 9 August 1912, Earthq. Engin. And Struc. Dynam., 15, 189-211.

Amraseys, N.N. and Finkel, C.F., 1990, Marmara sea earthquake of 1509, Terra Motae, 167-174.

Armijo, R., B. Meyer, A. Hubert, and A. Barka, 1999. Westward propagation of the North Anatolian fault into the Northern Aegian : timing and kinematics, *Geology*.

ATC-25, Seismic Vulnerability and Impact of Disruption of Lifelines in the Conterminous United States, Applied Technology Council, Redwood City, CA, 1991.

Barka, A. A., 1992, The North Anatolian Fault Zone, Annales Tectonicae, Special Issue, 6: 164-195.

Barka, A. A., 1996, Slip Distribution along North Anatolian Fault Associated with the Large Earthquakes of the Period 1939 to 1967, BSSA, 86: 1238-1254.

Barka, A. A., and K. Kadinsky-Cade, "Strike-Slip Fault Geometry in Turkey and Its

Barka, A. A., Kadinsky-Cade, K., 1988, Strike-slip Fault Geometry in Turkey and Its

Barka, A.A. and Kuşcu, İ, 1996, Extents of the North Anatolian fault in the İzmit, Gemlik and Bandırma bays, Turkish J. Marine Sci., 2, 93-106

Barka, A.A. and Toksöz, N.M., (1989), Seismic gaps along the North Anatolian fault, Abstract, IASPEI meeting in Istanbul, Turkey, S9-1.

Barka, A.A., 1991, İstanbul'un Depremselliğini oluşturan tektonik yapılar ve İstanbul için bir mikro-bölgelendirme denemesi, "İstanbul ve Deprem Sempozyumu" Inşaat Mü. Odası, 35-56.

Barka, A.A., 1993, Kuzey Anadolu Fayının Sapanca- İzmit ve Geyve- İznik Kolları Üzerinde Paleosismik Araştırmalar, Proje No: YBAG-4/7551, 85p.

Coburn, A. and R. Spence (1992), Earthquake Protection, Wiley, 355pp.

Dewey, J. F., and A. M. C. Şengör, "Aegean and Surrounding Regions: Complex Multi-Plate and Continuum Tectonic in a Convergent Zone," *Bull. Int. Assoc. Eng. Geol.*, 19, pp. 145-151, 1979.

Dewey, J.W., 1976, Seismicity of the Northern Anatolia, Bull. Seism. Spoc. Am., 66, 843-868.

EMS-98, *European Macroseismic Scale*, European Seismological Commission, Luxembourg, 1998.

Erdik, M. (1984), Seismic Hazard in Turkey, in Proc. Conf. On Science and Technology in Socio-Economic Developement, Technische Universitat Berlin, Massachusets Institute of Technology, Berlin, 1984.

Erdik, M. (1994), Developing a Comprehensive Earthquake Disaster Masterplan for Istanbul, in Issues in Urban Earthquake Risk, ed. B. Tucker et al., Kluwer Academic Publishers, Netherlands.

Erdik, M., Natural Hazards and Vulnerabilities in Turkey (unpublished report), Boğaziçi University, Istanbul, 1995.

Ergin, K., U. Güçlü and Z. Uz., *A Catalogue of Earthquakes for Turkey and Surrounding Area (11 A.D. to 1964 A.D.)*, Istanbul Technical University, Pub. No. 24, 1967.

Ergün, M. and Özel, E., 1995, Structural relationship between the sea of Marmara basin and the North Anatolian fault, Terra Nova, 7, 278-288.

Ergünay, O. and M. Erdik, Disaster Mitigation Program in Turkey, *Proc. of Int. Conf. on Disaster Mitigation Program Implementation*, Ocho Rios, Jamaica, 1984.

Eryilmaz, M., Eryilmaz, F.Y., Kirca, Z. and Dogan, E. (1995). Izmit Körfezinin çökel dagilimi ve buna etki eden faktörler, Izmit Körfezi Kuvaterner Istifi (ed: E. Meriç), 27-

Everenden, J. F., R. R. Hibbard and J. F. Schneider (1973), Interpretation of Seismic Intensity Data, Bull. Seism. Soc. Am., v.63, pp.399-422.

Evernden J.F. and J.M. Thompson (1985), Preceeding Seismic Intensities, in Evaluating Earthquake Hazards in Los Angeles Region, pp. 151-202, USGS Professional Paper No:1360, US Government Printing Office, Washington.

Evernden, J. F., W. M. Kohler, and G. D. Clow, Seismic Intensities of Earthquakes of Conterminous United States-Their Prediction and Interpretation, U.S. Geol. Surv. Professional Paper 1223, 50 p., 1981.

F. Finkel, N. N. Ambraseys, The Marmara Sea earthquake of 10 July 1894 and its effect on historic buildings, Anatolia Moderna Yeni Anadolu VII (Bibliothèque de l'Institut G. C. P. King, R. S. Stein, J. Lin, Bull. Seismol. Soc. Amer. 84, 935 (1994).

Gürbüz, C., Aktar, H. Eyidoğan, A. Cisternas, H. Haessler, and others, 2000. The seismotectonics of the Marmara region (Turkey) : results from a microseismic experiment, *Tectonophysics*, 316, 1-17.

Includes earthquakes in 1509, 1556, 1719, 1754, 1766, 1855, 1857, 1863, 1877, 1894, 1953, and 1964 from (12-14) and (35).

Ito, et al., Precise Distribution of Aftershocks of the Izmit Earthquake of August 17, 1999, Turkey, Eos Trans. 80, F662 (1999).

Jackson, J. and McKenzie, D. P., "Active Tectonics of the Alpine-Himalayan Belt Between Western Turkey and Pakistan", *Gophys. J. R. Ast. Soc.* 77, pp. 185-264, 1984.
Jackson, J., "Active Tectonics of the Aegean Region," *Annu. Rev. Earth Planet.Sci.*, pp. 239-271, 1994.

Kandilli Observatory and Earthquake Research Institute Web Site, http://www.koeri.boun.edu.tr.

Le Pichon, X., and J. Angelier, "The Hellenic Arc and Trench System: A Key to the Neotectonic Evolution of the Eastern Mediterranean Area," *Tectonophysics*, 60, pp. 1-42, 1979.

Le Pichon, X., T. Taymaz, and A.M.C. Şengör, 1999. The Marmara Fault and the future İstanbul earthquake, in *International Conference on the Kocaeli earthquake, 17 August*

1999, edited by M. Karaca, and D.N. Ural, pp. 41-54, İstanbul Technical University Press House, İstanbul.

M. N. Toksoz, A. F. Shakal, and A. J. Michael, Pageoph 117, 1258 (1979).

Meriç, E. (1995). Izmit Körfezi (Hersek Burnu-Kaba Burun) Kuvaterner'inin stratigrafisi ve ortamsal özellikleri, Izmit Körfezi Kuvaterner Istifi, (ed: E. Meriç), 251-258.

N. N. Ambraseys, C. F. Finkel, Annales Geophysicae 5B, 701 (1987).

N. N. Ambraseys, C. F. Finkel, Terra Nova 3, 527 (1991).

N. N. Ambraseys, C. F. Finkel, The Seismicity of Turkey and Adjacent Areas: A historical review, 1500-1800 (Muhittin Salih EREN, Istanbul, 1995).

Ohashi, O.,Y. Ohta, O. Ergünay, and A. Tabban, "Empirical Derivation of Seismic Intensity Distribution Laws Based upon Earthquake Data in Turkey," Hokkaido University, Sapporo, 1983.

Örgülü, G., and M. Aktar, 2001. Regional moment tensor inversion for strong aftershocks of the August 17, 1999 İzmit Earthquake (Mw = 7.4), *Geophysical Research Letters*, January issue.

Papazachos, B., and C. Papazachou, *The Earthquakes of Greece*, ZITI editions, Thessaloniki, 1997.

Pezeshk, M., T. S. Chang, K. C. Yiak and H. T. Kung, "Seismic Vulnerability Evaluation of Bridges in Memphis and Shelby Country, Tennessee," *Earthquake Spectra,* Vol. 11, No. 4, 1995.

Pınar, N., 1943, Marmara denizi basenlerinin jeolojisi, sismisitesi ve meteorolojisi, İst. Üni. Fen. Fak. Mec., 7, 314p.

Pınar, N., 1943. The geology, seismicity and meteorology of the basin of the Marmara Sea, *Université d'Istanbul*, Kenan Matbaası, İstanbul.

R. S. Stein, A. A. Barka, J. H. Dieterich, Geophys. J. Int. 128, 594 (1997).

Reichle, M. S. and J. E. Kahle, Written Communication, California Department of Conservation, Division of Mines and Geology, 1986.

RGELFE, *Estimating Losses From Earthquakes in China in Forthcoming 50 years*, State Seismological Bureau, Seismological Press, Beijing, 1992.

S. G. Wesnousky, Bull. Seismol. Soc. Amer. 89, 1131 (1999).

Seismic Hazard in Turkey," *Tectonophysics,* 117, pp. 295-344, 1985.

Sengör, A. M. C., 1979, The North Anatolian Transform Fault: Its Age, Offset and Tectonic Significance, *J. Geol. Soc.*, London, 136: 269-282.

Şengör, A.M.C., 1987, Cross-faults and differential streching of hanging walls in regions of low angle normal faulting: Examples from Western Turkey, in: Continenal exensional tectonics, edited by: M.P. Coward, J.F. Dewey and P.L. Hancock, Geological Society, London, Special Publication, No.28. 575-89.

Şengör, A.M.C., Görür, N. and Şaroğlu, F., 1985, Strike-slip faulting and related basin formation in zones of tectonic escape: Turkey as a case study, in: Strike-slip Faulting and Basin Formation, edited by: K.T. Biddle and N. Christie-Blick, Society of Econ. Paleont. Min. Sp. Publ., 227-264.

Smit, A. D., Taymaz, T., Oktay, F., Yüce, H., Alpar, B., Başaran, H., Jackson, A. J., Kara, S. And Şimşek, U., 1995, High Resolutionseismic profiling in the sea of Marmara (NW Turkey: Late Quaternary sedimentation and sea level changes, GSA Bull. 107/8, 923-936.

Stein, R. S., Barka, A. A., Dieterich, J. H., 1997, Progressive Failure on the North Anatolian Fault since 1939 by Earthquake Stress Triggering, *Geophysical Journal International,* 128: 594-604.

Stein, R., Barka, A. And Dieteich, J., 1997, Progressive failure on North Anatolian fault since 1939 by earthquake stress triggering, Geophys. J. Int., submitted.

Straub, C.S., 1996. Recent crustal deformation and strain accumulation in the Marmara sea region, NW. Anatolia, inferred from GPS measurements, ETH, Zurich.

T. Parsons, R. S. Stein, R. W. Simpson, P. A. Reasenberg, J. Geophys. Res. 104,

The most recent event for the Yalova segment is 1894.6; Izmit segment, 1999.7; Ganos fault, 1912.7; Prince's Islands fault, 1766.7; central Marmara fault, 1509.8.

Toppozada, R. T., J. H. Bennet, G. Borchardt, J. F. Davis, C. B. Johnson, H. J. Lagorio, K. V. Steinbrugge, Planning Scenario for A Major Earthquake on the Newport-Inglewood Fault Zone, California Department of Conservation, Division of Mines and Geology, special publication, 99, 207p., 1988.

Westaway, R., "Block Rotation in Western Turkey," *Journal of Geophysical Researches*, Vol. 95, No. B12, pp. 19857-19884, 1990.

Working Group Calif. Earthquake Probabilities, Seismic hazards in southern California: Probable earthquakes, 1994-2014, Bull. Seismol. Soc. Amer. 85, 379-439 (1995).
Y. Ogata, J. Geophys. Res. 104, 17995 (1999)

APPENDIX 1. Historical earthquakes that affected the Marmara Region (Ambraseys & Finkel, 1991)

Fault segment numbers that are based on the new segmentation presented in section 2.1, and are thought to be associated with historical earthquakes that took place in the region between 1500 and 1900, are provided in parenthesis following the description of each earthquake.

32 A.D.

An earthquake shook the province of Bithynia; most houses in Nicaea (Iznik) were destroyed. The shock has been experienced in Istanbul and even in Athens.

69 A.D.

Nicomedia (Izmit), the capital of Bithynia, was destroyed. The damage should be extensive, since the city was rebuilt.

121 A.D.

A major earthquake in Bithynia destroyed completely Nicomedia (Izmit) and the greater part of Nicaea (Iznik).

358 August 24

A catastrophic earthquake in Bithynia totally destroyed Nicomedia (Izmit) and its district killing, among others, the vice-governor and two bishops who happened to be in the city. Nicaea (Iznik), Constantinople, and Perinthus (n. Marmaraereğlisi), as well as many other towns, were damaged. Landslides, ground deformations and a seismic sea-wave in Nicomedia, followed by a conflagration, completed the destruction. The shock was strongly felt in Asia Minor as far as the district of Pontus.

362 December 2

Nicomedia (Izmit) was totally destroyed as well as a good part of Nicaea (Iznik). Springs dried up. As a measure of relief the authorities lowered the price of essentials.

The earthquake was felt in Constantinople (Istanbul) and allegedly damaged the newly built cathedral of St. Sophia.

396

An earthquake in Constantinople (Istanbul) and vicinity, followed by aftershocks that obliged the people to stay in the open. No evidence has been preserved about the degree of damage done in and outside the capital.

402 June

An earthquake felt in Constantinople (Istanbul) which caused considerable concern.

403

A strong earthquake was felt at Constantinople (Istanbul). Aftershocks continued for four months. The shock possibly originated at some considerable distance from the city.

407 April 1

An earthquake caused damage in Hebdomen (Bakırkoy) and in Constantinople (Istanbul) (particularly districts of Kaenupolis and Xerolophos). Sea wave is also reported to have occurred. The epicenter is estimated to be located offshore.

412

An earthquake in Constantinople (Istanbul) caused damage to the city walls.

447 November 6

Preceded by a damaging earthquake on 26 January, a catastrophic earthquake in the Sea of Marmara destroyed many towns in the provinces of Bithynia, Phrygia and Hellespont. In Constantinople (Istanbul), public buildings and houses damaged in January were ruined, and the greater part of the city wall and 57 of its 96 towers were overthrown. The shock was followed by a damaging sea-wave and by aftershocks that continued for months.

460 April 7

This earthquake caused extensive damage in the province of the Hellespont and in the greater part of Thrace. Cyzicus (n. Erdek) and villages in the interior were totally destroyed, with great loss of life. In places the ground opened up.

478 September 25

A destructive earthquake in the eastern part of the Sea of Marmara totally destroyed Helenopolis (Karamürsel) and Nicomedia (İzmit) and caused severe damage in Constantinople (Istanbul). Damaging sea wave and aftershocks are also reported.

484

A destructive shock in the western part of the Marmara Sea region caused damage in Thrace and serious loss of life. Sistos (Şehitlikler) and Callipolis (Gelibolu) were 'destroyed completely' and Tenedos (Bozcaada) sustained serious damage. Lampsacus (Lapseki) and Abydus (Çanakkale) were heavily damaged and the Long Walls of the Chersonesus at Hexamili (n. Ortaköy) were breached. Near Sistos tar oozed out of the ground. Minor damage extended to Constantinople.

542 August 16

A severe earthquake in Constantinople (Istanbul) caused considerable damage and loss of many lives. Many houses and a number of churches collapsed and the walls near the Golden Gate were damaged. The shock overturned a number of statues and other free-standing monuments.

543 September 6

An earthquake that destroyed half of the city of Cyzicus (Erdek), was severe at Constantinople (Istanbul) where it caused minor damage.

554 August 16

A destructive earthquake caused severe damage in Nicomedia (İzmit) and in Constantinople (Istanbul). Several other towns have also been affected. Sea flooded the cost inland to a distance of two miles and aftershocks continued for a long time.

557 December 11

A destructive shock affected the northern coast of Marmara Sea, especially west of Regium (K. Çekmece) and Constantinople (Istanbul). The destruction extended over a large area, but the limits are unknown.

740 October 26

The earthquake caused enormous material and human loss in many towns of Thrace and Bithynia, especially in Nicomedia (İzmit), Praenetos (Karamürsel) and Nicaea (İznik). The sea retired form the land permanently, changing the coastline. In Constantinople (Istanbul) a considerable part of the city walls were destroyed and buildings were damaged.

861 April 10

A severe earthquake in Constantinople (Istanbul) was preceded and followed by many shocks. A number of houses, public buildings and a small section of the city walls were damaged. Aftershocks continued 40 days.

869 January 9

An earthquake caused considerable damage in Constantinople (Istanbul), killing a number of people. The shock damaged the cathedral of Sta Sophia, part of which collapsed. The church of the Apostles which was damaged by the earthquake of 861, collapsed, together with the church of the Virgin at Sigma. A long series of aftershocks, some of them strong enough to cause additional damage in the city, continued for 40 days.

925 August

A major earthquake somewhere in Thrace produced an enormous cleft in the ground. Many villages and churches were totally destroyed. The shock apparently caused some damage to Athos as well.

989 October 25

A destructive earthquake in the eastern part of the Sea of Marmara caused extensive damage to villages and towns in the provinces of Thrace and Bithynia. In Constantinople (Istanbul) many houses collapsed and public buildings and parts of the city walls were damaged or destroyed. Damage was equally heavy in Nicomedia (Izmit) and was in places aggravated by a seismic sea-wave.

1011 March 9

Preceded by a strong foreshock in January, a destructive earthquake in the provinces of Byzantium caused great loss of life. In Constantinople (Istanbul) a few public buildings and houses were destroyed.

1032 August 13

A destructive earthquake centering somewhere on the Asiatic side of the Marmara Sea region, caused the collapse of public buildings and of an aqueduct. In Constantinople (Istanbul) the shock damaged the land walls.

1037 December 18

An earthquake, probably a large aftershock of the major earthquake on the North Anatolian Fault Zone of May 1035 in Gerede, caused some damage in Constantinople (Istanbul).

1063 September 23

This was a severe earthquake that spread desolation particularly along the north coast of the Sea of Marmara, and ruined many districts which lay between Constantinople (Istanbul) and Dardanelles. The walls of town, aqueducts, churches and public buildings were thorn down throughout all southern Thrace particularly at Myriophyto (Mürefte), Panion (n. Barbaros), and Redestos (Tekirdağ). In Constantinople (Istanbul), houses were ruined and a few public buildings were damaged or destroyed. Aftershocks continued to be felt in Constantinople (Istanbul) for two years. Most probably the shock originated from the Sea of Marmara off shore Cyzicus.

1296 June 1

An earthquake in Constantinople (Istanbul) caused considerable damage, particularly to a number of old houses, public buildings and free-standing structures and to the city walls as well. The earthquake, which was followed by aftershocks for many days, affected even more the Asiatic provinces, but details are lacking. As a consequence of the earthquake, the emperor was obliged to return to Constantinople.

1323

An earthquake in Constantinople (Istanbul) caused severe damage to buildings, churches and monumental columns. There is good evidence that this earthquake destroyed Militopolis (n. Karacabey), and perhaps Apollonia (Apolyontköy). This shock marks the beginning of a period of seismic activity in this part of the Marmara region, during which the earthquakes of 12 May 1327, which destroyed Lopadion (Ulubad), and of 17 January 1332, were widely felt.

1332 January 17

This earthquake was felt very strongly in Constantinople (Istanbul) and was followed by violent thunderstorms and heavy seas which caused serious damage to buildings and the sea walls. The shock itself caused no damage.

1343 October 18

Followed by an almost equally destructive aftershock, an earthquake in the western part of the Marmara Sea caused extensive damage to Thrace and along the coast to Chersonesus (Gelibolu Peninsula). Among other towns, Myriophyto (Mürefte) and Hora (Hoşköy) were almost destroyed with great loss of life and Lysimachia (Bolayir) was ruined. In Constantinople (Istanbul) the city walls were breached and some of the fortification towers were partly destroyed. Houses, public buildings and churches suffered different degrees of damage. The aftershock, that took place a few hours after the earthquake, was equally damaging throughout the region. It was followed by a seismic sea-wave that flooded the coast to a great distance and cast sailing ships on land, the sea advancing 12 stadia (2.2 km) inland on flat ground and causing extensive

damage to settlements and towns along the coast of Thrace. Aftershocks continued to be felt for almost a year. The earthquake had serious social and financial repercussions.

1344 November 6

This was probably a large aftershock of the earthquake of 1343 in Thrace. It destroyed completely the region of Ganohora (Gaziköy) on the west coast of the Sea of Marmara, including the castles of Ganos (Gaziköy), Hora (Hoşköy), Marmara Island, and the Long Walls of the Chersonesus or Tihos at Hexamili (n. Ortaköy). The shock seems to have been experienced very strongly at Constantinople (Istanbul), where it caused some damage to the city walls. Aftershocks continued for a few weeks.

1346 May 19

During the autumn of 1345 and again in the spring of 1346 new shocks were felt in Constantinople (Istanbul). The earthquake of 19 May 1346 caused some damage to a number of free-standing structures and to the church of Sta Sophia, the eastern part of which collapsed. It is not possible to locate the epicentral area of this event.

1354 March 1

This earthquake ruined the region along the coast of the Marmara Sea, from Redestos (Tekirdağ) to Madytos (Hacıabad), including Callipolis (Gelibolu), and other places in Thrace where many lives were lost. The earthquake damaged houses and the walls of Constantinople as well as numerous settlements south of Madytos and in the districts of Thrace and Macedonia as well as in Tenedos (Bozcaada).The shock was felt over a large area.

1400 January

An earthquake was strongly felt in Constantinople (Istanbul) as well as Bursa.

1419 March 15

This earthquake most probably occurred in the eastern North Anatolian fault but its effects extended to Constantinople (Istanbul).

1489 January 16

An earthquake in Istanbul caused the collapse of a number of minarets. The earthquake probably had an epicenter some distance from Istanbul, but no information is available for the damage caused outside the city.

1509 September 10

A destructive earthquake that caused considerable damage throughout the Marmara Sea area, from Gelibolu to Bolu and from Edirne and Demitoka to Bursa. Damage was particularly heavy in Istanbul where many mosques and other buildings, part of the city walls, and about 1000 houses were destroyed, and 5000 people were killed. Many houses and public buildings sustained various degrees of damage in Demitoka, Gelibolu, Iznik and Bolu. The shock was felt within a radius of 750 km and was followed by a seismic sea-wave in the eastern part of the Sea of Marmara. Aftershocks, some of them destructive, continued intermittently for almost two years.

1542 June 12

A destructive earthquake in Thrace caused extensive damage and great loss of life in the region between Gelibolu, Edirne and Istanbul. In Istanbul, 1700 houses are said to have been ruined and 4500 people killed. The epicentral area involved cannot be identified, but a possible location would be the central part of the north coast of the Sea of Marmara.

1556 May 10

A destructive shock in the east part of the Sea of Marmara ruined many places including Aydıncık (n. Erdek), and killed a large number of people. Damage extended to Bursa and Istanbul where many houses, mosques and parts of the city walls were ruined. The walls of Aya Sofya were cracked and the Fatih Mosque had to be repaired. The details of this event suggest that its epicenter must be sought offshore in the Sea of Marmara. Ambraseys (2000) locates this earthquake near the Kapıdağ peninsula. Based on the

damage description above we have decided to locate this earthquake at a location closer to Istanbul.

1567 October 1

This earthquake caused damage in the Sapanca area and to some unnamed villages in a district where a landslide was triggered by the shock. Damage extended to Izmit and to Istanbul, where a few houses collapsed. It is unlikely that the damaging effects of the earthquake extended beyond the limits of Sapanca.

1648 June 28

This earthquake damaged multistorey houses, chimneys and the spires of minarets in Istanbul. There is no information that the shock was felt elsewhere. The details of the effects of the shock in Istanbul suggest that the city was some distance from the epicentral region of a relatively large-magnitude earthquake, possibly in Transylvania.

1659 February 17

A large earthquake was felt throughout the western part of the Ottoman Empire. In Tekirdağ churches and mosques and in Istanbul old buildings, houses and chimneys were ruined. The effects of the earthquake suggest that the shock was of large magnitude and originated possibly in the Aegean Sea.

1688 September 10

This earthquake was felt rather strongly in Istanbul. The absence of any other information than causing heavy damage inland, suggest that the earthquake originated from somewhere in Karesi province.

1689 April 25

An earthquake was felt over a large area of northwestern Anatoila and Thrace, particularly along the west coast of the Black Sea. In Istanbul and Edirne several houses, mosques and towers were damaged by the shock and most probably by the high

winds documented at about this time, which necessitates repairs to various buildings in Istanbul. The epicentral area involved is impossible to identify, but a likely location would be the Maritsa Valley.

1690 July 11

A damaging earthquake in Istanbul caused a number of houses to collapse killing 20 people. At Büyük Çekmece a minaret collapsed. The absence of data from other towns suggests the possibility that this was a local shock with an epicenter offshore. Aftershocks continued to be felt for several days.

1707 June 2

This earthquake caused non-structural parts of the castle of Sedd ül-bahr to collapse. The shock was felt strongly at Izmir and was predictable in Istanbul. The data suggest and epicentral region south of the Dardanelles.

1719 May 25

Preceded by damaging foreshocks a major earthquake in the east part of the Sea of Marmara. Villages and towns on either side of the Gulf of Izmit, in Yalova, Pazarköy, Karamürsel, Kazıklı, Izmit, in the region of Sevenit (Sapanca ?) and as far as Düzce were destroyed or badly damaged; it is said that more than 6000 (?) people were killed in this earthquake. Considerable damage was done to houses, buildings and to the city walls of Istanbul, where 40 mosques and 27 towers were ruined. There was also significant damage in Akviran, Çatalca, Çekmece, and Heybeliada. The shock was strongly felt in Edirne, where it caused some minor damage, and in Chios, Izmir, Athos, Thessaloniki, Nish (?) and in Anatolia (?). Aftershocks continued for about a month.

1730 June 10

In this earthquake, the greater part of the castle in the district of Evreşe (n. Kadiköy) was destroyed (?) and much damage was done to villages along the road from Athos to Istanbul. The shock was strongly felt in Athos and was reported from Istanbul. Ambraseys and Finkel assume that the epicentral area was located offshore, in the Gulf of Muariz (Saros).

1752 July 29

A destructive earthquake in Thrace: Zerna (n. Ibriktepe), Hafsa and Hasköy were completely ruined and many people were killed. Considerable damage was done to houses and public buildings in Edirne where 100 people were killed; almost all minarets collapsed and part of the castle and wall were ruined. The ground was rent in places and elsewhere it liquefied, filling up wells. Aftershocks continued for more that a year.

1754 September 2

A great earthquake in the Gulf of Izmit and further to the east where villages were totally destroyed and the ground was opened. It is said that about 2000 people were killed. The lighthouse at Bendereğli (Ereğli) on the Black Sea was destroyed. There was much damage done at Üsküdar and in the Balat, and in Istanbul many old masonry houses and buildings collapsed and 60 people were killed by the main shock and by damaging aftershocks that continued for weeks; some mosques and parts of the city walls were also damaged. The main shock was associated with a seismic sea-wave which caused no damage. The shock was also reported from Izmir and Ankara (?). The shock does not seem to have caused serious damage to the south of Marmara Sea. Possible location of the epicentral area would be in the Izmit area.

1766 May 22

A destructive earthquake in the east part of the Sea of Marmara caused heavy damage extended from Rodosto (Tekirdağ) to Izmit and to the south coast of the Sea from Mudanya to Karamürsel. Damage to buildings and tall structures were reported from as far as Gelibolu, Edirne, Izmit and Bursa. In Istanbul many houses and public buildings collapsed, killing 880 people. Part of the underground water supply system was destroyed. The Ayvad dam on the upper Kağithane, north of Istanbul, was damaged, and in the vicinity of Sultanahmet, the roof of an underground cistern caved in. It is said that about 4000 people lost their lives. The earthquake was associated with a seismic sea-wave which was particularly strong along the Bosphorus and in the Gulf of Mudanya where it caused considerable damage. Damage extended inland, mainly to the north and west, as far as Edirne and to Gelibolu. In Çatalca and surrounding villages all

masonry houses were totally destroyed. It is said that about 4000 people lost their lives. The shock was felt strongly along the west coast of Black Sea. Damaging aftershocks continued for weeks, the sequence lasting for over a year. Ambraseys and Finkel (1991) assume that the epicentral region of this earthquake was offshore in the Sea of Marmara.

1766 August 5

A major earthquake in the west of the Sea of Marmara completed the destruction caused by the shock of 22 May and enlarged the affected area west of Rodosto (Tekirdağ). The region between Silivri and Tenedos (Bozcaada) was ruined with loss of life. The district of Ganohora (Tekirdağ) was totally destroyed and that of Gelibolu suffered heavy losses. The castles along the Dardanelles up to Sedd ül-bahr and in Evreşe were damaged. Damage extended to Bursa, Istanbul, throughout Thrace to Edirne, and in the district of Biga. Damaging aftershocks throughout the Marmara Sea area continued for almost a year.

1776 May 29

An earthquake caused widespread but minor damage along the coast from Gelibolu to Istanbul. Buildings and houses affected by the large earthquakes of 1766 and since repaired, were again damaged. Most probably this earthquake originated offshore.

1800 September 26

A series of earthquakes was felt in Istanbul as a result of which a public building was damaged.

1802 October 26

A large earthquake in eastern Transylvania caused some damage to the houses and to the covered bazaars in Istanbul and Edirne. The epicentral area of this event is outside the Marmara region.

1809 February 7

A large earthquake with an epicenter probably located offshore the Dardanelles, almost totally destroyed the region of Eskistanbul (the part of the mainland opposite Bozcaada (Tenedos), and caused damage on the island of Gökçeada (Imroz).

1855 February 28

The main shock came 15 minutes after a violent foreshock in the Hüdavendigar district - Bursa. Some old buildings and walls partly collapsed.

1859 August 21

A damaging earthquake with an epicenter offshore the Dardanelles caused heavy damage and liquefaction on the island of Gökçeada. This earthquake can be associated with fault segment 11 (Figure 2.23) (Ambraseys (2000)).

1877 October 13

An earthquake with an offshore epicentral area in the Sea of Marmara caused heavy damage to the Marmara Islans.

1893 February 9

This earthquake had an offshore epicenter in the Gulf of Saros. It caused considerable damage to Gökçeada.

1894 July 10

A destructive earthquake in the Gulf of Izmit and further to the east caused extensive damage in the area between Silivri, Istanbul, Adapazarı and Katırlı. Maximum effects were reported from the region between Heybeliada, Yalova and Sapanca where most villages were totally destroyed with great loss of life.. The shock caused the Sakarya river to flood its banks and the development of mud volcanoes. In Adapazarı 83 people were killed and another 990 in the Sapanca area. In Istanbul damage was widespread and in places very serious. Many public buildings, mosques, and houses were shattered and left on the verge of collapse, while most of the older constructions fell down, killing 276 and injuring 321 people. Three of the dams for the water supply of Istanbul were

badly damaged. The shock was associated with a seismic sea-wave, which at St. Stephanos (Yeşilköy) had a height of 1.5 m., and caused the failure of submarine cables. Liquefaction of the ground and landslides were reported from the epicenter region, particularly from the area between Sapanca and Adapazarı. The shock was felt as far as Bucharest, Sofia, Yannina, Crete and Konya, and it was not followed by a significant aftershock sequence.